Characterization of the spatio-temporal dynamics in thymic epithelial development

Inauguraldissertation

zur
Erlangung der Würde eines Doktors der Philosophie
vorgelegt der
Philosophisch-Naturwissenschaftlichen Fakultät
der Universität Basel

von

Carlos Eduardo Mayer

von Weinfelden (TG)

Basel, 2016

Genehmigt von der Philosophisch-Naturwissenschaftlichen Fakultät

auf Antrag von

Prof. Dr. Georg Andreas Holländer

Prof. Dr. Prime Leo Schär

Basel, den 23. Juni 2015

Prof. Dr. Jörg Schibler
Dekan

"¿Que dejamos atrás cuando cruzamos cada frontera? Cada momento parece romperse en dos: melancolía por lo que dejamos atrás y el entusiasmo de entrar en una nueva tierra."

-

„What do we leave behind when we cross each frontier? Each moment seems split in two: melancholy for what was left behind and the excitement of entering a new land."

Dr. Ernesto „Che" Guevara
Diarios de motocicleta (1952/53)

Acknowledgments

The past few years had a great impact on my life. During this time, I have had the chance to grow professionally and personally and, like many of such landmark experiences in life, I had many people accompanying me along the way.

First and foremost, I want to thank Professor Georg A. Holländer for his mentorship during the past six years during which I could always count on his wisdom and support. You introduced me to the world of science and encouraged me to keep learing and widening the horizon, in the lab as well as outside by sending me to several conferences abroad. Your ability to continuously keep an eye at the bigger picture and to always keep moving forward has been very inspiring and a great life lesson. Joining your lab was one of the best decisions of my life.

My deep gratitude also goes to Doctor Saulius Zuklys for being an outstanding colleague and friend. You taught me most of the skills I know today and always had an open ear for my thoughts. Your patience and positivism are great attributes that I will always remember. I will miss our 10 am coffee/brainstorm sessions.

And of course I would also like to thank all present and former members of the Pediatric Immunology Laboratory in Basel: Thomas Barthlott, Chiara Beilin, Caroline Berkemeier, Angela Bosch, Marita Bostincardi, Marco Catucci, Elli Christen, Simone Dertschnig, Martha Gaio, Sanjay Gawade, Jason Gill, Werner Krenger, Sébastien Loeffler, Gretel Nusspaumer, Annick Peter, Noriko Shikama, Gabor Szinnai, Hong Ying Teh, Tatjana Zalac, and Saule Zhanybekova. You all have made my PhD interesting, educational, and a very good time.

To Nicolas Beck, Raffael Beck, Claudio Galli, Damian Germann, Lukas Greuter, Alasdair Hall, and Vincenzo Maira I say: good friends are needed on every journey, and I couldn't think of better people to accompany me. May we keep on brewing beer together for many years.

I dedicate my doctoral thesis to my family for their unconditional love and support. To my parents Hilda and Eduardo for all the sacrifices they made in life in order to offer their children the best future they could imagine, and to my sisters Laura and Flavia for being the most important people in my life.

Table of Contents

Abbreviations

APC	Antigen-presenting cell
CK#	Cytokeratin #
CMJ	Cortico-medullary junction
cTEC	Cortical thymic epithelial cell
DC	Dendritic cell
DETC	Vγ5+ dendritic epithermal T cell
DNA	Deoxyribonucleic acid
Dox	Doxycycline
DP	CD4/CD8 double-positive thymocyte
dpc	days post coitum
E#	Embryonic day of Development #
i.p.	Intraperitoneal injection
IHC	Immunohistochemistry
ISP	Immature CD8 single positive thymocyte
LTi cell	Lymphoid tissue-inducer cell
MHC	Major histocompatibility complex
miRNA	Micro RNA
mRNA	messenger RNA
mTEC	Medullary thymic epithelial cell
n.s.	Not significant
P#	Postnatal day #
PCR	Polymerase chain reaction
pGE	Promiscuouse gene expression
qPCR	Quantitative PCR
RISC	RNA-induced silencing complex
RNA	Ribonucleic acid
RNAi	RNA interference
rtTA	Reverse tetracycline transactivator
TCR	T cell receptor
TEC	Thymic epithelial cell
TRA	Tissue restricted antigens
TRE	Tetracycline response element

1 Introduction

1.1 The thymus in history

In his book *The Wealth of Nations* (1) the Scottish economist Adam Smith took first attempts to define the basic concepts of supply and demand that rule the trading of goods. Interestingly, what he described in the context of competition in modern economies is also the inevitable consequence of life, namely the raising scarcity and the thereby emerging competition for goods, in this case nutriments and habitats. As a consequence of that competition organisms required to acquire survival mechanisms that increased their fitness by either adapting to extreme habitats and different nutrients, forming multicellular organisms and/or acquiring the ability to attack or defend from other life forms. In this context, the immune system can therefore be seen as a critical adaptation to competitive living that has co-evolved with life itself. Simple defensive mechanisms such as the production of antimicrobial peptides, establishment of pathogen-recognition systems (e.g. Toll-like receptors) and the formation of the complement system that can be found in bacteria or lower animals have been complemented with complex, multi-layered and adaptive defense systems such as the ones found in mice and humans today. As a crucial component of the adaptive immune system, the thymus is a remarkable example of that adaptation because it is not per se a vital organ but a mere module of adaptation to increase survival. Or as Henry G. Wright stated it in his 1852 publication in the London Journal of Medicine: "The purpose served by the thymus gland, according to the foregoing theory, tends to illustrate a physiological circumstance of great interest, (…), namely the progressive perfectionation of the framework of man in obedience to an all-pervading law."

1.2 Anatomy of the Thymus

The murine thymus is a bi-lobulated, encapsulated organ situated in the upper anterior thorax adjacent to the heart. The nature of the thymus can be described as dualistic as it is comprised of a static stromal structure and a dynamic, largely hematopoietic 'fluid phase'. The stromal structure, which could arguably be called the real thymic tissue, as it is stationary and permanent, makes up only a minor

number of cells in what is the total thymic cellularity. Within the stromal compartment thymic epithelial cells (TEC) play an important role in supporting thymopoiesis by providing soluble and cell-bound factors that are required to guide developing cells through the distinct steps of thymopoiesis (2, 3).

The thymus is roughly compartmentalized into two spatially and functionally distinct regions, an outer cortex and inner medulla. Developing T cells are mostly located in the cortical region making that compartment very dense and rich in cells. The prominent stromal cells within the cortex are cortical TEC (cTEC), which are very large, sponge-like cells that contain various developing thymocytes within what is a single cell's volume. This micro-unit of cTEC with associated thymocytes is a very good representation for the whole cortical structure as the cortex is basically a multimeric, sponge-like structure of micro-units structured by stromal cells that provide the required signals to T cell progenitor cells that move through it. Other abundant cell populations within the cortex are macrophages, which help in clearing thymocytes undergoing apoptosis, mesechymal cells and in small numbers endothelial cells, through which early T cell progenitors (ETP) enter the thymus (4–6). In contrast to the cortex, the medulla is a more complex structure composed of a number of cell types. As described below, only a small number of the developing thymocytes pass the selection processes in the cortex and are able to translate to the medulla, which leads to an overall lower cellular density in that compartment. mTEC are a prominent cell type within the medullar stroma and, as antigen factories, play an important role for the last step of T cell development where potentially auto-reactive cells are eliminated (3). Various subsets of dendritic cells (DC) within the medulla additionally support this process by importing foreign antigens and cross-presenting antigens picked up from dying cells, which in turn are removed by macrophages(7, 8). Moreover, in contrast to the cortex, endothelial cells are very prominent within the medulla because they are required for the export of finally matured T cells(9). Taken together, the thymus is a complex organ composed of many different cell types that ultimately serve the same purpose, namely to produce functional and tolerant T cells.

1.3 Thymus Organogenesis

The organogenesis of the murine thymus is a well-structured sequence of developmental steps that is initiated with the formation of the thymic primordium that develops from the ventral region of the third pharyngeal pouch with contribution from the surrounding neural crest cells (NCC) at embryonic day of development (E) 9.5(10). As this early structure grows, it starts to pattern into the two areas that will eventually give rise to the thymus and the parathyroid, whose corresponding areas is characterized by the expression of Glial cells missing 2 (Gcm2) very early on. The thymic epithelium develops from the endodermal lining that commences to express the transcription factor Forkhead box protein N1 (Foxn1) at around E10.5. Although Foxn1 is not required for the initial formation of the thymic epithelial precursor pool or the first steps of TEC development, it is required for the attraction and commitment of hematopoietic precursor cells to the thymus by regulating the expression of Dll4, CCL25, and other molecules involved in thymopoiesis (further described below) (11).

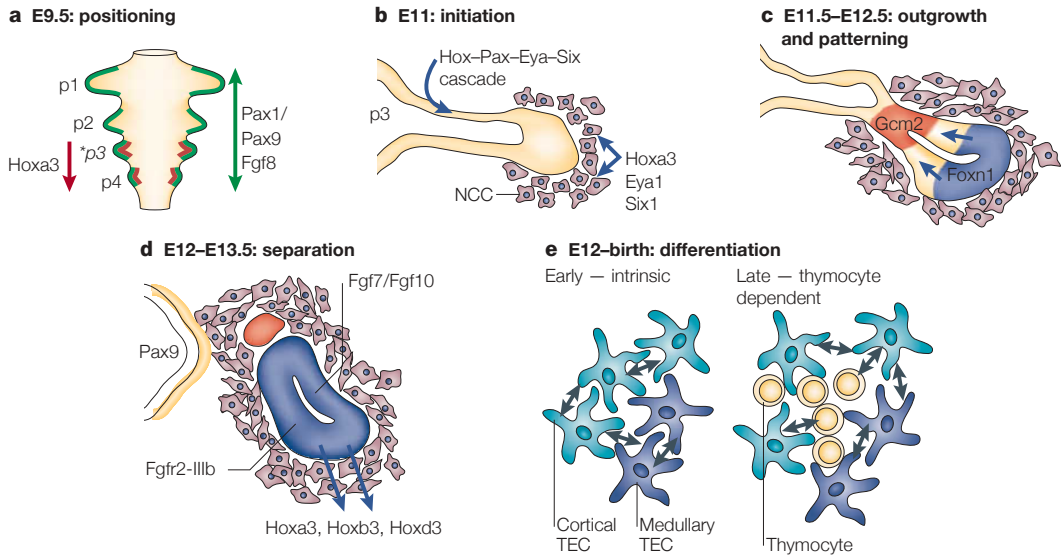

Figure 1.3-1. *A current model showing the distinct stages of early thymus organogenesis.* Thymus and parathyroid develop from a common anlage at the third pharyngeal pouch. Subsequently, influenced by various transcription factors, they separate and form distinct organs. TEC development is uniform in the initial stages, but starts to diverge later on. Image from Blackburn et al. (10).

With the immigration of hematopoietic cells TEC lineage divergence and specification is initiated. Interactions of mTEC progenitors with cells of hematopoietic origin through the Nuclear Factor κ B pathway induce the differentiation and maturation of mTEC (12–15). This contact is initially mediated by lymphoid tissue-inducer (LTi) cells and invariant Vγ5+ dendritic epidermal T cell (DETC) progenitor cells, but replaced by post-selection thymocytes (described below) in the mature thymus. As a consequence of these inductive signals the first mTEC start to differentiate and proliferate, thereby forming small medullary islets. There is scientific evidence that the initially emerging medullas are derived from single cells, meaning that they are each of one clonal origin (16). Although this aspect of medulla development is still debated, it is possible that, once these initially small medullary islets continue to grow, they start to fuse and form the large and multiclonally-derived medullas that are observed in adult mice (further described in chapter 3.4). With the onset of large-scale thymopoiesis and the emergence of medullary islets, the thymus starts to grow tremendously. This growth is continued during the first weeks after birth until the thymus reaches its maximal cellularity at around 5-7 weeks of life. Thereafter, the thymus experiences an early onset of involution that leads to a reduced T cell output and narrower TCR repertoire with age (17). The mechanisms driving this unique form of early organ involution are poorly understood, although changes in the neuroendocrine-immune axis are suggested by either increases or losses in the production of particular hormones and growth factors (18).

In conclusion, thymus organogenesis is a complex development that is orchestrated by the bi-directional interactions of various cell types. This inter-lineage dependency is crucial for the initial formation of thymic tissues, and continues to be important in the fully-grown organ as defects of specific signaling pathways or single cell types can lead to a disturbance of thymic structure and function. Despite the growing understanding of TEC biology, TEC development and the precise phenotypic characterization of TEC subsets during differentiation remain largely unknown.

1.4 T cell Development

The most important feature of the thymus is its capacity to promote T cell development. This process is initiated by the immigration of blood-borne T cell progenitor cells, derived from hematopoietic cells in the bone marrow, through the engagement of P-selecting expressed on endothelial cells of the thymic vasculature (6). At this stage, early thymic progenitor cells (ETP) are not yet committed to the T cell fate and have a wide lineage potential, including $\alpha\beta$ T cells (the most common T cell subset on which the following description of T cell development will focus), $\gamma\delta$ T cells, B cells, Dendritic cells and NK cells (19–22). The immediate progeny of immigrating ETP are called double-negative (DN) cells due to the lack of expression of the typical T cell co-receptors CD4 and CD8. These cells can further be subcategorized into DN1 cells based on the expression of CD44 in the absence of CD25. The further differentiation of DN1 cells and commitment to the T cell fate is dependent on the engagement of the Notch ligand Delta like protein 4 (Dll4) expressed by cTEC (23). Upon further development, the maturing lymphocytes acquire a CD25+ CD44+ phenotype (defined as the DN2 stage) and show a reduced potential to give rise to B cells, DCs, and monocytes (24). This progression through the early steps of development is accompanied by a migration of differentiating cells towards the subcapsular zone of the thymus and the upregulation of the recombination activating genes (RAG) 1 and 2, which are critically required for the rearrangement the locus encoding the TCR β chain.

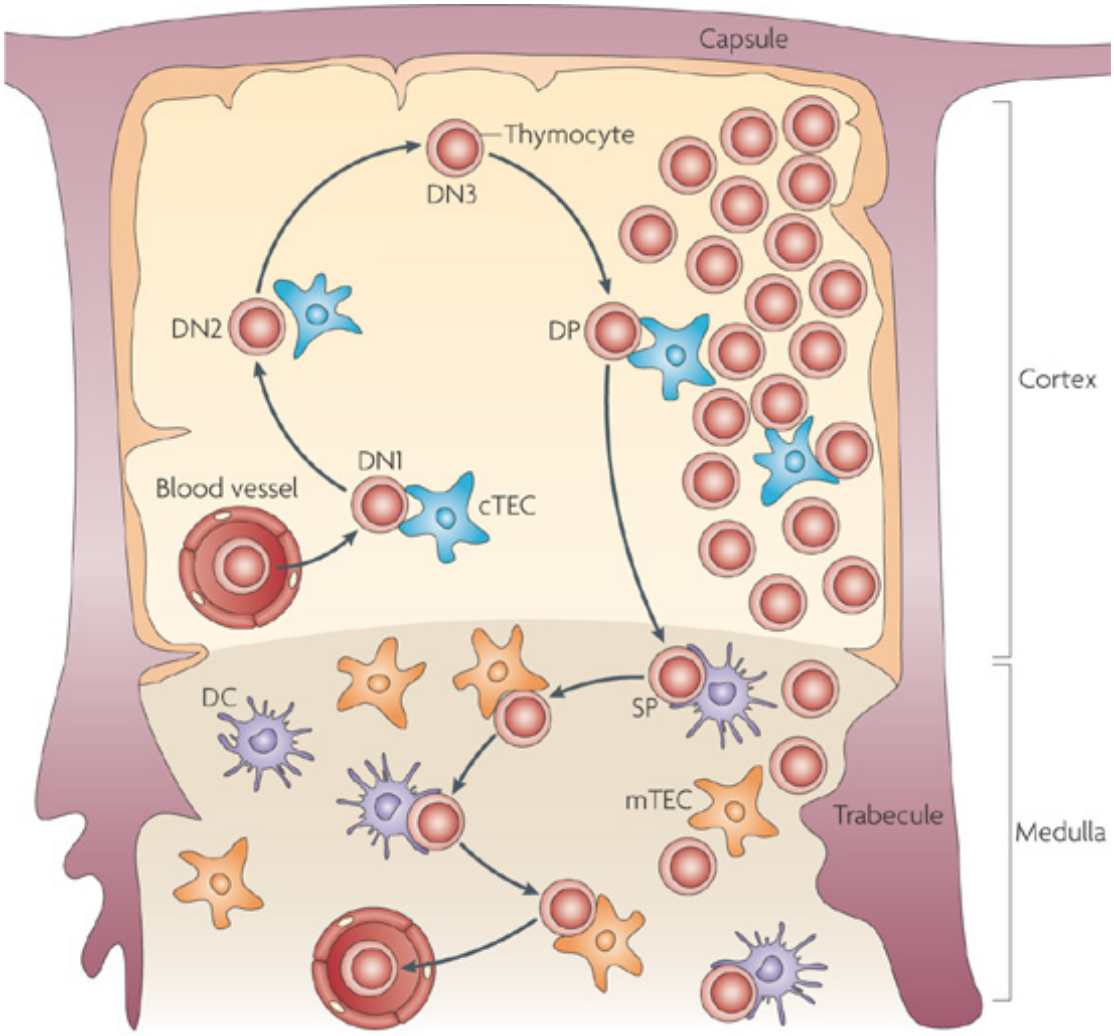

Figure 1.41-2. *Schematic representation of T cell development in the thymus.* Blood-borne T cell progenitor cells enter the thymus through blood vessels near the cortico-medullary junction. Attracted by signals from the cortical stroma, they move to the cortex, committing to a T cell fate, and start to rearrange their TCR loci. These first stages of T cell development are characterized by the differential expressions of CD25 and CD44 and called DN1-4. Upon successful rearrangement and expression of a functioning pre-TCR, developing T cells upregulate the expression of co-receptors CD4 and CD8, thereby entering the DP stage. On the journey towards the medulla, T cells experience positive selection, meaning that cells recognizing antigens bound to MHCs obtain signals for further development, while the others 'die by neglect'. In the medulla, potentially self-reactive T cells get negatively selected upon the strong interactions with self-antigens presented by antigen-presenting cells (APCs). The remaining cells leave the thymus as MHC restricted and self-tolerant naïve T cells. Image from Klein et al. (25).

The somatic DNA recombination of variable (V), diversity (D) and joining (J) gene segments within this locus allows the generation of TCR β chains with different antigen-binding capacities (26). Cells at this stage are named DN3 cells and express CD25 in absence of CD44. They express the TCR β chain from the newly rearranged locus as well as a surrogate TCR α chain (named pTα) that together form the pre-T-

cell receptor. The pre T-cell receptor is expressed on the cell surface in a complex with CD3, a molecule that provides the signaling components of T cell receptors. Receptor complexes containing a successfully rearranged TCR β chain are able to signal and pass the so-called β chain-selection process, after which the developing cells arrest the further rearrangement of the TCR β chain locus, start to heavily proliferate and downregulate CD25, thereby entering the DN4 stage. At this stage the TCR α chain locus is rearranged and the expression of the TCR co-receptor CD8 is initiated. Subsequently, these immature (CD8) single positive (ISP) cells commence the expression of CD4 and enter the prominent CD4 and CD8 double positive (DP) stage. The upregulation of the TCR co-receptors is accompanied by various rounds of proliferation that leads to the DP population of approximately 90% of total cellularity found in the mature thymus. At this very critical step of T cell development DP cells are tested on their ability to recognize peptide-MHC complexes presented on TEC, dendritic cells, B cells and possibly additional antigen-presenting cells (APC) (8). Only a small fraction of cells (~5%) that express a TCR composed of signaling-proficient α and β chains are 'positively selected' and able to proceed to the final developmental steps. An important parameter during positive selection is the affinity to the presented antigen and the resulting TCR signaling strength, as described by the affinity model of thymocyte selection (8, 27). The vast majority of cells baring a TCR that has none or very low affinity to peptide-MHC complexes undergo apoptosis in a process termed 'death by neglect'. Cells with an intermediate affinity are properly selected and continue T cell development, whereas thymocytes with a TCR that binds with very high affinity are negatively selected, whereby potentially auto-reactive cells are removed. Because there is no sharp threshold at which thymocytes are positively or negatively select, there is a range at which cells of equal affinity to the presented antigen are stochastically selected. Thymocytes at this range usually develop into the T regulatory cell (Treg) lineage, which is critically required for the establishment of peripheral tolerance (28).

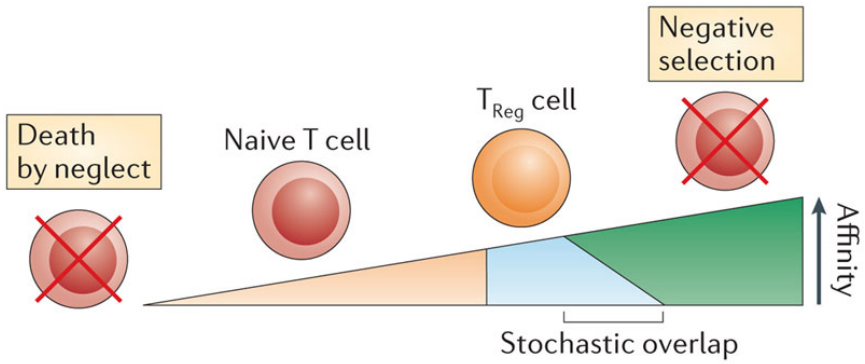

Figure 1.4-3. *The affinity model of thymocyte selection.* Newly generated T cell receptors (TCR) are tested during development on their ability to recognize antigens presented by thymic epithelial cells and other antigen presenting cells. The affinity model states the four possible outcomes of that testing depend on the affinity by which TCR recognize peptide/MHC complexes. Very low affinity (or lack thereof) leads to 'death by neglect' at which thymocytes undergo apoptosis. Cells baring a TCR with intermediate affinity are positively selected and continue to the next steps of T cell development. Intermediate to high affinity to presented antigens leads to the generation of regulatory T cells, whereas thymocytes with very high affinity are negatively selected and removed due to their potentially auto-reactive nature. Because there is no clear affinity threshold at which cells are either diverged to the regulatory T cell lineage or negatively selected there is a stochastic overlap at which some cells with same affinities to presented antigens can face either fate. Image from Klein et al. (8).

Depending on the class of MHC recognized, the positively selected T cells maintain the expression of either the CD4 or CD8 co-receptor and down regulate the other, but transiently express activation markers such as CD69 (29). Because positively selected T cells may still bare a TCR with high affinity towards 'self-antigens' expressed in other tissues of the body they move from the cortex to the medulla of the thymus where potentially auto-reactive cells are negatively selected. mTEC are professional antigen-producing cells that are able to ectopically express a large variety of peripheral tissue self-antigens thereby providing a 'genetic mirror' of the whole body on which T cells can be quality-tested (3, 25, 30). Developing T cells that recognize these self-antigens with high affinity could potentially be harmful and are triggered to undergoing apoptosis and then removed by a very effective clearing system composed of macrophages and other phagocytic cells. T cells that have passed all these checkpoints during the course of a 4 week development in the thymus are finally ready to leave the thymus and contribute to the immune system, tolerating self-antigens, but recognizing and attacking foreign peptides.

1.5 Thymic Epithelial Cell Function

TEC are roughly categorized by their position in the two main compartments of the thymus and therefore named cortical and medullar TEC. This simplified characterization does not however account for the many, only partially described subsets of TEC within each compartment. For instance, only few different types of TEC have been described in the cortex and a proper functional differentiation of cTEC subsets remains elusive. For that reason it is currently unknown how many of the molecules described below are expressed on a single cells or in different TEC subsets.

cTEC play an important role in the commitment of ETP (24). When T cell progenitors enter the thymus they have still a broad lineage potential that is only restricted once they encounter the ligand of the Notch signaling pathway Delta-like ligand 4 (Dll4) expressed by cTEC. This is a critical step in T cell development, because a deficiency in Dll4 in cTEC leads to the in situ development of B cells in the thymus instead (31). During the early steps of thymopoiesis T cell progenitors move through the cortex towards the subcapsular region. The general outward movement is guided by CXCL12 expressed on cTEC that is detected by CXCR4 on the developing cells (32). Subcapsular cTEC additionally express CCL25 that directs DN2 and DN3 cells to the edge of the cortex just below the capsule (33). After rearranging the genomic loci encoding the α and β chains of the TCR, T cells are tested on their ability to recognize peptide-MHC complexes presented by cTEC. The presentation of antigens is probably the main hallmark of thymic epithelial cells. Two of the most important steps during thymopoiesis heavily rely on it, positive and negative selection. It is therefore not surprising that TEC possess a sophisticated machinery to process and present antigens. Proteolytic enzymes cleave proteins into small peptides that are then loaded onto MHC class I and II molecules through very well described mechanisms (8). It was recently discovered that cTEC form a proteasome composed of a unique subunit named β5t that is only found in the thymic epithelium (34). The β5t subunit replaces the β5 and β5i subunits usually found in the two β heptameres that span the proteolytic core structure of the proteasome. This exchange results in the production of peptides with high affinity to the MHCI molecule, which are

required for the production of CD8 single positive thymocytes, as a lack in β5t leads to significantly lower development of this T cell subset (34). Another protease involved in the processing of antigens that are presented to developing thymocytes is Cathepsin L (Ctsl). This enzyme cleaves proteins within lysosomes and is not only important of the maturation of MHCII molecules (35), but also required for the processing of antigens that are needed for CD4 T cell development (36). Similarly, the thymus specific serine progease (TSSP) is required for the processing of proteins, which are then presented on MHCII (37). Taken together, β5t, Ctsl and TSSP are three examples of the sophisticated antigen processing machinery that is present in cTEC and that is required for proper selection of thymocytes. There are more proteolytic enzymes and enzyme complexes that are required for the processing of antigens supporting T cell development, and more research will have to be conducted to further enhance the knowledge on this complex machinery.

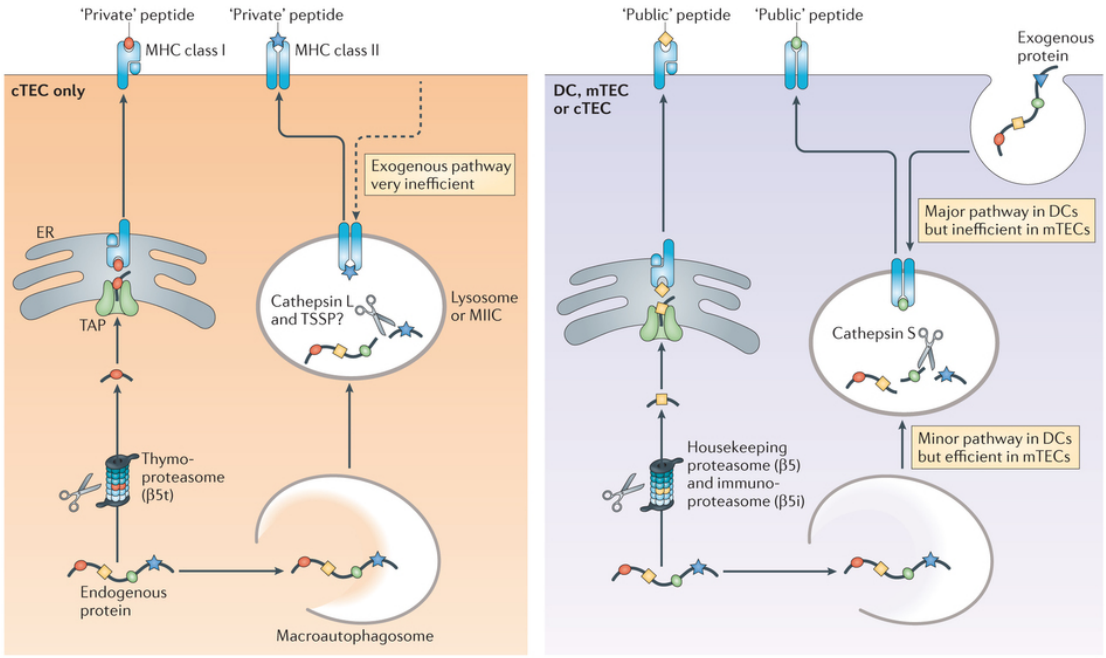

Figure 1.5-1. *Antigen presentation on thymic epithelial cells requires unique proteolytic pathways.* During thymopoiesis T cells are tested on their ability to recognize antigens presented on MHC molecules. Cells that present antigens use multiple antigen-processing pathways for the generation of peptides. Endogenous proteins are generally presented on MHC class I molecules. Proteasomes in the cytoplasm cleave proteins into small peptides, which are then transported to the endoplasmic reticulum where they loaded on MHCI molecules. This peptide-MHC complex is then transported to the surface where it can be detected by passing thymocytes. The proteasomes may contain different subunits in various cell

types that generate peptides with different affinities to MHCI. Endosomes in thymic epithelial cells process antigens that are presented on MHCII molecules. Various proteolytic enzymes process proteins that are derived from macroautophagosomes or endocytic vesicles, depending on the cell type. Image from Klein et al. (8).

After being positively selected thymocytes upregulate the CCR7 receptor and are able to sense CCL19 and CCL21 secreted predominantly by mTEC. As a result they migrate from the deep cortex into the medulla where they directly engage with mTEC and other APC. mTEC are a very special cell type that has the remarkable capability to express many tissue restricted antigens (TRA) ectopically in the thymus (30, 38). On a population level up to 19'000 genes are expressed by mTEC covering a large number of the protein-coding sequences within the genome, however only a few hundreds of TRA are expressed by a single cell (40). To achieve this extraordinary coverage of the genome a finely regulated transcriptional program is implemented in mTEC that involves epigenetic regulatory mechanisms at the DNA and histone level (39–42). In addition, the autoimmune regulator (Aire), a transcription factor that is specifically expressed in mTEC, regulates the transcription of a fraction of TRA (30). Mutations in its gene leading to a loss of function cause the severe autoimmune disorder Autoimmune polyendocrinopathy-candidiasis-ectodermal dystrophy (APECED) in humans (43, 44) and the emergence of auto-reactive T cells in mice (45). The wide palette of TRA expressed by mTEC is ultimately presented to developing T cells on MHCI and MHCII molecules. Thymocytes that recognize self-antigens with high affinity undergo apoptosis and are removed by a very effective clearing system involving macrophages and other phagocytic cells (46). The presentation of TRA by mTEC (together with other APC in the medulla) to the developing thymocytes is therefore important to ensure the production of self-tolerant T cells.

1.6 References

1. Adam, S. 1776. The wealth of nations.
2. Takahama, Y. 2006. Journey through the thymus: stromal guides for T-cell development and selection. *Nat. Rev. Immunol.* 6: 127–35.
3. Anderson, G., P. J. Lane, and E. J. Jenkinson. 2007. Generating intrathymic microenvironments to

establish T-cell tolerance. *Nat. Rev. Immunol.* 7: 954–63.

4. Sarang, Z., É. Garabuczi, G. Joós, B. Kiss, K. Tóth, R. Rühl, and Z. Szondy. 2013. Macrophages engulfing apoptotic thymocytes produce retinoids to promote selection, differentiation, removal and replacement of double positive thymocytes. *Immunobiology* 218: 1354–1360.

5. Anderson, G., E. Jenkinson, N. Moore, and J. Owen. 1993. MHC class II-positive epithelium and mesenchyme cells are both required for T-cell development in the thymus. *Nature* 362: 70–73.

6. Rossi, F. M., S. Y. Corbel, J. S. Merzaban, D. A. Carlow, K. Gossens, J. Duenas, L. So, L. Yi, and H. J. Ziltener. 2005. Recruitment of adult thymic progenitors is regulated by P-selectin and its ligand PSGL-1. *Nature immunology* 6: 626–34.

7. Brocker, T. 1999. The role of dendritic cells in T cell selection and survival. *J. Leukoc. Biol.* 66: 331–5.

8. Klein, L., B. Kyewski, P. M. Allen, and K. A. Hogquist. 2014. Positive and negative selection of the T cell repertoire: what thymocytes see (and don't see). *Nat. Rev. Immunol.* 14: 377–91.

9. Matloubian, M., C. Lo, G. Cinamon, M. Lesneski, Y. Xu, V. Brinkmann, M. Allende, R. Proia, and J. Cyster. 2004. Lymphocyte egress from thymus and peripheral lymphoid organs is dependent on S1P receptor 1. *Nature* 427: 355–360.

10. Blackburn, C. C., and N. R. Manley. 2004. Developing a new paradigm for thymus organogenesis. *Nat. Rev. Immunol.* 4: 278–89.

11. Itoi, M., N. Tsukamoto, and T. Amagai. 2007. Expression of Dll4 and CCL25 in Foxn1-negative epithelial cells in the post-natal thymus. *International immunology* 19: 127–32.

12. Rossi, S. W., M.-Y. Y. Kim, A. Leibbrandt, S. M. Parnell, W. E. Jenkinson, S. H. Glanville, F. M. McConnell, H. S. Scott, J. M. Penninger, E. J. Jenkinson, P. J. Lane, and G. Anderson. 2007. RANK signals from CD4(+)3(-) inducer cells regulate development of Aire-expressing epithelial cells in the thymic medulla. *J. Exp. Med.* 204: 1267–72.

13. Akiyama, T., Y. Shimo, H. Yanai, J. Qin, D. Ohshima, Y. Maruyama, Y. Asaumi, J. Kitazawa, H. Takayanagi, J. M. Penninger, M. Matsumoto, T. Nitta, Y. Takahama, and J.-I. Inoue. 2008. The tumor necrosis factor family receptors RANK and CD40 cooperatively establish the thymic medullary microenvironment and self-tolerance. *Immunity* 29: 423–37.

14. Desanti, G. E., J. E. Cowan, S. Baik, S. M. Parnell, A. J. White, J. M. Penninger, P. J. Lane, E. J. Jenkinson, W. E. Jenkinson, and G. Anderson. 2012. Developmentally regulated availability of RANKL and CD40 ligand reveals distinct mechanisms of fetal and adult cross-talk in the thymus medulla. *J. Immunol.* 189: 5519–26.

15. Roberts, N. A., A. J. White, W. E. Jenkinson, G. Turchinovich, K. Nakamura, D. R. Withers, F. M. McConnell, G. E. Desanti, C. Benezech, S. M. Parnell, A. F. Cunningham, M. Paolino, J. M. Penninger, A. K. Simon, T. Nitta, I. Ohigashi, Y. Takahama, J. H. Caamano, A. C. Hayday, P. J. Lane, E. J. Jenkinson, and G. Anderson. 2012. Rank signaling links the development of invariant γδ T cell progenitors and Aire(+) medullary epithelium. *Immunity* 36: 427–37.

16. Rodewald, HR, S Paul, C Haller, H Bluethmann, and C Blum. 2001. Thymus medulla consisting of epithelial islets each derived from a single progenitor. *Nature* .

17. Rudd, Venturi, Li, Samadder, Ertelt, Way, Davenport, and Nikolich-Zugich. 2011. Nonrandom attrition of the naive CD8+ T-cell pool with aging governed by T-cell receptor:pMHC interactions. *Proceedings of the National Academy of Sciences* 108: 13694–13699.

18. Velardi, E., J. J. Tsai, A. M. Holland, T. Wertheimer, V. W. Yu, J. L. Zakrzewski, A. Z. Tuckett, N. V. Singer, M. L. West, O. M. Smith, L. F. Young, F. M. Kreines, E. R. Levy, R. L. Boyd, D. T. Scadden, J. A. Dudakov, and M. R. van den Brink. 2014. Sex steroid blockade enhances thymopoiesis by modulating Notch signaling. *J. Exp. Med.* 211: 2341–9.

19. Akashi, Richie, Miyamoto, Carr, and Weissman. 2000. B Lymphopoiesis in the Thymus. *The Journal of Immunology* 164: 5221–5226.

20. Wu, L., M. Antica, G. R. Johnson, R. Scollay, and K. Shortman. 1991. Developmental potential of the earliest precursor cells from the adult mouse thymus. *The Journal of experimental medicine* 174: 1617–27.

21. Vargas, C. L., J. Poursine-Laurent, L. Yang, and W. M. Yokoyama. 2011. Development of thymic NK cells from double negative 1 thymocyte precursors. *Blood* 118: 3570–8.

22. Shortman, K, and L Wu. 1996. Early T lymphocyte progenitors. *Annual review of immunology* .

23. Lind, E. F., S. E. Prockop, H. E. Porritt, and H. T. Petrie. 2001. Mapping precursor movement through the postnatal thymus reveals specific microenvironments supporting defined stages of early lymphoid development. *J. Exp. Med.* 194: 127–34.

24. Rothenberg, EV, JE Moore, and MA Yui. 2008. Launching the T-cell-lineage developmental programme. *Nature Reviews Immunology* .

25. Klein, L., M. Hinterberger, G. Wirnsberger, and B. Kyewski. 2010. Antigen presentation in the thymus for positive selection and central tolerance induction. *Nature reviews. Immunology* 9: 833–44.

26. Tonegawa, S. 1983. Somatic generation of antibody diversity. *Nature* 302: 575–81.

27. Palmer, E., and D. Naeher. 2009. Affinity threshold for thymic selection through a T-cell receptor-co-receptor zipper. *Nat. Rev. Immunol.* 9: 207–13.

28. Hsieh, C.-S., H.-M. Lee, and C.-W. Lio. 2012. Selection of regulatory T cells in the thymus. *Nature Reviews Immunology* .

29. Barthlott, T., H. Kohler, and K. Eichmann. 1997. Asynchronous coreceptor downregulation after positive thymic selection: prolonged maintenance of the double positive state in CD8 lineage differentiation due to sustained biosynthesis of the CD4 coreceptor. *The Journal of experimental medicine* 185: 357–62.

30. Kyewski, B., and L. Klein. 2006. A central role for central tolerance. *Annual review of immunology* 24: 571–606.

31. Hozumi, K., C. Mailhos, N. Negishi, K. Hirano, T. Yahata, K. Ando, S. Zuklys, G. A. Holländer, D. T. Shima, and S. Habu. 2008. Delta-like 4 is indispensable in thymic environment specific for T cell development. *The Journal of experimental medicine* 205: 2507–2513.

32. Plotkin, J., S. E. Prockop, A. Lepique, and H. T. Petrie. 2003. Critical role for CXCR4 signaling in progenitor localization and T cell differentiation in the postnatal thymus. *Journal of immunology (Baltimore, Md. : 1950)* 171: 4521–7.

33. Benz, C., K. Heinzel, and C. C. Bleul. 2005. Homing of immature thymocytes to the subcapsular microenvironment within the thymus is not an absolute requirement for T cell development. *European journal of immunology* 34: 3652–63.

34. Murata, S., K. Sasaki, T. Kishimoto, S.-I. Niwa, H. Hayashi, Y. Takahama, and K. Tanaka. 2007. Regulation of CD8+ T cell development by thymus-specific proteasomes. *Science (New York, N.Y.)* 316: 1349–53.

35. Nakagawa, T, W Roth, P Wong, A Nelson, and A Farr. 1998. Cathepsin L: critical role in Ii degradation and CD4 T cell selection in the thymus. *Science* .

36. Honey, K., T. Nakagawa, C. Peters, and A. Rudensky. 2002. Cathepsin L regulates CD4+ T cell selection independently of its effect on invariant chain: a role in the generation of positively selecting peptide ligands. *The Journal of experimental medicine* 195: 1349–58.

37. Gommeaux, J., C. Grégoire, P. Nguessan, M. Richelme, M. Malissen, S. Guerder, B. Malissen, and A. Carrier. 2009. Thymus-specific serine protease regulates positive selection of a subset of CD4+ thymocytes. *Eur. J. Immunol.* 39: 956–64.

38. Derbinski, J., A. Schulte, B. Kyewski, and L. Klein. 2001. Promiscuous gene expression in medullary thymic epithelial cells mirrors the peripheral self. *Nature immunology* 2: 1032–9.

39. Waterfield, M., I. S. Khan, J. T. Cortez, U. Fan, T. Metzger, A. Greer, K. Fasano, M. Martinez-Llordella, J. L. Pollack, D. J. Erle, M. Su, and M. S. Anderson. 2014. The transcriptional regulator Aire coopts the repressive ATF7ip-MBD1 complex for the induction of immunotolerance. *Nat. Immunol.* 15: 258–65.

40. Sansom, S. N., N. Shikama-Dorn, S. Zhanybekova, G. Nusspaumer, I. C. Macaulay, M. E. Deadman, A. Heger, C. P. Ponting, and G. A. Holländer. 2014. Population and single-cell genomics reveal the Aire dependency, relief from Polycomb silencing, and distribution of self-antigen expression in thymic epithelia. *Genome Res.* 24: 1918–31.

41. Tykocinski, L.-O. O., A. Sinemus, E. Rezavandy, Y. Weiland, D. Baddeley, C. Cremer, S. Sonntag, K. Willecke, J. Derbinski, and B. Kyewski. 2010. Epigenetic regulation of promiscuous gene expression in thymic medullary epithelial cells. *Proceedings of the National Academy of Sciences of the United States of America* 107: 19426–31.

42. Derbinski, J., J. Gäbler, B. Brors, S. Tierling, S. Jonnakuty, M. Hergenhahn, L. Peltonen, J. Walter, and B. Kyewski. 2005. Promiscuous gene expression in thymic epithelial cells is regulated at multiple levels. *The Journal of experimental medicine* 202: 33–45.

43. Villaseñor, J., C. Benoist, and D. Mathis. 2005. AIRE and APECED: molecular insights into an autoimmune disease. *Immunological reviews* 204: 156–64.

44. Unknown. 1997. An autoimmune disease, APECED, caused by mutations in a novel gene featuring two PHD-type zinc-finger domains. *Nature genetics* 17: 399–403.

45. Kuroda, N., T. Mitani, N. Takeda, N. Ishimaru, R. Arakaki, Y. Hayashi, Y. Bando, K. Izumi, T. Takahashi, T. Nomura, S. Sakaguchi, T. Ueno, Y. Takahama, D. Uchida, S. Sun, F. Kajiura, Y. Mouri, H. Han, A. Matsushima, G. Yamada, and M. Matsumoto. 2005. Development of autoimmunity against transcriptionally unrepressed target antigen in the thymus of Aire-deficient mice. *Journal of immunology (Baltimore, Md. : 1950)* 174: 1862–70.

46. Starr, T. K., S. C. Jameson, and K. A. Hogquist. 2003. Positive and negative selection of T cells. *Annual review of immunology* 21: 139–76.

2 Aim of Thesis

The work presented in this thesis is centered on the development and maturation of the epithelial compartment in the murine thymus and consequently its functional capacity to promote normal thymopoiesis. Two main aspects have been investigated in depth:

1. The role of the Dicer in thymic epithelial cell development and function

The endoribonuclease Dicer is critically required for the processing of most miRNA, a class of evolutionary conserved non-coding RNA that plays an important role in transcriptional regulation. The aim of the present study was to investigate the role of Dicer, and hence miRNA in general, in thymic epithelial cell development during embryogenesis and its function in maintaining thymopoiesis in the adult mouse. Specifically, I wished to investigate: A) the requirement of Dicer for TEC development, lineage specification and maintenance; B) the transcriptional changes upon a loss of Dicer expression targeted to the thymic epithelia and its consequences for thymic function; and C) the competence of T lymphocytes educated by a Dicer-deficient epithelial scaffold.

2. The capacity of β5t-expressing progenitor cells to form the cortical and medullar thymic epithelial compartments

Results obtained from a mouse experimental model that allows for conditional lineage tracing at early stages of thymic development suggested that most (if not all) thymic epithelial cells display hallmarks of having once adopted features characteristic of a cortical epithelial phenotype, i.e. the expression of the thymoproteasome subunit β5t. I extended these findings to probe: A) the precise timepoint of β5t expression during thymic epithelial development; B) the phenotype of β5t-expressing progenitor cells; C) the activity of β5t-expressing progenitor cells in later stages of thymus development; and D) the regenerative capacity of those cells in the post-natal thymus.

Taken together, these two research programs will provide unprecedented insight into the spatio-temporal dynamics of thymic epithelial cell development and function.

3 Results

3.1 miRNAs control the maintenance of thymic epithelia and their competence for T lineage commitment and thymocyte selection

3.1.1 Introductory notes

3.1.1.1 Summary

Since the discovery of RNA interference (RNAi) in the 1998, interest in the biological role of non-coding RNA has continuously grown. In this context, the evolutionary conserved class of microRNA (miRNA) has attracted special attention. miRNA are a class of small, non-coding RNA and are generated through the post-transcriptional processing of miRNA precursor sequences by the RNA-endonuclease-complexes Drosha/DGCR8 in the nucleus and then Dicer/AGO2 in the cytoplasm. After processing, the ensuing miRNA are then transported and incorporated into the RNA-induced silencing complexes (RISC), which execute RNA-interference. miRNA have been identified to play an important role in the transcriptional regulation during development. Hence, I was interested to investigate the role of Dicer in TEC for thymic organogenesis and maintenance of function. Using a conditional cre/lox system, Dicer was deleted in thymic epithelia as early as embryonic day of development (E) 12.5 using conditional Dicer alleles and the expression of the Cre recombinase under the transcriptional control of the Foxn1 locus. This deletion resulted in a marked reduction of individual miRNA, which could be detected at E16 and later developmental stages. Interestingly, the apparent loss of Dicer expression did not perturb thymic organogenesis but altered both the postnatal development and maintenance of the organ, resulting in a decreased thymic cellularity as early as the first week of life. This change was caused by a progressive loss of developing T lymphocytes consequent to a partial block in thymus positive selection. This limitation suggested a deficiency in the capacity of cTEC to provide an environment appropriate for this essential step in thymocyte maturation. In addition, the commitment of hematopoietic progenitor cells to a T cell fate was affected and paralleled an increased in-situ development of B cells. This deficiency to establish the T cell lineage in lieu of B lymphogoiesis correlated with a decreased expression on cTEC of Dll4, a Notch ligand critically for the commitment to a T cell fate. On closer

examination, further differences in the composition of the thymic epithelial compartment could be observed in mice deficient in Dicer expression in their TEC. For example, the expansion of the mTEC compartment, a feature typically observed in the first weeks of life, was largely absent. Moreover, immature ($MHCII^{lo}$) mTEC were especially affected suggesting a partial though progressive maturational block in mTEC differentiation from a yet to be phenotypically precisely defined TEC progenitor (see chapter 3.4). Mature mTEC revealed a higher proliferation rate as revealed by increased BrdU incorporation. The apparent dysbalance between immature and mature mTEC may reflect a progressive exhaustion of a mTEC-committed precursor pool or, alternatively, could be the consequence of a failure in differentiation accompanied by a compensatory increase in the maintenance of mature mTEC by way of proliferation. Mice three weeks and older revealed a lack of mTEC characteristic markers in the medullar including cytokeratins 5 and 14 that resulted in large supposedly mTEC-free areas in the thymic medullas of these mice. In parallel, an extensive loss of TEC density could be observed within the cortical scaffold, marking the functional disintegration of the dense cortex. The loss of Dicer resulted in a marked transcriptomic change in two-week-old cTEC and mTEC. A gene ontology analysis of up- and downregulated transcripts predicted multiple cellular processes affected in cTEC and mTEC, including transcription, cell signaling, differentiation, adhesion, apoptosis, and the organization of extracellular matrix. In spite of the lack of precise miRNA target prediction algorithms it became evident that the broad loss of miRNA resulted in a transcriptomic imbalance in TEC that affected critical pathways.

T cell selected in a microenvironment composed of TEC deficient in Dicer expression failed to cause overt autoimmunity even in 30-week-old mice. However, the thymic generation and export of regulatory T cells during the first weeks of life establish a peripheral T cell pool able to keep newly emerging auto-reactive T cells under control and thus disease-free. To avoid this protective mechanism and to uncover the auto-reactive potential of T cells selected by TEC devoid of Dicer expression, T cells were depleted in vivo in two-week-old mutant mice. The screening of these mice revealed mononuclear infiltrates in several organs of treated mice once the

peripheral T cell pool was re-established. Hence, central T cell tolerance induction was defective in these animals. To correlate these findings with a lack in regular negative selection against self-antigens, mTEC from 2 week old mutant mice were screened for the expression of Aire-dependent and –independent TRA. In the absence of miRNA transcripts individual TRA were either decreased or increased, thus suggesting a change in the repertoire of self representation by TEC. This alteration likely accounted (at least in part) for a defective negative selection of autoreactive T cells.

Taken together these results reveal a critical requirement for Dicer, and therefore miRNA, for postnatal TEC development, maintenance and function. We therefore hypothesise that a change in normal TRA expression in mTEC at a time of critical thymic growth fails to enforce regular central T cell tolerance induction allowing for auto-reactive T cells to escape selection and to exit to the periphery where these cells may harm peripheral organs. It remains, however, to be defined, which miRNA secure regular mTEC function under physiological conditions. This issue will need to be investigated using experimental mouse models in which single miRNA (clusters) are deleted in TEC, which will only be able once single, potentially functionally relevant miRNA can be identified. Unfortunately, current miRNA target prediction algorithms fail to precisely identify key miRNA that account for the functionally relevant transcriptomic changes observed in cTEC and mTEC upon the loss of Dicer. Therefore more work will have to be conducted in order to find the miRNA molecules that control key TEC features.

3.1.1.2 Contribution

The work described above was published in 2012 in the Journal of Immunology (PMID:22972926) and reflects a body of work to which several have contributed. I was responsible for the analysis of TEC cellularity at distinct developmental stages (Figure 1A; Supplementary Figure 1B), for the flowcytometric characterization of the distinct TEC subpopulations (Figures 3C,E-F; Supplementary Figures 1C, 3B), for the assessment of thymic and splenic T and B cell development (Figures 1E-F, 2A, 4A-B,

6A-B; Supplementary Figures 1D, 3C), for the analyses of thymic, adrenal, occular, kidney, pancreatic, liver, salivary gland and skin tissue sections (Figures 3A-B *lower panels*, 7A; Supplementary Figures 1A *lower panels*, 3A *lower panels*, 3D) and their scoring (Figure 7A). I quantified the changes of miRNA expression during embryonic development following the ablation of Dicer (Figure 1D). I assisted in the preparation of cells for and analysis of gene expression profiles (Figure 5), the transplantation of embryonic thymic lobes (Supplementary Figure 3) and the in vivo depletion of T cells (Figure 7A). These contributions were considered significant so that I was acknowledged as a co-first author of the work published.

3.1.1.3 Authors and affiliations in the publication

Saulius Zuklys [*1], **Carlos E. Mayer** [*1], Saule Zhanybekova [*], Heather Stefanski [†], Gretel Nusspaumer [*], Jason Gill [*], Thomas Barthlott [*], Stephan Chappaz [‡], Takeshi Nitta [§], James Dooley [¶], Ruben Nogales-Cadenas [||], Yousuke Takahama [§], Daniela Finke [‡], Adrian Liston [¶], Bruce R. Blazar [†], Alberto Pascual-Montano [||] and Georg A. Holländer [*,#]

[*] Pediatric Immunology, Department of Biomedicine, University of Basel, and The Basel University Children's Hospital, Basel, Switzerland

[†] Cancer Center and Department of Pediatrics, Division of Blood and Marrow Transplantation, University of Minnesota, Minneapolis, USA

[‡] Developmental Immunology, Department of Biomedicine, University of Basel, and The Basel University Children's Hospital, Basel, Switzerland

[§] Division of Experimental Immunology, University of Tokushima, Japan

[¶] Autoimmune Genetics Laboratory, VIB and University of Leuven, Leuven, Belgium

|| Functional Bioinformatics Group, National Center for Biotechnology-CSIC , Universidad Autónoma de Madrid , Madrid, Spain

Developmental Immunology, Department of Paediatrics, University of Oxford, Oxford, United Kingdom

1 Contributed equally to the work

3.1.2 Abstract

Thymic epithelial cells provide unique cues for the life-long selection and differentiation of a repertoire of functionally diverse T cells. Rendered miRNA deficient, these stromal cells in the mouse lose their capacity to instruct the commitment of haematopoietic precursors to a T cell fate, to effect thymocyte positive selection and to achieve promiscuous gene expression required for central tolerance induction. Over time, the microenvironment created by miRNA-deficient thymic epithelia assumes the cellular composition and structure of peripheral lymphoid tissue where thympoiesis fails to be supported. These findings emphasize a global role for miRNA in the maintenance and function of the thymic epithelial cell scaffold and establish a novel mechanism how these cells control peripheral tissue antigen expression to prompt central immunological tolerance.

3.1.3 Introduction

The thymus provides a unique stromal microenvironment that instructs the differentiation of blood-borne precursors to functionally mature T lymphocytes proficient to effect an immune response against microbial pathogens whilst unable to elicit an autoimmune reaction (1). The major structural components of the thymus are thymic epithelial cells (TEC) that can further be classified as cortical (c) or medullary (m) TEC subpopulations based on distinct structural, antigenic and

functional features (2,3). The molecular programs that control TEC growth, differentiation, and maintenance are, however, only incompletely characterized.

The most immature T cell precursors differentiate within the thymic cortex where they acquire the expression of both CD4 and CD8 (double positive, DP stage of development) and eventually express the complete $\alpha\beta$ T cell antigen receptor (TCR) (4). As their antigen specificity is randomly generated, DP thymocytes are subjected to a selection process aimed at testing their suitability for a given individual. Known as positive selection, thymocytes with a TCR that recognizes self-peptide/MHC complexes on cTEC with sufficient affinity will continue their intrathymic maturation and migrate to the medulla. There, thymocytes are exposed to a negative selection. This process purges TCR-bearing cells with an affinity for self-peptide/MHC complexes above a critical threshold and thus prevents self-antigen recognition by T cells of extra thymic tissue which may elicit autoimmunity.

Micro RNA (miRNA) represent an essential class of small (19-25 nucleotides, nt), non-coding RNAs indispensible for biological processes including cell fate determination, self-renewal, differentiation, proliferation, apoptosis and cellular homeostasis (5). Primary miRNA transcripts are processed by nuclear RNAse III enzyme Drosha and its co-factor DGCR8 to intermediate miRNAs, which are exported to the cytoplasm. There, a second RNAse III enzyme, designated Dicer, catalyzes the formation of miRNA duplexes. These short sequences are integrated into the RNA-induced silencing complexes (RISC) and control protein synthesis by interacting with target messenger RNA either repressing translation or mediating RNA cleavage and degradation (6). A single miRNA species may regulate the expression of hundreds of proteins, though the repression is usually mild and frequently the result of both downregulation of mRNA levels and inhibition of translation (7-9). Cell- and tissue-specific miRNA expression patterns have been identified, suggesting unique biological roles for specific miRNA. However, the precise functions for almost all of the at least 1055 mouse miRNA remain to be experimentally verified (10). To judge the global role of miRNA for the

development, function and homeostasis of TEC, we generated mice with a TEC targeted Dicer deficiency.

3.1.4 Results

3.1.4.1 Thymus cellularity and T lymphopoietic activity are decreased in the absence of Dicer expression in TEC

To study the integrated and global role of miRNA in TEC development and function, we generated mice that lack *dicer1* expression in thymic epithelia. For this purpose, mice with a conditional *dicer1* allele (Dicer$^{fl/fl}$, (14)) were crossed to transgenic animals expressing the Cre recombinase in all TECs (15). Because Cre expression in heterozygote Foxn1-Cre transgenic mice is non-toxic to TECs (Supplemental Fig. 1 and ref (16)), Dicer$^{fl/fl}$ mice negative for the expression of Cre were used as controls and compared to heterozygous Cre-transgenic Dicer$^{fl/fl}$ mice (designated Foxn1-Cre::Dicer$^{fl/fl}$). Thymus cellularity was unaffected in fetal and early post-natal Foxn1-Cre::Dicer$^{fl/fl}$ mice despite a complete deletion of the *dicer1* locus and the absence of distinct miRNA species in TEC at day 16.5 of gestation (E16.5) (Fig. 1A, 1B, 1D). A significant reduction in thymus size and absolute cell number was first observed in three week old Foxn1-Cre::Dicer$^{fl/fl}$ mice (Fig. 1A, 1C). In contrast, changes in intrathymic T cell differentiation were already apparent in Foxn1-Cre::Dicer$^{fl/fl}$ mice as early as the first week of life (Fig. 1E, 1F). While the frequency of double negative (DN) cells was increased, CD4^{-}CD8^{+} single positive (SP) thymocytes with a mature phenotype (CD24^{lo}CD3^{hi}) were diminished. At 3 weeks and later, the relative frequency of double positive (DP) thymocytes was consistently increased though all subsequent maturational stages were diminished (Fig. 1E, 1F). By 30 weeks of age, DP thymocytes were almost completely absent in Foxn1-Cre::Dicer$^{fl/fl}$ mice . The competence of Dicer-deficient TEC to support regular T cell development was thus progressively compromised affecting both the generation of DP thymocytes and their subsequent maturation to single positive, naïve T cells.

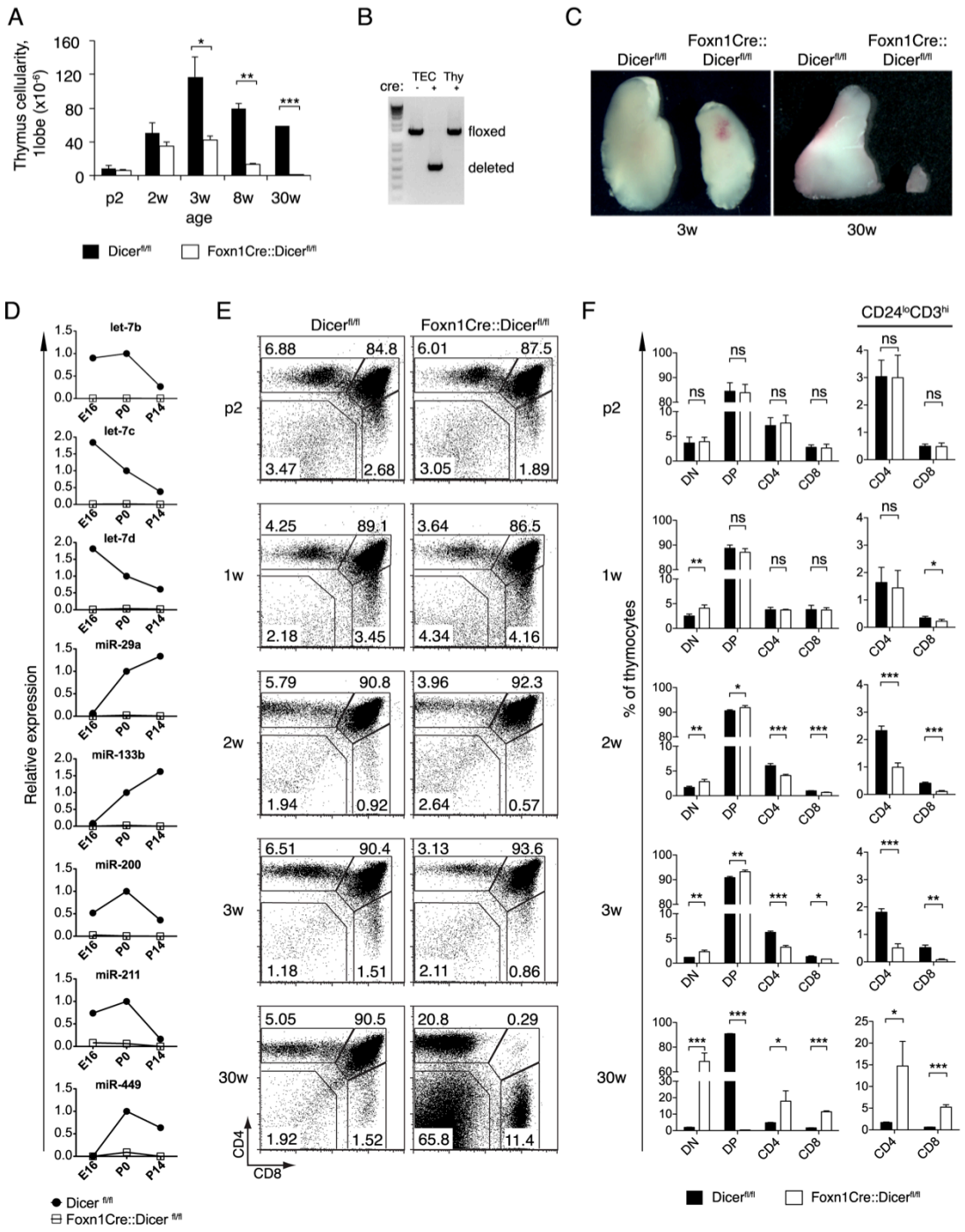

Figure 3.1-1. *Reduced thymic cellularity and gradual failure of T cell development in Foxn1-Cre::Dicer$^{fl/fl}$ mice.* (A) Total thymic cell numbers of Dicer$^{fl/fl}$ (black bars) and Foxn1-Cre::Dicer$^{fl/fl}$ (white bars) mice at indicated ages (p: post-natal days; w: weeks); *denotes p<0.05; ** p<0.01; *** p<0.001. (B) PCR-based detection of the conditional *dicer1* locus in purified thymocytes (Thy) and TECs from Dicer$^{fl/fl}$ (*cre* -) and Foxn1-Cre::Dicer$^{fl/fl}$ (*cre*+) embryos at day 16.5 (E16.5). (C) Macroscopic analysis of single thymus lobes from 3 and 30 week old Dicer$^{fl/fl}$ and Foxn1-Cre::Dicer$^{fl/fl}$ mice. (D) Decreased miRNA expression in TECs from Foxn1-Cre::Dicerfl/fl mice. TECs (CD45-EpCAM+) were isolated by cell sorting from Dicerfl/fl (closed circles) and Foxn1-Cre::Dicerfl/fl (open squares) mice at the indicated ages and were subjected to quantitative RT-PCR analysis using primers specific for the indicated mature miRNAs. Small nuclear RNA U6 was used as an endogenous control. Data were normalized to the expression of miRNA in newborn (P0) Dicerfl/fl mice. (E) Flow cytometric analysis for the cell surface expression of CD4 and CD8 on thymocytes isolated from Dicer$^{fl/fl}$ and Foxn1-Cre::Dicer$^{fl/fl}$ mice at indicated ages.

Numbers denote the percentage of cells within the given gates in a representative experiment. (F) Frequencies of thymocyte subpopulations (left panel) and of mature (i.e. $CD3^{hi}CD24^{lo}$) CD4 and CD8 single positive thymocytes (right panel) in $Dicer^{fl/fl}$ (black bars) and Foxn1-Cre::$Dicer^{fl/fl}$ mice (white bars) at indicated ages. Data signify the mean ± SD; ns, not significant; *denotes $p<0.05$; ** $p<0.01$; *** $p<0.001$. Data are representative of at least two independent experiments for each time point with at least three mice per group.

3.1.4.2 Commitment to the T cell lineage requires Dicer expression in cTEC

We next investigated the nature of the $CD4^{-}CD8^{-}$ thymocytes as these cells were already increased in Foxn1-Cre::$Dicer^{fl/fl}$ mice as early as 1 week of age and represented more than half of all the thymocytes in 30 week old mutant animals (Fig. 1E). The screening of these cells for the expression of non-T cell lineage markers identified a relative and absolute increase of $CD19^{+}$ cells (Fig. 2A). Although a substantial proportion of these cells expressed high levels of CD93 similar to the pattern observed for B cells in the bone marrow of both wild type and mutant mice (Fig. 2A) , they did not express IgM. We therefore conclude that these were immature thymic B cells that developed in situ, possibly due to changes in the microenvironment. Indeed the thymic medulla progressively displayed increased numbers of Lyve-1^{+} lymphatic vessels, $PNAd^{+}$ high endothelial venules and CR-1^{+} follicular dendritic cells (Fig. 2B), that in aggregate resulted in older animals in a histological structure reminiscent of secondary lymphoid tissue.

Since commitment to a T cell fate is dependent on Dll4 expression by cTEC (17), we next tested whether Foxn1-Cre::$Dicer^{fl/fl}$ mice lacked the correct expression of $Dll4^{+}$. The relative frequency and absolute cell number of $Dll4^{+}$ cTEC was halved in 3 week old Foxn1-Cre::$Dicer^{fl/fl}$ mice when compared to controls (Fig. 2C). The relative frequency of early thymic progenitors (ETP, defined as $Lin^{-}CD25^{-}CD44^{hi}$c-kit^{+} cells) among thymocytes was in parallel decreased by two-fold when compared to age-matched controls (0.02±0.011 vs 0.04±0.017; $p<0.05$, n=4). Thus, Dicer deficient TECs created an altered microenvironment reduced in the molecular cues critical for the attraction of early thymic progenitors and their commitment to the T cell lineage.

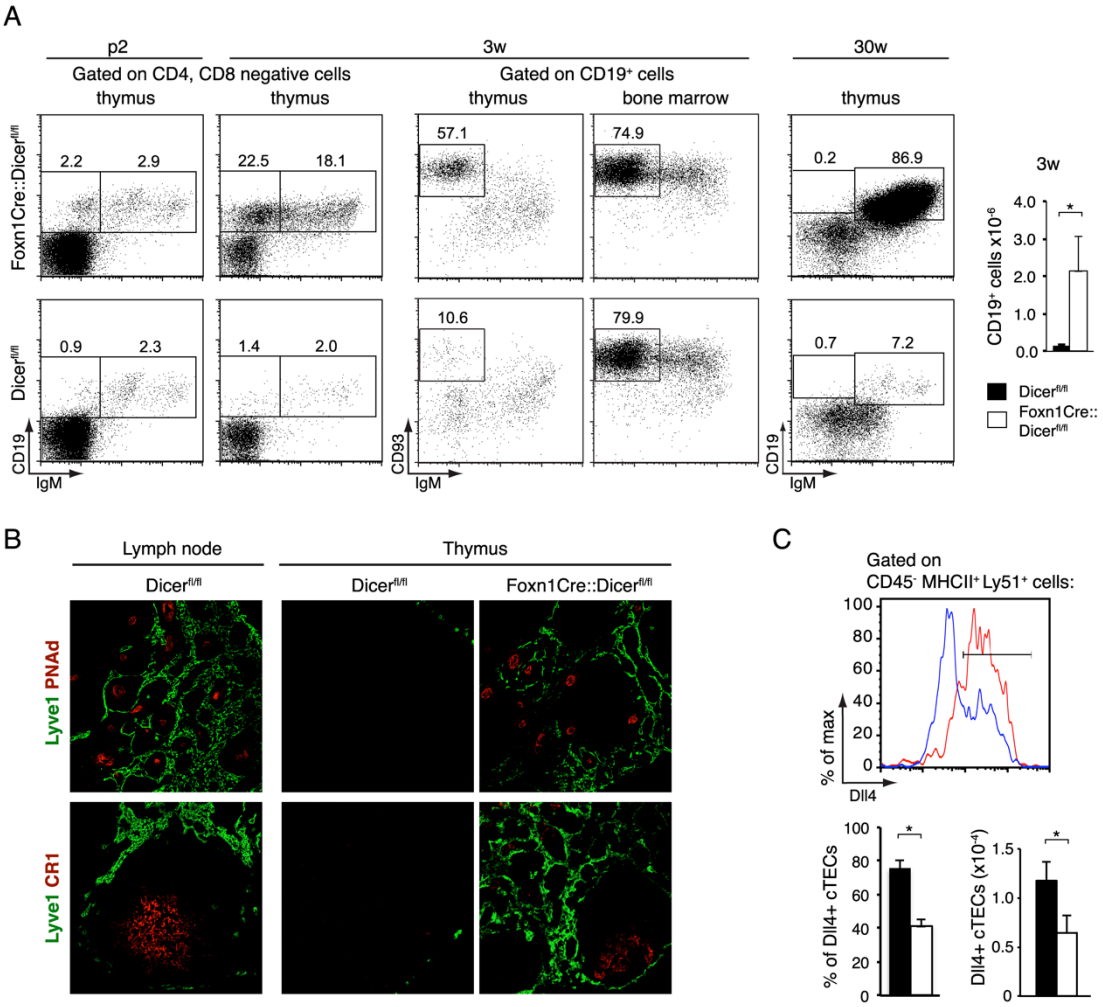

Figure 3.1-2. *Dicer-deficient TEC create a microenvironment permissive for in-situ B-cell development.* (A) Left panels: Flow cytometry of $CD4^{-}CD8^{-}$ double negative cells from thymus and bone marrow for the expression of CD19, IgM, and CD93. Numbers denote the frequency observed in a representative experiment for each of the indicated subpopulations. Right panel: Absolute numbers of thymic $CD19^{+}$ cells in 3 week old $Dicer^{fl/fl}$ (black bars) and Foxn1-Cre::$Dicer^{fl/fl}$ (white bars) mice. * denotes $p<0.05$. Three independent experiments with at least 3 mice per group were performed. (B) Immunofluorescence analysis of lymph node and thymus tissue from 30 week old mice for the expression of lymphatic vessel endothelial hyaluronan receptor Lyve-1 (identifying lymphatics), peripheral lymph node addressin PNAd (staining high endothelial venules) and complement receptor CR1 (detecting follicular dendritic cells). Data are representative of at least two separate experiments using each two mice each. (C) FACS analysis of Delta-like 4 (Dll4) expression by cTEC ($CD45^{-}MHCII^{+}UEA\text{-}1^{-}Ly51^{+}$) in 3 week old $Dicer^{fl/fl}$ (red line) and Foxn1-Cre::$Dicer^{fl/fl}$ (blue line) mice (upper panel); relative frequency and cellularity of $Dll4^{+}$ cTEC (lower panels); Data signify the mean ± SD; *denotes $p<0.05$. Two independent experiments with at least 3 mice per group were performed.

3.1.4.3 Dicer-deficient TEC fail to maintain a regular thymic microenvironment

To further investigate the consequences a TEC-restricted loss of Dicer-dependent miRNA expression, control and mutant thymus tissue sections were analyzed for the composition and organization of their stroma. In 2 day and 3 week old mice of both

groups, histological analyses demonstrated well demarcated medullary islands surrounded by a cell-dense cortex (Fig. 1A and Supplemental Fig. 2). In 3 week old mutant mice, the cortical TEC network was however, less dense and, in contrary to the wild type thymus, mainly composed of cytokeratin (CK)5^{+}CK8^{+}, cTEC (MTS10^{-}). The thymic cortex of mutant mice had also changed in as much as its epithelia expressed lower amounts of Psmb11 (a.k.a. β5t), a cTEC-specific component of the thymoproteasome pivotal for the differentiation of MHC class I restricted CD8 SP thymocytes (18) (Fig. 3A, 3B). mTEC (CK5^{+}MTS10^{+}) were reduced in number and mostly located at the cortico-medullary junction. In parallel, ERTR7^{+} fibroblasts had accumulated in the presumed medulla where the few remaining mTEC were usually less reactive with UEA-1 though Aire^{+} epithelia and dendritic cells could still be detected (Fig. 3A and G.N., G.A.H unpublished observation).

The small thymus remnant detected in 30 week old Foxn1-Cre::Dicer$^{fl/fl}$ mice had lost its typical cortico-medullary organization and the few remaining TEC were now arranged in several solitary islands devoid of mTEC contributions (Fig. 3B). Though almost all of the epithelia displayed a cortical phenotype (CK8^{+}MTS10^{-}UEA-1^{-}), the expression of Psmb11 could not anymore be detected. The loss of Dicer expression differentially affected TEC cellularity of Foxn1-Cre::Dicer$^{fl/fl}$ mice, in contrast to absolute mTEC, both absolute and relative cTEC numbers of cTEC were increased (Fig. 3C), a change that correlated with a higher proliferation rate (Fig. 3D). Thus, a lack of Dicer expression in TEC progressively precludes the normal differentiation, patterning, maintenance and function of these cells.

To assess whether miRNAs are specifically required by TEC for MHC expression and their differentiation from immature (MCH^{lo}) to mature (MHC^{hi}) mTEC, we next analyzed TEC for their MHCII expression and mTEC for the detection of the autoimmune regulator (Aire). Both cTEC and mTEC from Foxn1-Cre::Dicer$^{fl/fl}$ and Dicer$^{fl/fl}$ mice expressed comparable amounts of MHC class I and II molecules (Fig. 3E). However, the relative frequency of MHCII^{lo}Aire^{-} mTEC was reduced and that of MHCII^{hi}Aire^{-} and MHCII^{hi}Aire^{+} mTEC was increased in Foxn1-Cre::Dicer$^{fl/fl}$ mice. Thus, miRNAs appear to be required for the regular maintenance of MHCII^{lo} mTEC

but dispensable for their differentiation into MHCII^{hi}Aire^{+} mTEC, which express an array of peripheral tissue-specific antigens (PTA) and are critical for negative selection of maturing thymocytes (see below).

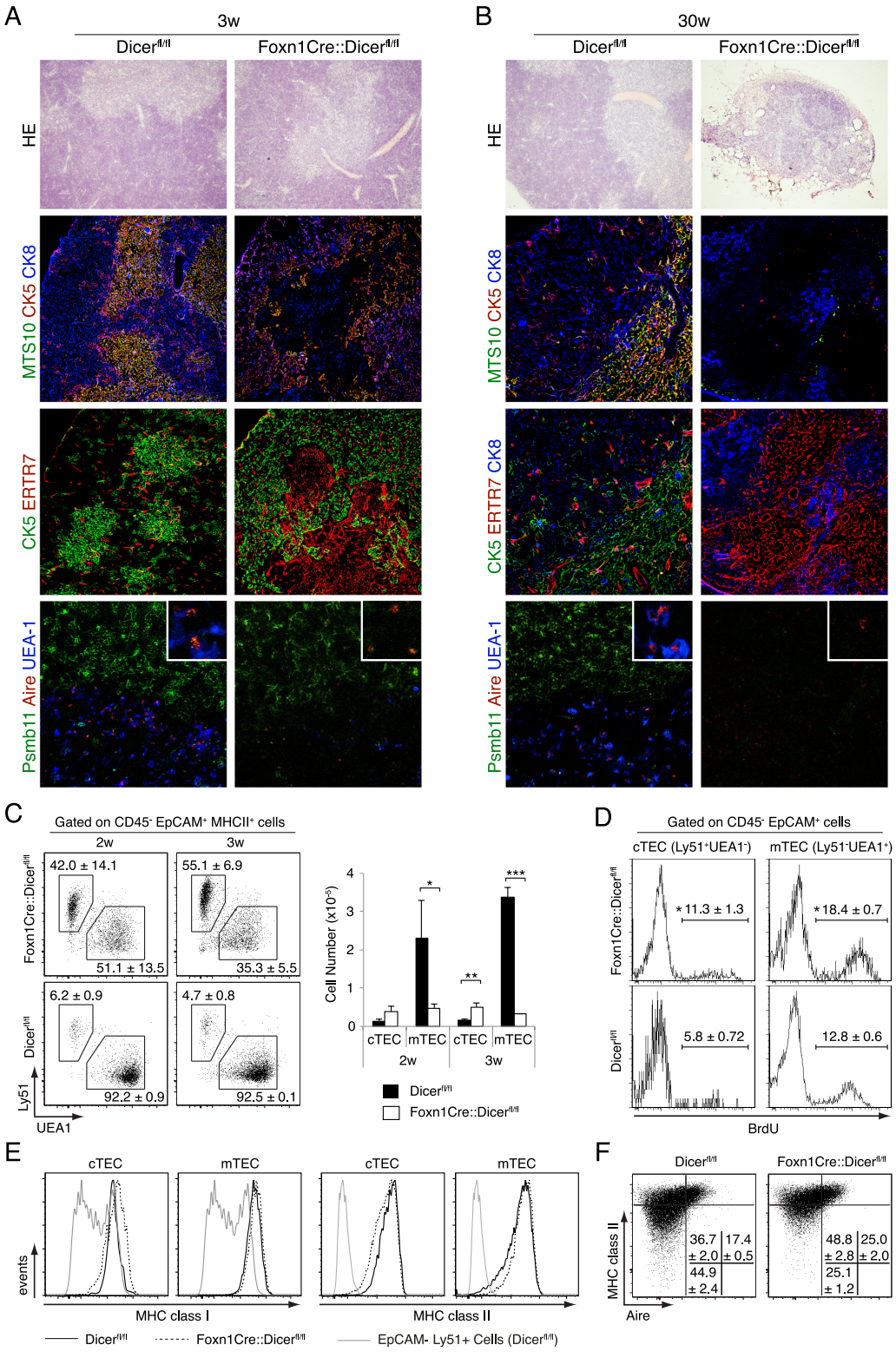

Figure 3.1-3. *Dicer deficient TEC fail to maintain a regular thymic microenvironment.* Hematoxilin and eosin (HE) staining (top row) and immunofluorescence analysis of thymic tissue sections from 3 week old (A) and 30 week old (B) Dicer$^{fl/fl}$ or Foxn1-Cre::Dicer$^{fl/fl}$ mice. For immunohistology, antibodies specific for ERTR7 were used to identify fibroblasts, CK8 and Psmb11 for the detection of cTEC, and MTS10, CK5, and Aire as well as reactivity with UEA-1 for the identification of mTEC. Original magnification 20x; the bottom panels display close-ups in the right upper corner. Data are representative of at least three separate experiments with at least two mice each. (C) Flow cytometric analysis of TEC (CD45-

EpCAM^{+}MHCII^{+}) subpopulations isolated from 2 and 3 week old mice. The relative frequency (left panels) and absolute cell numbers (right graph) of cTEC (UEA^{-}1-Ly51^{+}) and mTEC (UEA-1^{+}Ly51^{-}) in Dicer$^{fl/fl}$ (black bars) and Foxn1-Cre::Dicer$^{fl/fl}$ (white bars) mice are shown. Data indicate the mean ± SD of at least 3 mice per group; *denotes $p<0.05$; ** $p<0.01$; *** $p<0.001$. Data are representative of three independent experiments. (D) BrdU incorporation in cTEC and mTEC isolated from 2 week old Dicer$^{fl/fl}$ and Foxn1-Cre::Dicer$^{fl/fl}$ mice pulsed for 4 hours. The percentage of TEC incorporating the label (mean ± SD, *denotes $p<0.05$; 3 mice per group) is shown. Data are representative of at least two separate experiments. (E) MHC cell surface expression on Dicer deficient TEC. Cortical and medullary thymic epithelial cells from Dicer$^{fl/fl}$ (solid lines) and Foxn1-Cre::Dicer$^{fl/fl}$ (dotted lines) mice were stained for the cell surface expression of MHC class I (left panels) and MHC class II molecules (right panels) and analyzed by flow cytometry. The histograms are representative of two independent experiments with three mice per group. (F) Flow cytometric analysis of MHCII and autoimmune regulator (Aire) expression in TECs (CD45^{-}EpCAM^{+}) isolated from 2 week old mice. Numbers denote the percentage of cells (mean ± SD) within the given quadrant. The plots are representative of two independent experiments with three mice per group.

3.1.4.4 Dicer-deficient cTEC fail to impose efficient positive selection

Given the changes in cTEC we next investigated in Foxn1-Cre::Dicer$^{fl/fl}$ and control mice the sequential changes in thymocyte CD3 and CD69 cell surface expressions as phenotypic markers of positive selection (19). Under physiological conditions, positive selection sets off a transient up-regulation of CD69 among CD3^{int} DP thymocytes. In turn, these cells sequentially adopt a CD3^{hi}CD69^{+} and eventually a CD3^{hi}CD69^{-} cell surface phenotype. The relative frequencies of these distinct thymocyte populations were undisturbed in 1 week old Foxn1-Cre::Dicer$^{fl/fl}$ mice implying thymocyte positive selection to be normal (Fig. 4A). In contrast, 2 week and older mutant mice displayed a progressively compromised positive selection as the frequencies of their CD3^{int}CD69^{+} and CD3^{hi}CD69^{+} DP thymocytes were gradually reduced (Fig. 4A) despite an increased frequency of cTEC (Fig. 3C). To detail early post-selection steps in DP thymocyte differentiation, we also analyzed changes in CD4 and CD8 expression on either CD3^{int}CD69^{+} or CD3^{hi}CD69^{+} DP cells (Fig. 4B). Although the downregulation of CD8 on CD3^{int}CD69^{+} cells occurred normally in 1 and 2 week old Foxn1-Cre::Dicer$^{fl/fl}$ mice, this was impaired in 3 week old mutants (Fig. 4B, left panels). Focusing on younger Foxn1-Cre::Dicer$^{fl/fl}$ mice with a seemingly undisturbed cortical epithelial microenvironment, we also noticed a gradual defect in the progression of CD3^{hi}CD69^{+} DP thymocytes (via the intermediate CD8^{hi}CD4^{lo} stage) to cells with a mature SP CD8 phenotype (Fig. 4B, right panels). Thus, positive selection of DP thymocytes is significantly impaired in Foxn1-Cre::Dicer$^{fl/fl}$ mice as

early as the second week of life and is preceded by a defect in DP maturational progression towards the CD8 SP lineage.

Since Dicer-deficient mice express an impaired thymoproteasome (Fig. 3A), we next investigated the development of MHC class I restricted thymocytes expressing a T cell antigen receptor known to depend on Psmb11 expression for its efficient positive selection (20). For this purpose, sub-lethally irradiated neonatal Foxn1-Cre::Dicer$^{fl/fl}$ and Dicer$^{fl/fl}$ mice were engrafted with day 14 fetal liver cells from OT-I TCR transgenic mice. The OT-I TCR (composed of the Vα2 and V β5 chains) recognizes ovalbumin and is selected by self-peptides derived from β-catenin and other proteins (21). The selection of OT-I TCR transgenic thymocytes was severely compromised in chimeric Foxn1-Cre::Dicer$^{fl/fl}$ mice and this resulted in a significant reduction of cells with an immediate post-selection phenotype, i.e. CD4^{hi}CD8^{int} and CD4^{neg}CD8^{hi} (Fig. 4C). The partial block in positive selection resulted in parallel in an increase in pre-selection DP thymocytes and a concomitant reduction in OT-I transgenic T cells committed to the CD8 lineage (Fig. 4C, left and middle panel). Moreover, chimeric Foxn1-Cre::Dicer$^{fl/fl}$ mice displayed a reduced frequency of mature transgenic SP CD8 thymocytes expressing high surface Vα2 concentrations (Fig. 4C, right panel). Taken together, the absence of Dicer expression in TEC resulted in reduced positive thymocyte selection and an altered antigen receptor repertoire.

To test whether the thymus phenotype in Foxn1-Cre::Dicer$^{fl/fl}$ mice was affected by Foxn1-Cre mediated recombination in keratinocytes and consequent systemic influences, we transplanted embryonic thymic tissue from both Dicer$^{fl/fl}$ and Foxn1-Cre::Dicer$^{fl/fl}$ mice under the kidney capsule of a nu/nu recipients. Analysis of the grafted tissue 4 weeks after transplantation revealed a phenotype identical to that observed in age-matched Foxn1-Cre::Dicer$^{fl/fl}$ mice (Supplemental Fig.3A-C). This finding is in keeping with the observation that Foxn1-Cre::Dicer$^{fl/fl}$ mice have a normal skin (Supplemental Fig3D).

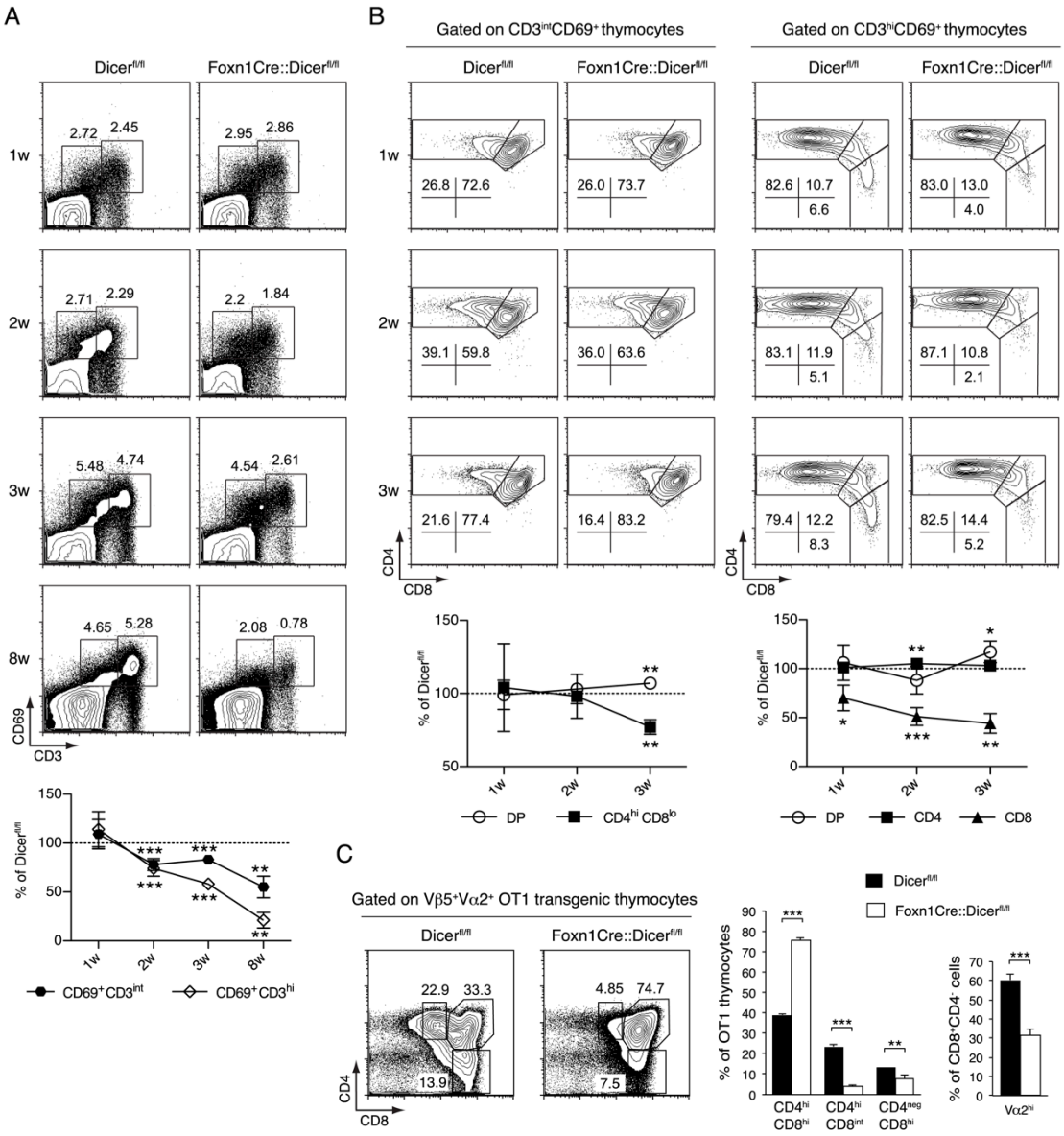

Figure 3.1-4. *Dicer expression in TECs is required for efficient thymocyte positive selection.* (A) Upper panels: Flow cytometric analysis was performed on all thymocytes excluding double negative cells isolated from Dicer$^{fl/fl}$ and Foxn1-Cre::Dicer$^{fl/fl}$ mice of indicated ages. Representative plots of CD69 and CD3 expression analyses of total thymocytes are shown. Lower graph: Changes in the relative frequency of CD69^{+}CD3^{int} and CD69^{+}CD3^{hi} thymocytes over time in Foxn1-Cre::Dicer$^{fl/fl}$ mice in comparison to Dicer$^{fl/fl}$ animals; ** indicates $p<0.01$; *** $p<0.001$. Data are representative of at least two separate experiments with three mice per group. (B) Representative plots of CD4 and CD8 expression analyses of CD69^{+}CD3^{int} (upper left panels) and CD69^{+}CD3^{hi} thymocytes (upper right panels). Lower left graph: Kinetic changes in the relative frequency of the DP and CD4^{+}CD8^{int} phenotypes among CD69^{+}CD3^{int} thymocytes in Foxn1-Cre::Dicer$^{fl/fl}$ mice when compared to Dicer$^{fl/fl}$ animals. Lower right graph: Kinetic changes in the relative frequency of the DP, SP CD4 and SP CD8 phenotypes among CD69^{+}CD3^{hi} thymocytes in Foxn1-Cre::Dicer$^{fl/fl}$ mice when compared to Dicer$^{fl/fl}$ animals. The data in the lower graphs shows the mean ± SD; *denotes $p<0.05$; ** $p<0.01$; *** $p<0.001$. The results are representative of 2 independent experiments with at least 3 mice per group. (C) Flow cytometric analysis of 4 week old Dicer$^{fl/fl}$ and Foxn1-Cre::Dicer$^{fl/fl}$ mice reconstituted at birth with OT-1 TCR transgenic fetal liver cells. Left panels: CD4 and CD8 expression on OT1 TCR transgenic thymocytes. The dot blot graphs are representative of at least three independent experiments. The bar graphs demonstrate the relative frequency of OT1 TCR transgenic CD4^{hi}CD8^{hi}, CD4^{hi}CD8^{int} and CD4^{-}CD8^{hi} cells in each gate of left

panels (left graph) and the relative frequency of $CD4^{-}CD8^{hi}$ thymocytes expressing high $V\alpha2^{+}$ cell surface amounts as an indicator of thymocyte positive selection (right graph). Black bars: $Dicer^{fl/fl}$ mice; white bars: Foxn1-Cre::$Dicer^{fl/fl}$ mice. The values represent mean ±SD with at least 3 mice per group; ** denotes $p<0.01$; *** $p<0.001$. Data are representative of at least 2 separate experiments with each three or more mice per group.

3.1.4.5 Gene expression analysis in Dicer-deficient TEC uncover miRNA-sensitive cellular processes

Gene expression profiles were established for both cortical and medullary TEC subpopulations to identify transcripts that are significantly up- or down-regulated as a consequence of Dicer deficiency (Fig. 5A, 5B). For this purpose, Foxn1-Cre::$Dicer^{fl/fl}$ and $Dicer^{fl/fl}$ mice were investigated at two weeks of age since the former animals still had a relatively intact cTEC cellularity though already displayed functional deficiencies. Gene Ontology (GO) analysis of significantly upregulated and downregulated transcripts (corrected $p<0.05$) predicted multiple cellular processes to be affected in cortical, medullary and both types of TEC (Fig. 5C, 5D). Specifically, transcription, cell signaling, differentiation, adhesion, apoptosis and the organization of extracellular matrix were predicted to be altered as a consequence of Dicer deficiency in TEC.

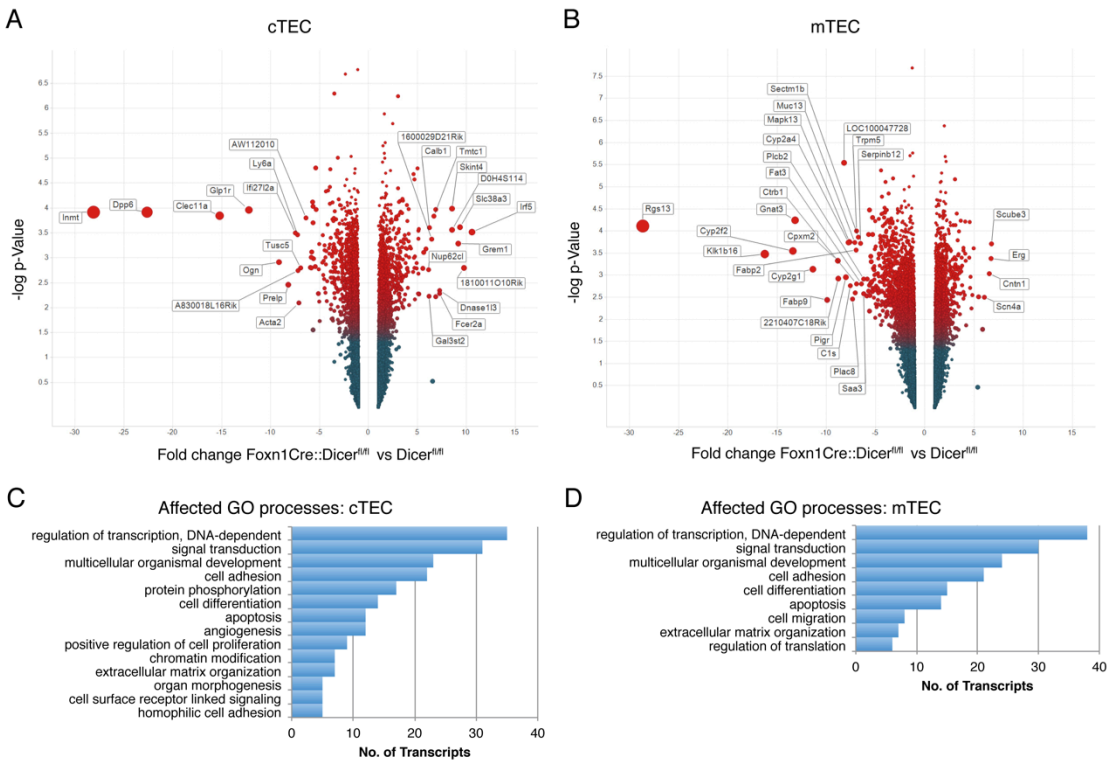

Figure 3.1-5. *Analysis of gene expression changes in Dicer-deficient TEC and its impact on cell signaling.* Volcano plot analysis of mRNA expression changes in cTEC (A) and mTEC (B) from two week old Foxn1-Cre::Dicer$^{fl/fl}$ mice compared to Dicer$^{fl/fl}$ mice. Positive values on the X-axis indicate an up-regulation of transcripts in mutant TEC presented as fold changes, whereas negative values specify down-regulated transcripts shown as fold changes. The Y-axis represents a log scale revealing the corrected p-value for a two-way analysis of variance of the differences between samples. The data represents two separate biological replicates with at least 10 mice per group. The bar graphs show gene ontology pathways significantly affected (corrected $p<0.05$) in cTEC (C) and mTEC (D), respectively.

3.1.4.6 Dicer-deficiency in TEC alters peripheral T cell phenotype

The lack of Dicer expression in TEC led to significant phenotypic changes among peripheral T cells. Both naïve CD4$^+$ and CD8$^+$ T cells (i.e. CD62L^{hi}CD44$^-$) were reduced in Foxn1-Cre::Dicer$^{fl/fl}$ mice at 8 weeks of age whilst the relative frequency of memory T cells was two- to three-fold more abundant, a finding likely caused by moderate T lymphopenia (Fig. 6A, 6B). Moreover, Foxn1-Cre::Dicer$^{fl/fl}$ mice displayed a proportional increase in CD8$^+$ effector (CD44^{hi}CD62L$^{low/-}$) and central memory (CD44^{hi}CD62L^{hi}) T cells. In keeping with the degree of lymphopenia, the relative frequency of FoxP3$^+$CD4$^+$ regulatory T cells was only modestly increased though their cellularity was not significantly different from that of Dicer$^{fl/fl}$ mice (Fig. 6C).

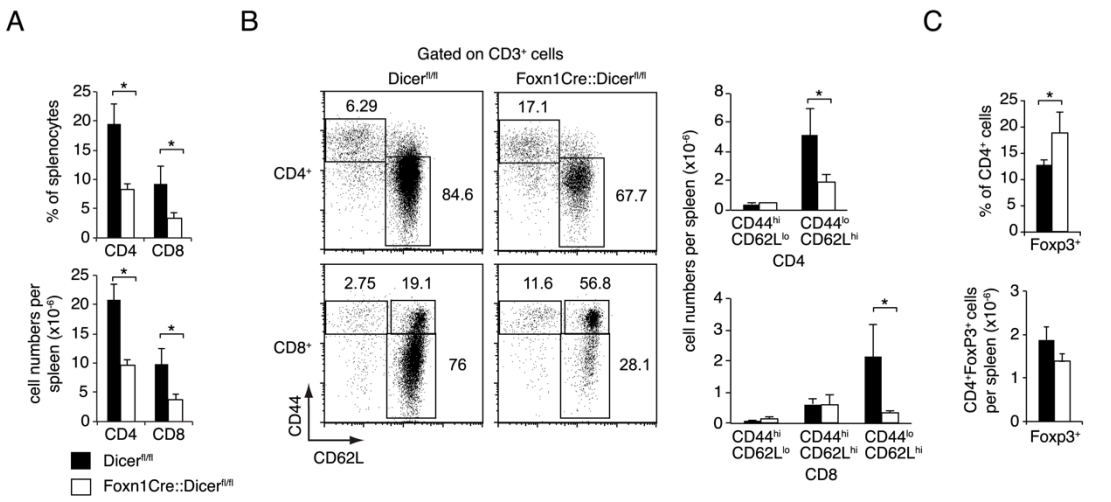

Figure 3.1-6. *Dicer deficiency in TECs results in altered T cell numbers.* (A) Relative frequencies and absolute cell numbers (mean ± SD) of splenic CD4 and CD8 T cells in 8 week old Dicerfl/fl (black bars) and Foxn1-Cre::Dicerfl/fl mice (white bars); * indicates $p<0.05$. Data are representative of three separate experiments with at least 3 mice per group. (B) Left panels: Representative analysis of CD44 and CD62L expression among splenic T cells from 8 week old Dicerfl/fl and Foxn1-Cre::Dicerfl/fl mice. The numbers show the relative frequency of a given subpopulation as identified by the drawn gate. Right graphs: Absolute numbers (mean ± SD) of T cells from 8 week old Dicerfl/fl (black bars) and Foxn1-Cre::Dicerfl/fl mice (white bars) with naïve and memory phenotypes; * indicates $p<0.05$. Data are representative of three separate experiments with at least 3 mice per group. (C) Relative frequency (upper graph) and absolute cell numbers (lower graph) of splenic CD4+Foxp3+ T cells in 8 week old Dicerfl/fl (black bars) and Foxn1-Cre::Dicerfl/fl mice (white bars); * indicates $p<0.05$. Data are representative of two separate experi- ments with at least 3 mice per group.

3.1.4.7 T cells selected in a thymus with Dicer deficient TEC elicit autoimmunity

We next examined whether T cells selected by Foxn1-Cre::Dicer$^{fl/fl}$ mice were prone to elicit autoimmunity since their selection was altered by thymic microenvironmental changes possibly resulting in a T cell repertoire with different functional properties. Although Foxn1-Cre::Dicer$^{fl/fl}$ mice were followed and regularly analyzed for as long as 45 weeks, spontaneous lymphocytic organ infiltrates were not observed at a frequency different to that of control mice (unpublished observations). As peripheral tolerance may have been maintained in Foxn1-Cre::Dicer$^{fl/fl}$ mice by T cells that had early on developed in a yet largely normal though already miRNA-deficient thymic epithelial microenvironment (22), mutant and wild type mice were efficiently T cell depleted at the age of 2 weeks using a mixture of anti-CD4, -CD8 and -Thy1.2 antibodies. In the course of autologous reconstitution, newly formed T cells were now selected in a thymic

microenvironment which in the case of Foxn1-Cre::Dicer$^{fl/fl}$ mice had adopted an altered architecture and had lost its capacity for normal TCR selection. Multi-organ infiltration developed in Foxn1-Cre::Dicer$^{fl/fl}$ but not control mice over the course of 28 weeks, variably affecting eyes, pancreas, salivary glands, and liver (Fig. 7A). The inflammatory cell infiltrations of the eyes altered the retinal architecture in its entire thickness leading to a partial destruction of the photoreceptor outer segment and the nuclear layer.

As thymic expression of self-antigens is critical for the maintenance of self tolerance, transcripts for selective single self-antigens were quantified in purified mTEC of 2 week old Foxn1-Cre::Dicer$^{fl/fl}$ and Dicer$^{fl/fl}$ mice (Fig. 7B, 7C). This time point had specifically been chosen since the relative frequency of MHCII^{hi}Aire^{+} mTEC was comparable for both mouse strains (Fig. 3F). A significant decrease in both Aire-dependent and -independent transcripts was detected with retinal (IRbp), salivary gland (Salivary protein 1, Spt1), hepatic (C-reactive protein, CRP) and pancreatic (Insulin-2, Ins2; Glutamic acid decarboxylase, Gad1) peripheral tissue antigens (PTA) invariably reduced in Dicer-deficient mTEC (Fig. 7B, 7C and 7D). These changes correlated with the pattern of tissue infiltrations linking defects in PTA expression to organ-specific autoimmune pathologies.

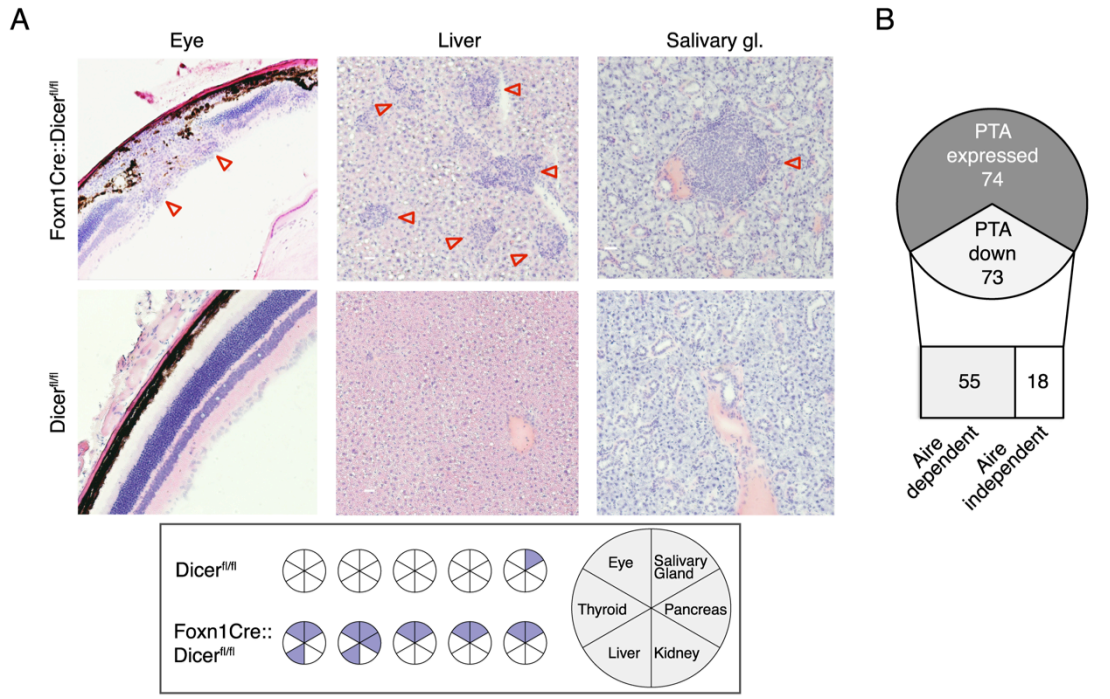

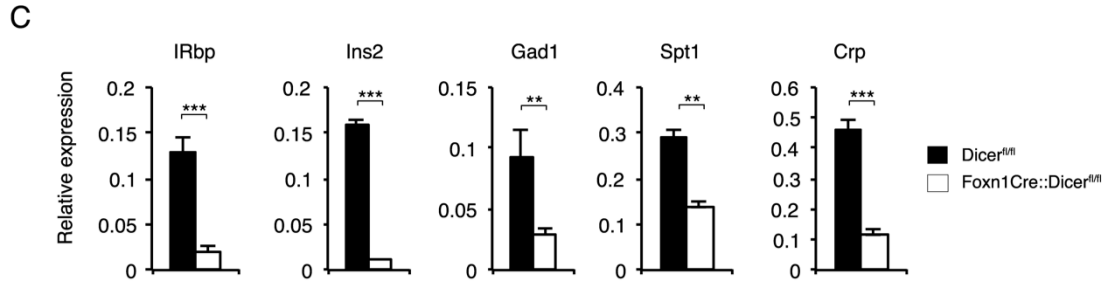

D

Gene	Fold Change	Aire Dep	Gene	Fold Change	Aire Dep	Gene	Fold Change	Aire Dep	Gene	Fold Change	Aire Dep	Gene	Fold Change	Aire Dep
Fabp9	8.6	no	Igf2	2.8	yes	Rptn	2.3	no	Mpo	1.9	yes	Mmp13	1.7	yes
Fabp2	7.3	yes	Mup4	2.7	yes	Pah	2.3	no	Klk6	1.9	yes	Slc5a1	1.6	yes
Fabp1	6.5	yes	Mcpt2	2.7	yes	Krt19	2.3	yes	Sprr2f	1.9	yes	Itih3	1.6	yes
Ear2	4.6	yes	Cyp11a1	2.7	yes	Apob	2.2	no	Ins2	1.8	yes	Ang4	1.5	yes
Saa2	4.6	yes	Dppa3	2.6	yes	Slpi	2.2	yes	Hbb-bh1	1.8	yes	Actc1	1.5	yes
Gc	4.2	no	Crp	2.6	no	Epx	2.1	yes	Myl7	1.8	yes	Hbb-y	1.5	yes
Apoc2	3.9	yes	Psp	2.6	yes	Tff2	2.1	yes	Pomc	1.8	yes	Gad1	1.5	no
Krt10	3.7	yes	Ngp	2.5	yes	Reg3g	2.1	yes	Prph	1.7	no	Gsta2	1.5	no
Fgg	3.6	yes	Tdo2	2.5	yes	Lta	2	yes	Tnnt2	1.7	no	Zp3	1.5	yes
Cyp3a13	3.6	no	Mup1	2.5	yes	Krt13	2	yes	Tac2	1.7	yes	Spt1	1.5	yes
Muc3	3.4	no	Slc12a3	2.5	yes	Anxa10	2	no	Alb	1.7	yes	Eomes	1.4	yes
Ear1	3.2	yes	Zp2	2.4	no	Fabp7	2	yes	Tm4sf5	1.7	no	Krt16	1.4	yes
Mmp7	3	no	Fbp1	2.4	yes	Nmb	1.9	yes	Ly6g	1.7	yes	S100a9	1.4	yes
Kng1	2.9	yes	S100a8	2.3	no	Prg2	1.9	no	Tff1	1.7	yes	Krt1	1.4	yes

Dep: dependency

Figure 3.1-7. *Autoimmunity in aged Foxn1-Cre::Dicer$^{fl/fl}$ mice.* (A) Upper panels: H&E staining of eye, liver and salivary gland tissue from 32 week old female Dicer$^{fl/fl}$ and Foxn1-Cre::Dicer$^{fl/fl}$ mice that had been T cell depleted at 2 weeks of age and allowed to autologously reconstitute their T cell compartment. Lower panel: Graphic summary of organ infiltrations in 32 week old Dicer$^{fl/fl}$ and Foxn1-Cre::Dicer$^{fl/fl}$ mice following transient T cell depletion at 2 weeks of age (each circle represents an individual mouse). Data is representative of two independent experiments with each 5 mice per group. (B) Graphic representation of changes in microarray measured expression of 147 Aire-dependent and Aire-independent peripheral tissue antigens (PTA) in purified mTEC from two week old Foxn1-Cre::Dicer$^{fl/fl}$ and Dicer$^{fl/fl}$ mice. (C) RT-PCR analysis for the expression of retinal (IRbp), salivary gland (Spt1), hepatic (CRP) and pancreatic (Ins2, Gad1) peripheral tissue antigens in purified mTEC from 2 week old Dicer$^{fl/fl}$ (black bars) and Foxn1-Cre::Dicer$^{fl/fl}$ mice (white bars). Gapdh was used as a reference for data

normalization. The data is representative of 2 separate experiments and indicate the mean ± SD of at least 3 mice per group; ** signifies $p<0.01$; *** $p<0.001$. (D) Decreased Peripheral Tissue Antigen (PTA) expression in mTEC as a consequence of Dicer deletion. PTA expression was analyzed in mTEC from 2 week old Foxn1- Cre::Dicerfl/fl mice using microarray and compared to the expression profile of age-matched, wild mTEC.

3.1.5 Discussion

Short, non-coding RNAs typically modulate the regulation of organ development via subtle though efficient parallel targeting of multiple components within a regulatory network (10,23). Because the molecular targets of most miRNA remain experimentally unverified, their role in tissue differentiation and function has largely been interrogated via global interference with their biogenesis (5). Here, the dependence of TEC differentiation and function on the biological properties of miRNA has been investigated in mice where Dicer is ablated after formation of the thymus primordium but before the complete patterning of its microenvironment. Our results reveal that miRNA are differentially expressed in separate TEC subpopulations and that this non-coding species of RNA is essential for the maintenance of a regularly composed and correctly functioning thymic microenvironment.

The TEC-targeted, embryonic loss of Dicer results in a sequential emergence of structural and functional alterations with defects apparent only after the first week of life. The asynchronous appearance of a complex phenotype is likely the result of a substantial variation in the decay of individual miRNA following *dicer1* gene ablation (24) and may also reflect a variable susceptibility of separate TEC subpopulations for the loss of specific miRNA.

The hematopoietic cells settling into the thymus require signals from Dll4 expressed by cTEC for their commitment to a T cell fate (17). In the absence of Dicer, fewer cTEC express Dll4 which suggest Dll4 as a likely indirect target of miRNA. Diminished expression of Dll4 on cTEC correlates with the observed reduction of ETPs and a robust B cell differentiation *in situ.* Since the Notch ligand density is important *in vitro* for the commitment of hematopoietic precursors to a T cell fate (25), quantitative signaling differences suffice to explain the *in situ* B cell

development in younger Foxn1-Cre::Dicer$^{fl/fl}$ mice. These findings provide a molecular mechanism (i.e. reduced Dll4 expression by cTEC) for the increase in intrathymic B-cell development (this report and ref. (26))

In older mutant animals, the microenvironment is unable to attract uncommitted hematopoietic precursors and consequently neither immature B nor T cells can be detected. Rather, the cellular composition and organization of the microenvironment demonstrates a structure reminiscent of secondary lymphoid tissues where lymphocyte homing is directed through PNAd^{+} venules (27) and new lymphatic vessels are established (in the absence of overt inflammation) possibly sprouting from pre-existing endothelial cells (28). The increase and persistence of the two vascular systems is likely mediated by different mechanisms including the presence of B cells, the expression of CCL21 by TEC and dendritic cells, and the stimulation of the lymphotoxin beta receptor on endothelial cells of blood and lymph vessels (29,30).

The almost complete attrition of TEC is an intriguing feature of older Foxn1-Cre::Dicer$^{fl/fl}$ mice. Given that miRNA expression patterns create a cell type-specific signature and help to reinforce cell fate specifications, it is conceivable that the pool of TEC precursor/stem cells is altered and/or that their differentiation into distinct TEC subsets is repressed following the targeted loss of Dicer expression. A reduction of MHC^{lo} mTEC suggests a defective maintenance of the progenitor pool in the absence of miRNA, a finding that is contrasting the higher frequency of p63^{+} TEC reported recently (26). The changes in gene expression in miRNA-deficient TECs infer that several pathways essential for cell pluripotency, differentiation and survival appear to be affected following the loss of Dicer. Indeed, the continuous replacement of immature and mature TEC was severely affected in older Foxn1-Cre::Dicer$^{fl/fl}$ mice. The loss of miRNA also resulted in the upregulation of multiple transcripts of key molecules known to affect TEC development and function. For example the correct control of Wnt signaling in TECs is required for thymus development since gain of canonical Wnt signaling activity is incompatible with regular thymus organogenesis and function (15). Similarly, changes in BMP signaling

in TEC affect both embryonic development (31) and thymopoietic function (32). Increased TgfβR3 expression in Dicer deficient TECs possibly contributes to the enhanced thymic involution via enhanced stimulation of TgfβR2 signaling (16),whereas the upregulation of insulin-like growth factor 1 receptor (Igf-1R) may, in response to Igf-1, account for increased TEC proliferation (Fig. 3D; and ref. (33)). Hence, distinct miRNA may directly control the expression, activation and/or availability of signaling elements essential for either TEC differentiation, proliferation or function. In keeping with this contention, the single loss of miR-29a enhances thymic involution in adult mice though neither thymic architecture nor function are affected (26).

Thymocyte differentiation such as the generation of post-selection thymocytes with a $CD3^{hi}CD69^{+}CD4^{-}CD8^{+}$ is already impaired in young Foxn1-Cre::$Dicer^{fl/fl}$ mice even though cellularity, MHC expression and architectural organization of the cTEC scaffold has not yet been compromised. This finding infers a previously unnoticed (26) qualitative cTEC deficiency in supporting the development of CD8 SP thymocytes. Later in life, mutant mice display a defect in positive selection that is marked by a partial block in the sequential upregulation of CD69 and CD3 on DP thymocytes. This fault points to a previously unrecognized critical element in positive selection since neither MHC nor Psmb11 are affected when the deficiency becomes first apparent (18,34-37). Though a reduced density of the epithelial network is likely to contribute to altered thymocyte development in older mice (26), overt TEC-free areas as observed in Kremen1-deficient mice were not sufficient to compromise T cell development (38). The continued selection of $CD3^{hi}CD69^{+}$ thymocytes and their differentiation along the SP CD8 lineage is MHC independent but requires other, additional cues (39-41). However, only few candidate molecules expressed by cTEC including ICAM and IL-7 (42,43) have so far been inferred to play a role in positive thymocyte selection, yet their transcripts remained unchanged in Dicer-deficient cTEC (unpublished observations). Thus, mice that lack Dicer expression in cTEC display significant defects in thymocyte development which appear to be unrelated to previously identified mechanisms controlling this multi-stage process.

Thymocyte negative selection is likely impaired in Foxn1-Cre::Dicer$^{fl/fl}$ mice since their mTEC display a significant deficiency in promiscuous gene expression. The molecular signature of this defect implies a common yet undefined mechanism that controls some but not all known PTA transcripts. Though the differentiation of Aire^{+} mTEChi was apparently independent of miRNAs, the expression of a significant number of Aire dependent PTAs was, however, affected by the lack of Dicer expression. It is thus conceivable that miRNAs may act either in concert or downstream of Aire to regulate the expression of a subset of Aire-dependent PTAs. In parallel, our data likewise reveal that miRNA also control the expression of a number of Aire-independent PTA, possibly via a common pathway. As a corollary, central tolerance induction is defective and autoimmunity ensues. Because PTA expression confined to the perinatal period suffices to induce long-lasting tolerance (22), functionally relevant defects in negative selection become only apparent once the initially chosen T cell pool is replaced by cells selected in the distorted thymic microenvironment of two and more week old Foxn1-Cre::Dicer$^{fl/fl}$ mice. The pattern of organ-specific autoimmunity observed in these mice correlates with the altered expression profile of tissue-specific self-antigens. It is therefore conceivable that some forms of autoimmunity may also occur as a consequence of known or not yet described miRNA polymorphisms that either affect the biogenesis of miRNA or influence their ability for target repression.

3.1.6 Material and Methods

Mice

Mice were kept under specific pathogen free conditions and used according to federal and institutional regulations. For developmental staging, the day of the vaginal plug was designated as embryonic day (E) 0.5. C57BL/6 mice were obtained in-house from the Departmental breeding facility whereas nude (nu/nu) mice were obtained from a commercial vendor (Janvier, France). Mice were kept and handled according to Cantonal and Federal regulations and permissions.

Histology and immunofluorescence

Frozen thymus tissue sections (8μm) were fixed in gradient ethanol solutions and stained with Mayer's hematoxyline (Réactifs RAL) and eosin (J.T.Baker). For immunohistochemistry, acetone-fixed sections (8μm) were stained using antibodies specific for cytokeratin (CK) 5 (Covance), CK8 (Progen), CK14 (Covance), MTS10 (a gift from R. Boyd, Melbourne, Australia), ERTR7 (provided by W.vanEwijk, Utrecht, Netherlands), Psmb11 (MBL), Lyve1 (ReliaTech), CR1 (8C12, Becton-Dickinson), Aire (5H12, provided by S. Hamish, Adelaide, Australia), PNAd (MECA-79, Becton-Dickinson), and reactivity to lectin UEA-1 (Reactolab). Alexa-Fluor conjugated anti-IgG antibodies (Invitrogen) were used as secondary reagents. Images were acquired using a Zeiss LSM510.

Flow cytometry, cell sorting and intracytoplasmic staining

Haematopoietic cells from thymus and spleen were stained with Abs against CD3 (KT-3), CD4 (GK1.5, BioLegend), CD8 (53-67, eBioscience), CD19 (ID3), CD25 (PC61.5, eBioscience), CD44 (IM7, eBioscience), CD62L (MEL-14, Becton-Dickinson), CD69 (H1.2F3, Becton-Dickinson), CD93 (aa4.1, eBioscience) and IgM (R33.24.12). For intracellular staining, cells were fixed and permeabilized using the Cytofix/Cytoperm Kit (Becton-Dickinson) and stained for Foxp3 expression (FJK-16s, eBioscience). For the analysis of TEC, thymic lobes were cut into small pieces, and then incubated at 37°C for 60 minutes in HBSS containing 2% (w/v) FCS (Perbio), 100μg/ml Collagenase/Dispase (Roche Diagnostics) and 40ng/ml DNaseI (Roche). TECs were enriched using AutoMACS (Miltenyi Biotec) and stained for the expression of EpCAM (G8.8, DSHB, University of Iowa), CD45 (30F11, eBioscience), MHCI (AF6-88.5, Biolegend), MHCII (AF6-120.1, BioLegend), Ly51 (6C3, BioLegend) Dll-4 (gift from Robson MacDonald, University of Lausanne) and UEA-1 (Reactolab). For intracellular staining, TECs were marked for cell surface molecules, fixed, permeabilized (Cytofix/Cytoperm, Becton-Dickinson) and stained with BrdU or Aire-specific antibodies. Flow cytometric analysis and cell sorting were performed (FACSAria) using FACSDiva (Becton-Dickinson) and FlowJo software (TreeStar).

MicroRNA detection and gene expression profiling

Total RNA was isolated from sorted cells with the miRNeasy Mini Kit (Qiagen). The QuantiMir RT Kit (System Biosciences) was utilized to analyze the expression of specific miRNA. cDNA was assessed by quantitative real-time PCR with SYBR Green (SensiMix, Bioline). Primer sequences are available upon request. Gapdh was used as an internal control for miRNA and mRNA analysis respectively. The mRNA expression profiles in TEC isolate from 2 week old Foxn1Cre::Dicer$^{fl/fl}$ and Dicer$^{fl/fl}$ mice were generated using the GeneChip Gene 1.0 ST Array System (Affymetrix). The array data were submitted to the ArrayExpress repository under accession E-MEXP-3303 (Username:Reviewer_E-MEXP-3303 password:aghiiesx).

Bioinformatic and statistical analysis

Differential expression analysis for mRNA was carried out using Partek® application software (www.partek.com) and visualized with Integromics Biomarker Discovery for Tibco Spotfire® (www.integromics.com). The gene expression data were normalized using Affymetrix Robust Multi-Array Analysis (RMA) and differential expression was obtained by analysis of variance (Two-way ANOVA). P-value correction for multiple hypothesis was performed with Benjamini-Hochberg´s false discovery rate (FDR) (11). Functional analyses of biological processes were determined by Genecodis determining the significantly enriched gene ontology terms in the list of gene targets (12,13).

BrdU analysis

Mice were injected intraperitoneally (i.p.) with 1mg BrdU in phosphate buffered saline and TECs were analyzed 4 hours later by flow cytometry (see above).

Bone marrow chimeric mice

Sub-lethally irradiated newborn Foxn1Cre::Dicer$^{fl/fl}$ and Dicer$^{fl/fl}$ mice were injected i.p. with OT1 transgenic fetal liver cells ($2x10^6$) from E13.5-14.5 old embryos. Successfully grafted animals (with an average chimerism of at least 30% for OT1) were analyzed 4 weeks later.

T-cell depletion

Two-week old mice were injected i.p. three times every three days with 200µg anti-CD4 (GK1.5), 100µg anti-CD8 (53-67) and 50µg anti-Thy1.2 (T24), a dose that efficiently deplete peripheral T cells.

Fetal thymus transplants

Thymic lobes were collected from E15.5 embryos and both lobes from a single embryo were placed under the kidney capsule of the recipient nu/nu mice. Four weeks later, thymic lobes were removed and analyzed.

Statistical analysis

Statistical analysis was performed using students t-test (unpaired, two-tailed). Probability values were classified into four categories: $P>0.05$ (not significant), $0.05\geq P>0.01$ (*), $0.01\geq P>0.001$ (**) and $P\leq 0.0001$ (***).

3.1.7 References

1. Klein, L., M. Hinterberger, G. Wirnsberger, and B. Kyewski. 2009. Antigen presentation in the thymus for positive selection and central tolerance induction. *Nat. Rev. Immunol.* 9: 833-844.
2. Klug, D. B., C. Carter, E. Crouch, D. Roop, C. J. Conti, and E. R. Richie. 1998. Interdependence of cortical thymic epithelial cell differentiation and T-lineage commitment. *Proc. Natl. Acad. Sci. U. S. A.* 95: 11822-11827.
3. Gray, D. H., N. Seach, T. Ueno, M. K. Milton, A. Liston, A. M. Lew, C. C. Goodnow, and R. L. Boyd. 2006. Developmental kinetics, turnover and

stimulatory capacity of thymic epithelial cells. *Blood.* 108: 3777-3785.

4. Takahama, Y. 2006. Journey through the thymus: stromal guides for T-cell development and selection. *Nat. Rev. Immunol.* 6: 127-135.

5. Bartel, D. P. 2009. MicroRNAs: target recognition and regulatory functions. *Cell.* 136: 215-233.

6. Kim, V. N. 2005. MicroRNA biogenesis: coordinated cropping and dicing. *Nat. Rev. Mol. Cell. Biol.* 6: 376-385.

7. Lewis, B. P., C. B. Burge, and D. P. Bartel. 2005. Conserved seed pairing, often flanked by adenosines, indicates that thousands of human genes are microRNA targets. *Cell.* 120: 15-20.

8. Baek, D., J. Villén, C. Shin, F. D. Camargo, S. P. Gygi, and D. P. Bartel. 2008. The impact of microRNAs on protein output. *Nature.* 455: 64-71.

9. Selbach, M., B. Schwanhäusser, N. Thierfelder, Z. Fang, R. Khanin, and N. Rajewsky. 2008. Widespread changes in protein synthesis induced by microRNAs. *Nature.* 455: 58-63.

10. Xiao, C., and K. Rajewsky. 2009. MicroRNA control in the immune system: basic principles. *Cell.* 136: 26-36.

11. Benjamini, Y., and Y. Hochberg. 1995. Controlling the false discovery rate: a practical and powerful approach to multiple testing. *Journal. of. the. Royal. Statistical. Society.* 57: 289-300.

12. Nogales-Cadenas, R., P. Carmona-Saez, M. Vazquez, C. Vicente, X. Yang, F. Tirado, J. M. Carazo, and A. Pascual-Montano. 2009. GeneCodis: interpreting gene lists through enrichment analysis and integration of diverse biological information. *Nucleic. Acids. Res.* 37: W317-W322.

13. Carmona-Saez, P., M. Chagoyen, F. Tirado, J. M. Carazo, and A. Pascual-Montano. 2007. GENECODIS: a web-based tool for finding significant concurrent annotations in gene lists. *Genome. Biol.* 8: R3.

14. Harfe, B. D., M. T. McManus, J. H. Mansfield, E. Hornstein, and C. J. Tabin. 2005. The RNaseIII enzyme Dicer is required for morphogenesis but not patterning of the vertebrate limb. *Proc. Natl. Acad. Sci. U. S. A.* 102: 10898-10903.

15. Zuklys, S., J. Gill, M. P. Keller, M. Hauri-Hohl, S. Zhanybekova, G. Balciunaite, K. J. Na, L. T. Jeker, K. Hafen, N. Tsukamoto, T. Amagai, M. M. Taketo, W. Krenger, and G. A. Holländer. 2009. Stabilized {beta}-Catenin in Thymic Epithelial Cells Blocks Thymus Development and Function. *J. Immunol.* 182: 2997-3007.

16. Hauri-Hohl, M. M., S. Zuklys, M. P. Keller, L. T. Jeker, T. Barthlott, A. M. Moon, J. Roes, and G. A. Holländer. 2008. TGF-beta signaling in thymic epithelial cells regulates thymic involution and postirradiation reconstitution. *Blood.* 112: 626-634.

17. Hozumi, K., C. Mailhos, N. Negishi, K. I. Hirano, T. Yahata, K. Ando, S. Zuklys, G. A. Holländer, D. T. Shima, and S. Habu. 2008. Delta-like 4 is indispensable in thymic environment specific for T cell development. *J. Exp. Med.* 205: 2507-2513.

18. Murata, S., K. Sasaki, T. Kishimoto, S. Niwa, H. Hayashi, Y. Takahama, and K. Tanaka. 2007. Regulation of CD8+ T cell development by thymus-specific proteasomes. *Science.* 316: 1349-1353.

19. Barthlott, T., H. Kohler, and K. Eichmann. 1997. Asynchronous coreceptor downregulation after positive thymic selection: prolonged maintenance of the double positive state in CD8 lineage differentiation due to sustained biosynthesis of the CD4 coreceptor. *J. Exp. Med.* 185: 357-362.

20. Nitta, T., I. Ohigashi, Y. Nakagawa, and Y. Takahama. 2010. Cytokine crosstalk for thymic medulla formation. *Curr. Opin. Immunol.* 23: 190-197.

21. Santori, F. R., S. M. Brown, and S. Vukmanović. 2002. Genomics-based identification of self-ligands with T cell receptor-specific biological activity. *Immunol. Rev.* 190: 146-160.

22. Guerau-de-Arellano, M., M. Martinic, C. Benoist, and D. Mathis. 2009. Neonatal tolerance revisited: a perinatal window for Aire control of autoimmunity. *J. Exp. Med.* 206: 1245-1252.

23. Tsitsiou, E., and M. A. Lindsay. 2009. microRNAs and the immune response. *Curr. Opin. Pharmacol.* 9: 514-520.

24. Soukup, G. A., B. Fritzsch, M. L. Pierce, M. D. Weston, I. Jahan, M. T. McManus, and B. D. Harfe. 2009. Residual microRNA expression dictates the extent of inner ear development in conditional Dicer knockout mice. *Dev. Biol.* 328: 328-341.

25. Dallas, M. H., B. Varnum-Finney, C. Delaney, K. Kato, and I. D. Bernstein. 2005. Density of the Notch ligand Delta1 determines generation of B and T cell precursors from hematopoietic stem cells. *J. Exp. Med.* 201: 1361-1366.

26. Papadopoulou, A. S., J. Dooley, M. A. Linterman, W. Pierson, O. Ucar, B. Kyewski, S. Zuklys, G. A. Hollander, P. Matthys, D. H. Gray, B. De Strooper, and A. Liston. 2012. The thymic epithelial microRNA network elevates the threshold for infection-associated thymic involution via miR-29a mediated suppression of the IFN-α receptor. *Nat. Immunol.* 13: 181-187.

27. Girard, J. P., and T. A. Springer. 1995. High endothelial venules (HEVs): specialized endothelium for lymphocyte migration. *Immunol. Today.* 16: 449-457.

28. He, Y., I. Rajantie, M. Ilmonen, T. Makinen, M. J. Karkkainen, P. Haiko, P. Salven, and K. Alitalo. 2004. Preexisting lymphatic endothelium but not endothelial progenitor cells are essential for tumor lymphangiogenesis and lymphatic metastasis. *Cancer. Res.* 64: 3737-3740.

29. Liao, S., and N. H. Ruddle. 2006. Synchrony of high endothelial venules and lymphatic vessels revealed by immunization. *J. Immunol.* 177: 3369-3379.

30. Muniz, L. R., M. E. Pacer, S. A. Lira, and G. C. Furtado. 2011. A Critical Role for Dendritic Cells in the Formation of Lymphatic Vessels within Tertiary Lymphoid Structures. *J. Immunol.* 187: 828-834.

31. Bleul, C. C., and T. Boehm. 2005. BMP Signaling Is Required for Normal Thymus Development. *J. Immunol.* 175: 5213-5221.

32. Tsai, P. T., R. A. Lee, and H. Wu. 2003. BMP4 acts upstream of FGF in modulating thymic stroma and regulating thymopoiesis. *Blood.* 102: 3947-3953.

33. Chu, Y. W., S. Schmitz, B. Choudhury, W. Telford, V. Kapoor, S. Garfield, D. Howe, and R. E. Gress. 2008. Exogenous insulin-like growth factor 1 enhances thymopoiesis predominantly through thymic epithelial cell expansion. *Blood.* 112: 2836-2846.

34. Grusby, M. J., R. S. Johnson, V. E. Papaioannou, and L. H. Glimcher. 1991. Depletion of $CD4^+$ T cells in major histocompatibility coplex class II-deficient mice. *Science.* 253: 1417-1420.

35. Cosgrove, D., D. Gray, A. Dierich, J. Kaufman, M. Lemeur, C. Benoist, and D. Mathis. 1991. Mice lacking MHC class II molecules. *Cell.* 66: 1051-1066.

36. Zijlstra, M., M. Bix, N. E. Simister, J. M. Loring, D. H. Raulet, and R. Jaenisch. 1990. β2-Microglobulin deficient mice lack $CD4\text{-}8^+$ cytolytic T cells. *Nature.* 344: 742-746.

37. Koller, B. H., P. Marrack, J. W. Kappler, and O. Smithies. 1990. Normal development of mice deficient in β2M, MHC class I proteins and $CD8^+$T cells. *Science.* 248: 1227-1231.

38. Osada, M., E. Ito, H. A. Fermin, E. Vazquez-Cintron, T. Venkatesh, R. H. Friedel, and M. Pezzano. 2006. The Wnt signaling antagonist Kremen1 is required for development of thymic architecture. *Clin. Dev. Immunol.* 13: 299-319.

39. Muller, K. P., and B. A. Kyewski. 1993. T cell receptor targeting to thymic cortical epithelial cells in vivo induces survival, activation and differentiation of immature thymocytes. *European. Journal. of. Immunology.* 1993: 1661-1670.

40. Hare, K. J., E. J. Jenkinson, and G. Anderson. 1999. CD69 expression discriminates MHC-dependent and -independent stages of thymocyte positive selection. *J. Immunol.* 162: 3978-3983.

41. Singer, A., S. Adoro, and J. H. Park. 2008. Lineage fate and intense debate: myths, models and mechanisms of CD4- versus CD8-lineage choice. *Nat. Rev. Immunol.* 8: 788-801.

42. Paessens, L. C., S. K. Singh, R. J. Fernandes, and Y. van Kooyk. 2008. Vascular cell adhesion molecule-1 (VCAM-1) and intercellular adhesion molecule-1 (ICAM-1) provide co-stimulation in positive selection along with survival of selected thymocytes. *Molecular. immunology.* 45: 42-48.

43. Park, J. H., S. Adoro, T. Guinter, B. Erman, A. S. Alag, M. Catalfamo, M. Y. Kimura, Y. Cui, P. J. Lucas, R. E. Gress, M. Kubo, L. Hennighausen, L. Feigenbaum, and A. Singer. 2010. Signaling by intrathymic cytokines, not T cell antigen receptors, specifies CD8 lineage choice and promotes the differentiation of cytotoxic-lineage T cells. *Nat. Immunol.* 11: 257-264.

3.1.8 Supplementary Material

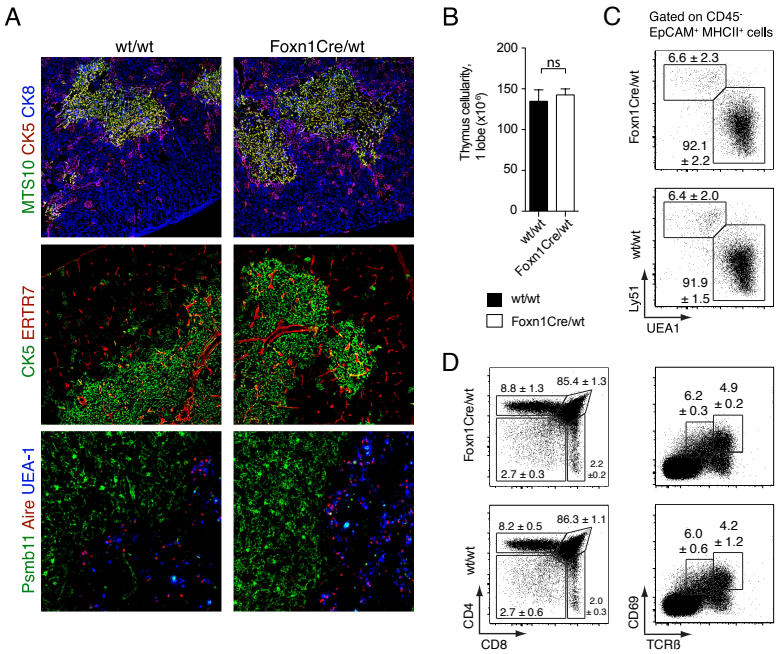

Supplemental Figure 1. Heterozygous Foxn1-Cre mice display a regular thymus size, cellular architecture and function. (A) Immunofluorescence analysis of thymic tissue sections from heterozygous Foxn1Cre transgenic (Foxn1Cre/wt) and wild type (wt/wt) mice using antibodies specific for ERTR7 to identify fibroblasts; for CK8 and Psmb11 to detect cTEC; and for MTS10, CK5, and Aire as well as reactivity with UEA-1 to recognize mTEC. Data are representative of two separate experiments with at least three mice each. (B) Total thymic cell numbers of wt/wt (black bars) and Foxn1-Cre/wt (white bars) mice at 3 weeks of age; ns: not significant. (C) Flow cytometric analysis of TEC (CD45-EpCAM+MHCII+) subpopulations isolated from thymic tissue of Foxn1Cre/wt and wt/wt mice. The relative frequency (right panels) and absolute cell numbers (left graph) of cTEC (UEA-1-Ly51+) and mTEC (UEA-1+Ly51-) from wt/wt (black bars) and Foxn1Cre/wt mice (white bars) are shown. Data indicate the mean ± SD of at least 3 mice per group; *denotes $p<0.05$; ** $p<0.01$; *** $p<0.001$. Data are representative of three independent experiments. (D) Flow cytometric analysis of thymocyte development using surface markers CD4 and CD8 (left panels), and markers for positive selection, CD69 and TCRbeta (right panels). The relative frequencies of the indicated populations isolated from wt/wt (lower panels) and Foxn1Cre/wt mice (upper panels) are shown. Data indicate the mean ± SD of at least 3 mice per group; *denotes $p<0.05$; ** $p<0.01$. Data are representative of three independent experiments.

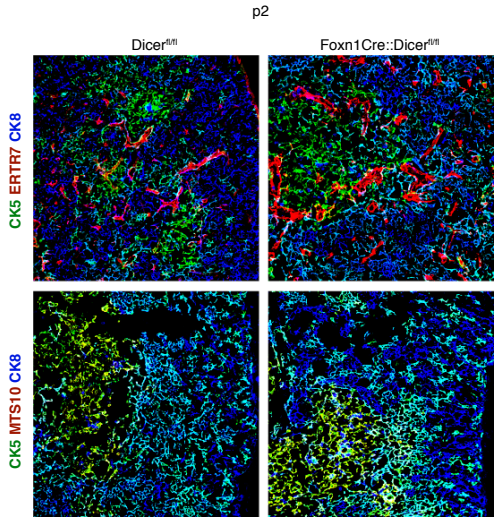

Supplemental Figure 2. Thymic microenvironment of 2 day old (p2) Foxn1-Cre::Dicer$^{fl/fl}$ mice. Immuno- fluorescence analysis of thymic tissue sections from p2 Dicer$^{fl/fl}$ or Foxn1-Cre::Dicer$^{fl/fl}$ mice. Antibodies were used to identify fibroblasts (ERTR7), cortical (CK8) and medullary (MTS10, CK5) TEC. Original magnification 20x. Data are representative of two separate experiments.

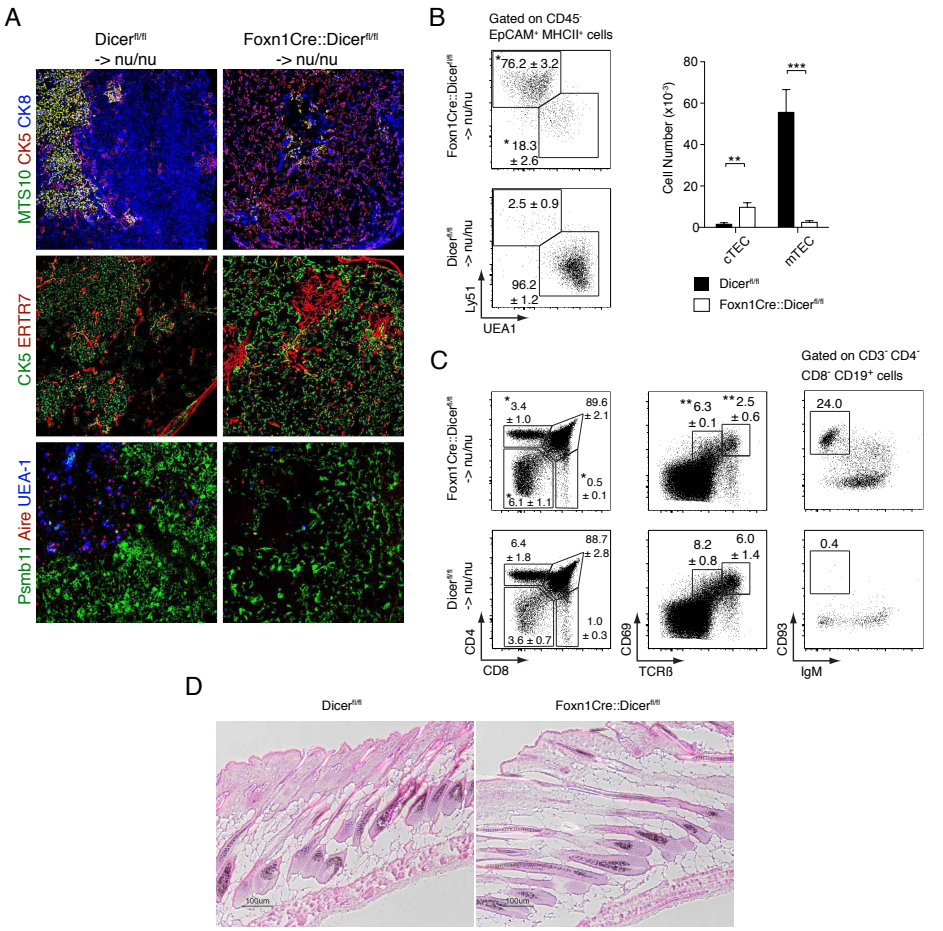

Supplemental Figure 3. TEC phenotype of Foxn1-Cre::Dicer$^{fl/fl}$ mice is uneffected by Cre-mediated recombination in keratinocytes. Fetal thymic lobes from E15.5 Dicer$^{fl/fl}$ or Foxn1-Cre::Dicer$^{fl/fl}$ embryos were transplanted under the kidney capsule of nu/nu recipients and grafts were analyzed 4 weeks later. (A) Immunofluorescence analysis of thymic tissue sections using antibodies specific for ERTR7 to identify fibroblasts; for CK8 and Psmb11 to detect cTEC; and for MTS10, CK5, and Aire as well as reactivity to UEA-1 to recognize mTEC. Data are representative of three separate experiments with at least two mice each. (B) Flow cytometric analysis of TEC (CD45-EpCAM+MHCII+) subpopulations isolated from thymic tissue grown under the kdney capsule of a nu/nu recipient mice. The relative frequency (left panels) and absolute cell numbers (right graph) of cTEC (UEA-1-Ly51+) and mTEC (UEA-1+Ly51-) from Dicer$^{fl/fl}$ (black bars) and Foxn1-Cre::Dicer$^{fl/fl}$ (white bars) of the indicated grafts are shown. Data show the mean ± SD of at least 3 mice per group; *denotes $p<0.05$; ** $p<0.01$; *** $p<0.001$. Data are representative of three independent experiments. (C) Flow cytometric analysis of lymphopoiesis in the grafts using surface markers CD4 and CD8 for T lineage development (left panels), markers for thymocyte positive selection CD69 and TCRbeta (middle panels) and .the expression of CD93 and IgM to identify B cell maturation in situ. The relative frequencies of the respective populations for Dicer$^{fl/fl}$ (lower panels) and Foxn1-Cre::Dicer$^{fl/fl}$ grafts (upper panels) are shown. Data indicate the mean ± SD of at least 3 mice per group; *denotes $p<0.05$; ** $p<0.01$. Data are representative of three independent experiments. (D) Hematoxilin and eosin (HE) staining of skin sections from 3 week old Dicer$^{fl/fl}$ or Foxn1-Cre::Dicer$^{fl/fl}$ mice.

3.2 Aire-expressing thymic medullary epithelial cells originate from β5t-expressing progenitor cells

3.2.1 Introductory notes

3.2.1.1 Summary

Staging TEC development, be it during organogenesis or homeostatic maintenance, has proven difficult in the past due to the paucity of appropriate cell markers. To overcome this limitation a mouse model was created in which we used the cTEC-specific expression pattern of the thymoproteasome unit β5t to genetically trace cells. With this strategy we intended to identify cTEC at very early stages during lineage commitment in thymus development. For this reason the sequence for the Cre recombinase was placed under the transcriptional control of the Psmb11 locus encoding the β5t proteasome subunit. Cre expression was detected only in thymic epithelial cells, mostly limited to cTEC, as defined by the expression of EpCAM and Ly51 in absence of CD45 and UEA1. Importantly, transcripts for β5t were absent from all peripheral organs investigated. Mice homozygous for the knock-in revealed a phenotype identical to that observed for conventional knock-out animals, namely a specific reduction of post-selection CD4-CD8+ thymocytes, confirming correct targeting of the Psmb11 locus. These knock-in mice, designated β5t-Cre, were crossed to a ZsGreen reporter line to mark cells that currently or previously had expressed β5t. Unexpectedly, we found that all TEC in adult mice expressed ZsGreen albeit mRNA specific for β5t and Cre were only detected in cTEC. Hence, cells giving rise to the mTEC lineage must have expressed at one point in their development β5t as they also express the ZsGreen reporter. We therefore wished to specify the β5t expression dynamics during foetal stages. β5t expression was initiated after E11.5 and almost all TEC expressed the ZsGreen reporter by E12.5. Interestingly, we also identified a few ZsGreen-positive cells of this developmental stage that did not express the β5t protein. These cells may have expressed the β5t protein not yet at all or sufficiently to be detected by immunohistochemistry. Alternatively, these cells may again have lost β5t expression and represented a TEC of a development stage different from the cTEC lineage.

Taken together these observations reveal an unexpected relationship between the cortical and medullar thymic epithelial cell lineages, which was previously not appreciated. They implied a possible relationship whereby a progenitor expressing β5t had the potential to differentiate into the cTEC lineage and maintain β5t protein expression or, alternatively, could adopt the mTEC fate, thus suspending β5t protein expression but maintaining reporter-positivity. Due to the non-inducible and permanent expression of the reporter, the dynamics of this relationship could not be further probed. To resolve this issue, another mouse experimental model was generated and analyzed (see chapter 3.4).

3.2.1.2 Contribution

The work described above was a collaborative work between the laboratory of Professor Yousuke Takahama in Tokushima (Japan) and our laboratory in Basel (Switzerland). Our results were published in 2013 in the Proceedings of the National Academy of Sciences of the United States of America (PNAS) (PMID:23720310).

My contribution to this project was the phenotypic characterization of the thymi in β5t-Cre::CAG-STOP-CAG-ZsGreen mouse line by flow cytometry. This included the initial analysis of animals in which the targeted Psmb11 locus contained the sequence for the Cre recombinase and the neomycin cassette, the latter of which was originally required for the generation of these mice. Here we observed an uneven expression of the Cre recombinase in TEC, which lead to an inconsistent variability in ZsGreen-expression on a mouse per mouse basis. Because of this inexplicable phenomenon we decided to remove the neomycin cassette by crossing β5t-Cre mice to a transgenic mouse line that ubiquitously expressed flippase. The ensuing, neomycin cassette-deficient, animals expressed Cre more reliably and consistently and were therefore used for all experiments in this project. After circumventing this anomaly, I focused the analysis on the detection of reporter-positive TEC at various developmental stages and on T cell development (to exclude potential functional deficiencies of TEC in this transgenic mouse model) (Figure 3 A-B). Finally, although this data was not included in the final publication, I analyzed sorted ZsGreen- and + cell populations

for the expression of various transcripts to ensure the specificity and reliability of this mouse model. All together, my contributions significantly contributed to the establishment of the experimental mouse model and the key findings observed in that mouse line, and were acknowledged in the final Japanese-Swiss co-publication.

3.2.1.3 Authors and affiliations in the publication

Izumi Ohigashi[a,1], Saulius Zuklys[b,1], Mie Sakata[a], **Carlos E. Mayer**[b], Saule Zhanybekova[b], Shigeo Murata[c], Keiji Tanaka[d], Georg A. Holländer[b,e,2,3], and Yousuke Takahama[a,2,3]

a Division of Experimental Immunology, Institute for Genome Research, University of Tokushima, Tokushima 770-8503, Japan

b Laboratory of Pediatric Immunology, Department of Biomedicine, University of Basel and University Children's Hospital Basel, 4058 Basel, Switzerland

c Graduate School of Pharmaceutical Sciences, University of Tokyo, Tokyo 113-0033, Japan

d Tokyo Metropolitan Institute of Medical Science, Tokyo 156-8506, Japan

e Department of Paediatrics and the Weatherall Institute of Molecular Medicine, University of Oxford, Oxford OX3 9DU, United Kingdom

1 Contributed equally

3.2.2 Abstract

The thymus provides multiple microenvironments that are essential for the development and repertoire selection of T lymphocytes. The thymic cortex induces the generation and positive selection of T lymphocytes, whereas the thymic medulla

establishes self-tolerance among the positively selected T lymphocytes. Cortical thymic epithelial cells (cTECs) and medullary TECs (mTECs) constitute the major stromal cells that structurally form and functionally characterize the cortex and the medulla, respectively. cTECs and mTECs are both derived from the endodermal epithelium of the third pharyngeal pouch. However, the molecular and cellular characteristics of the progenitor cells for the distinct TEC lineages are unclear. Here we report the preparation and characterization of mice that express the recombinase Cre instead of β5t, a proteasome subunit that is abundant in cTECs and not detected in other cell types, including mTECs. By crossing β5t-Cre knock-in mice with loxP-dependent GFP reporter mice, we found that β5t-Cre–mediated recombination occurs specifically in TECs but not in any other cell types in the mouse. Surprisingly, in addition to cTECs, β5t-Cre-loxP–mediated GFP expression was detected in almost all mTECs. These results indicate that the majority of mTECs, including autoimmune regulator-expressing mTECs, are derived from β5t-expressing progenitor cells.

3.2.3 Introduction

Thymic epithelial cells (TECs) are derived from the endodermal epithelium of the third pharyngeal pouch (1-3). Cortical TECs (cTECs) provide a microenvironment that induces the generation of T cells and the positive selection of functionally competent T cells, whereas medullary TECs (mTECs) essentially contribute to the establishment of self-tolerance by the deletion of self-reactive T cells and the generation of regulatory T cells (4, 5). The nuclear protein Autoimmune regulator (Aire) expressed by a subpopulation of mTECs is essential, especially during the perinatal period, for the establishment of self-tolerance in T cells (6, 7). Although the importance of the forkhead transcription factor Foxn1 for the development of both cTECs and mTECs has been established (2, 8), it remains unknown how the endodermal epithelium of the third pharyngeal pouch gives rise to cTECs and mTECs. In particular, the molecular and cellular mechanisms underlying the separate development of the cTEC and mTEC lineages remain unclear.

We previously reported β5t, a proteasome subunit expressed in cTECs (9, 10). β5t is pivotal for the positive selection of immunocompetent $CD8^+$ T cells (11, 12). β5t mRNA and protein are prominently expressed in cTECs and not detected in other cell types, including mTECs (10). To examine whether β5t-expressing cells could contribute to the development of cells other than cTECs, we engineered mice in which the β5t-encoding genomic sequence was replaced with the sequence that encodes the loxP-specific recombinase Cre. Analyzing mice that are crossed to carry the β5t-Cre knock-in allele and the loxP-dependent GFP reporter allele, we demonstrate that β5t-Cre-loxP–mediated GFP expression is detected in practically all cTECs and, surprisingly, in almost all mTECs, including $Aire^+$ mTECs, but not in any other cell types in the body. The results indicate that β5t expression is highly specific for TECs and that in addition to mature cTECs, β5t is expressed in TEC progenitor cells that give rise to mTECs, including $Aire^+$ mTECs.

3.2.4 Results

3.2.4.1 Generation of β5t-Cre Knock-In Mice.

We produced β5t-Cre knock-in mice by homologous recombination in embryonic stem cells using a gene-targeting vector in that the sole exon sequence encoding the β5t gene was replaced with a sequence encoding the codon-improved Cre recombinase (Fig. S1). Homologous recombination with the targeting vector was confirmed by Southern blot analysis, in which a 5.6-kb BamHI fragment appeared after hybridization with a 3′ probe (Fig. S1 *A* and *B*) and by PCR analysis of genomic DNA through amplification of a recombination-specific 765-bp fragment (Fig. S1 *A* and *C*). Because the β5t-Cre knock-in allele lacks the sequence encoding β5t protein (Fig. S1*A*), mice homozygous for the β5t-Cre knock-in alleles were deficient in functional β5t protein and therefore defective in the generation of $CD8^+$T cells (Fig. 1*A*). Identical to previously reported β5t-deficient mice (9, 11), homozygous β5t-Cre knock-in mice were defective in the generation of ~80% of $CD4^-CD8^+$ T cell antigen receptor $(TCR)^{high}$ mature thymocytes but were comparable to normal mice in the generation of $CD4^-CD8^-$ and $CD4^+CD8^+$ immature thymocytes as well as

$CD4^+CD8^-$ TCR^{high} mature thymocytes (Fig. 1*A*). In contrast, mice heterozygous for the β5t-Cre knock-in allele showed no alterations or defects in thymocyte cellularity (Fig. 1*A*), in agreement with the normal T-cell development detected in $\beta5t^{+/-}$ heterozygous mice previously produced (9, 11). These results indicate that homologous recombination of the genome was successfully engineered to knock in the β5t-Cre allele, as designed in Fig. S1*A*. Because homozygous β5t-Cre knock-in mice lacked β5t protein expression and hence were defective in the generation of $CD8^+$ T cells, the remainder of this article describes the results obtained from mice heterozygous for the β5t-Cre knock-in allele. We first examined the tissue specificity of Cre expression in β5t-Cre knock-in mice. In agreement with the highly specific expression of β5t gene in cTECs (9, 10), Cre mRNA expression in β5t-Cre knock-in mice was specifically detected in cTECs but not in other thymic cell types, including mTECs and a population of non-TEC thymic stromal cells (containing fibroblasts and endothelial cells) (Fig. 1*B*). All other tissues tested failed to express Cre mRNA (Fig. 1*B*); thus, the specificity of Cre expression in β5t-Cre knock-in mice faithfully reproduces the expression specificity of β5t.

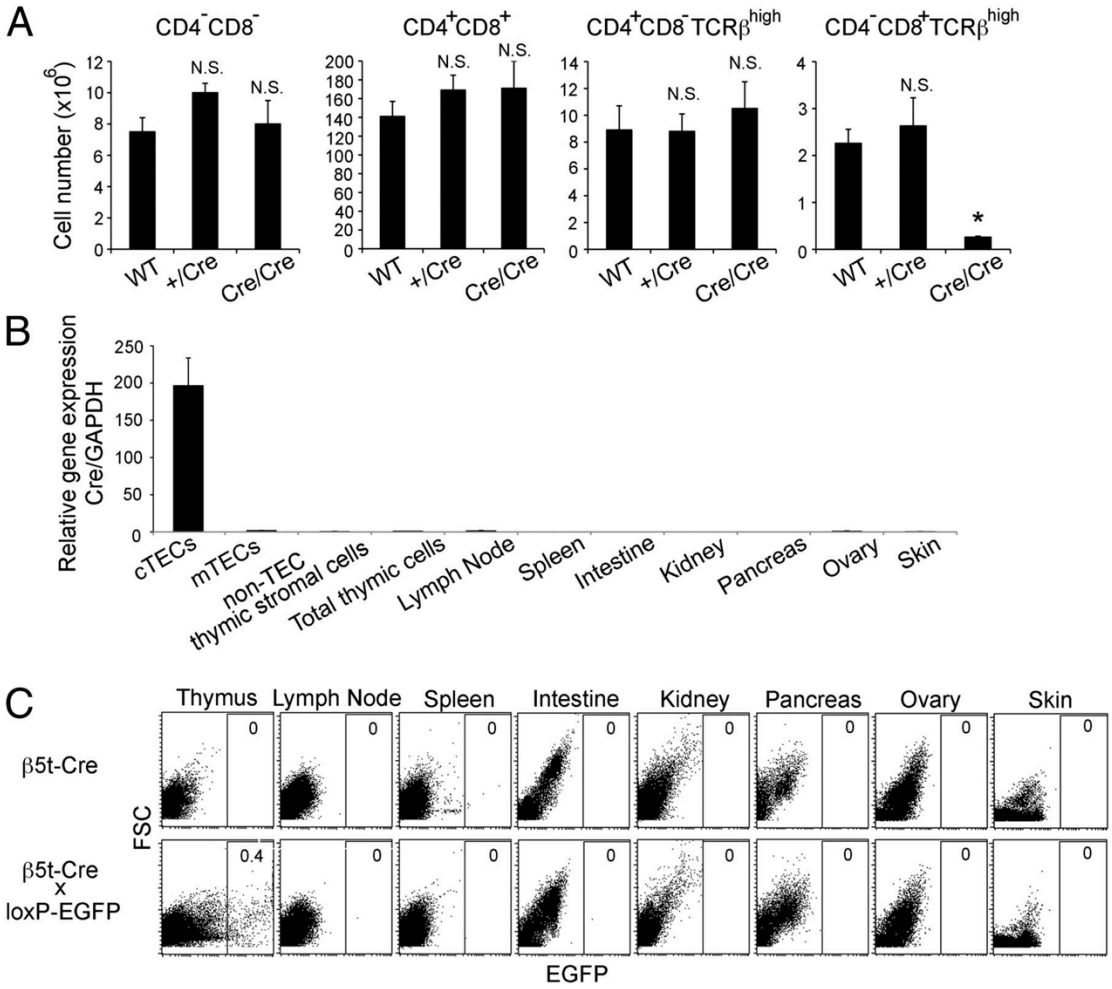

Figure 3.2-1. *β5t-Cre knock-in mice.* (*A*) Numbers (means and SEs, $n = 3$) of $CD4^-CD8^-$, $CD4^+CD8^+$, $CD4^+CD8^-TCR\beta^{high}$, and $CD4^-CD8^+$ $TCR\beta^{high}$ thymocytes in 4-wk-old WT (+/+) and β5t-Cre knock-in heterozygous (+/Cre) and homozygous (Cre/Cre) mice. $^*P < 0.005$; N.S., not significant. (*B*) Relative mRNA expression of Cre in indicated cells and organs isolated from 4- to 5-wk-old β5t-Cre knock-in heterozygous mice. The expression levels (means and SEs, $n = 3$) of Cre measured by quantitative RT-PCR were normalized to that of GAPDH and compared with the level measured in total thymic cells. (*C*) Representative flow cytometry profiles of forward scatter intensity and EGFP expression in collagenase-digested cells obtained from indicated tissues of 4- to 5-wk-old β5t-Cre knock-in mice and β5t-Cre x loxP-EGFP mice. Numbers indicate frequency of $EGFP^+$ cells in total cells. $n = 3$.

3.2.4.2 β5t-Cre-loxP–Mediated GFP Expression Is Specifically Detected in TECs.

To trace the developmental potential of β5t-expressing cells in vivo, β5t-Cre knock-in mice were crossed with CAG-loxP-stop-loxP-EGFP-transgenic (loxP-EGFP) mice, in which EGFP would be ubiquitously expressed under the control of the CAG promoter only when the loxP-flanked stop sequences had been excised by Cre recombinase (13). In β5t-Cre × loxP-EGFP mice, EGFP reporter expression specifically visualizes cells that either express β5t presently or expressed β5t during

their development. We initially examined EGFP expression in adult β5t-Cre × loxP-EGFP mice by flow cytometric analysis of collagenase-digested cells isolated from various organs. We found that $EGFP^+$ cells were detected only in the thymus but not in any other organs (Fig. 1*C*). The thymus-specific EGFP expression in β5t-Cre × loxP-EGFP mice was confirmed by macroscopic fluorescence observation using a transilluminator and by fluorescence microscopy analysis of tissue sections. Within collagenase-digested thymic cells, $EGFP^+$ cells were clearly detected in CD326 [epithelial cell adhesion molecule (EpCAM)]$^+$ TECs but not in $CD326^-$ non-TECs, indicating that β5t-Cre-loxP–mediated EGFP is specifically expressed in TECs (Fig. 2*A*). Immunofluorescence analysis of thymic sections prepared from adult β5t-Venus knock-in mice confirmed that only the cortex but not the medulla expressed the Venus fluorescence (Fig. 2*B*). In striking contrast, EGFP expression in the adult thymus of β5t-Cre × loxP-EGFP mice was detected throughout the thymus (Fig. 2*B*). Specifically, the EGFP signals not only identified CD249 $(Ly51)^+$ cTECs localized in the thymic cortex but also keratin 14 $(K14)^+$ mTECs and keratin 5 $(K5)^+$ mTECs localized in the medulla (Fig. 2*B*). These results indicate that β5t-Cre-loxP–mediated EGFP expression is specifically detected in TECs, and surprisingly, in both cTECs and mTECs.

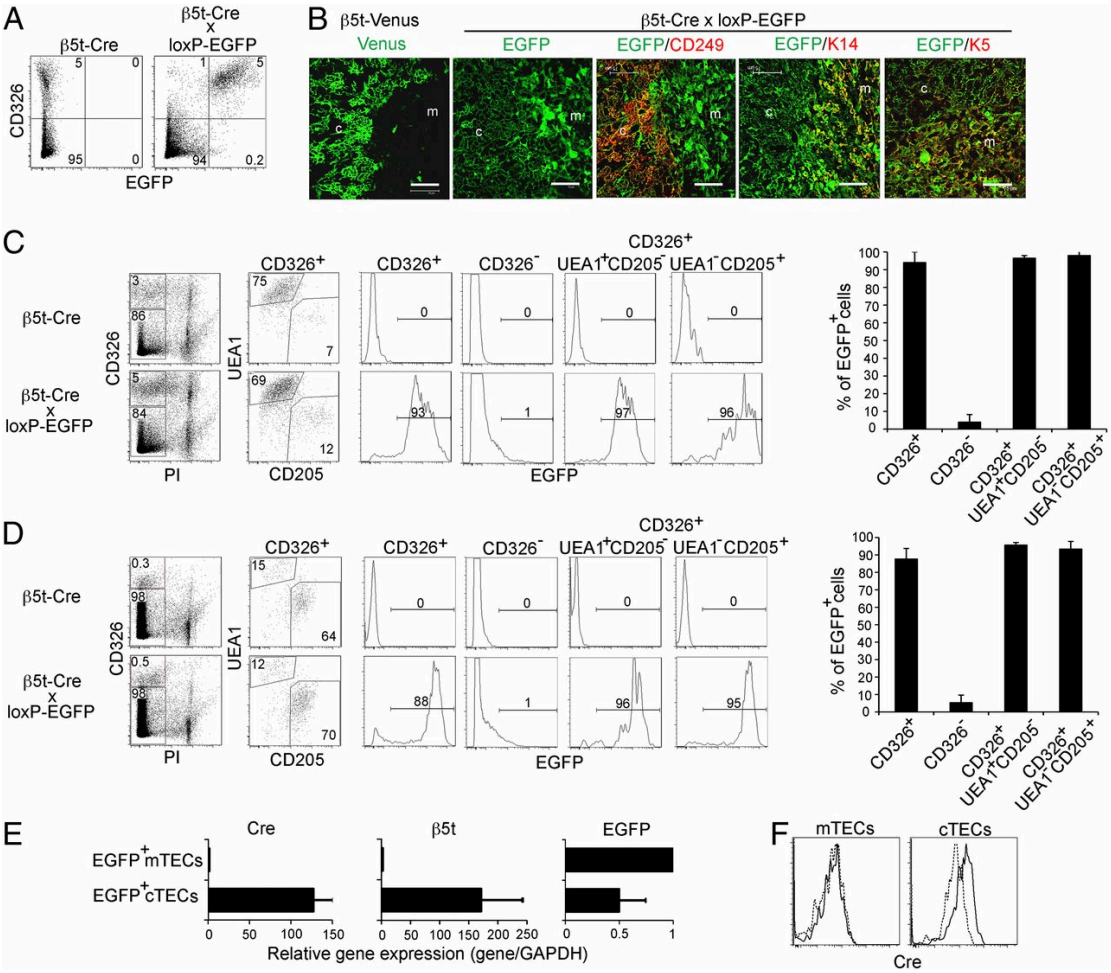

Figure 3.2-2. *β5t-Cre-loxP–mediated GFP expression is detected in mTECs and cTECs.* (*A*) Representative flow cytometry profiles of CD326 and EGFP expression in collagenase-digested thymic cells from 6- to 7-wk-old mice. Thymocytes were depleted from the thymic cells by using magnetic bead–conjugated anti-CD45 antibody. Numbers indicate frequency of cells within indicated areas. $n = 3$. (*B*) Cryosections of the thymus from 6- to 7-wk-old β5t-Venus mice and β5t-Cre × loxP-EGFP mice were analyzed by confocal microscopy. Venus expression and EGFP expression are shown in green. Where indicated, the sections were also stained for CD249 (Ly51), keratin 14 (K14), or keratin 5 (K5) (red). c, cortex; m, medulla. (Scale bar: 75 μm.) Representative results are shown ($n = 3$). (*C* and *D*) Collagenase-digested thymic cells from indicated mice were stained with CD326 antibody and propidium iodide (PI) to identify $CD326^+PI^-$ viable TECs (*Left*). EGFP expression on $CD326^+$ TECs, $CD326^-$ non-TEC thymic cells, $CD326^+UEA1^+CD205^-$mTECs, and $CD326^+UEA1^-CD205^+$ cTECs from 6- to 7-wk-old (*C*) and 0-d-old (*D*) mice (*Center*). Numbers in dot plots and histograms indicate frequency within indicated area. Frequencies (means and SEs, $n = 3$) of $EGFP^+$ cells within indicated cell populations (*Right*). (*E*) The amounts of Cre, β5t, and EGFP mRNAs in $EGFP^+CD326^+UEA1^+CD205^-$ mTECs and $EGFP^+CD326^+UEA1^-CD205^+$ cTECs obtained from 2- to 3-wk-old β5t-Cre × loxP-EGFP mice were measured by quantitative RT-PCR analysis and were normalized to the amount of GAPDH mRNAs. Data represent means and SEs of three independent measurements. (*F*) Flow cytometric analysis of Cre expression in $CD45^-CD326^+CD80^+CD249^-$ mTECs and $CD45^-CD326^+CD80^-CD249^+$ cTECs from 1-wk-old β5t-Cre mice (solid line) or WT mice (dashed line). Data are representative of three independent experiments.

3.2.4.3 β5t-Cre-loxP–Mediated GFP Expression Is Detected in the Majority of mTECs and cTECs.

The histological analysis (Fig. 2*B*) indicated that large proportions of mTECs and cTECs expressed β5t-Cre-loxP–mediated EGFP. To measure the frequency of β5t-Cre-loxP–mediated EGFP expression in cTECs and mTECs, collagenase-digested thymic cells from β5t-Cre × loxP-EGFP mice were multicolor stained for cell-surface markers of cTECs and mTECs. The cells were also stained with propidium iodide to distinguish between viable and dead cells. Analyzed by flow cytometry, $EGFP^+$ viable cells were detected among TECs (i.e., $CD326^+$ cells) but not $CD326^-$ non-TEC thymic cells from both adult (Fig. 2*C*) and newborn (Fig. 2*D*) β5t-Cre × loxP-EGFP mice but not β5t-Cre mice, confirming our previous results (Fig. 2*A*). It was further found that EGFP expression was detected in the majority of both $CD326^+$*Ulex europaeus* agglutinin 1 $(UEA1)^+CD205^-$ mTECs and $CD326^+UEA1^-CD205^+$ cTECs (95 ± 3% in mTECs and 98 ± 2% in cTECs in adult thymus, $n = 3$; and 96 ± 1% in mTECs and 93 ± 4% in cTECs in newborn thymus, $n = 3$) (Fig. 2 *C* and*D*). These results indicate that the majority of mTECs and cTECs in newborn and adult mice exhibit a developmental signature that indicates their current or previous expression of β5t. Because most cTECs are positive for β5t protein (10), β5t-Cre-loxP–mediated EGFP detected in cTECs likely reflects the present expression of β5t in these cells. On the other hand, because β5t protein expression is not detected in mTECs (10), the detection of EGFP in the majority of mTECs from β5t-Cre × loxP-EGFP mice must reflect a previous expression of the β5t gene during development. In keeping with this interpretation, mRNA specific for EGFP but for neither Cre nor β5t was robustly detected in $EGFP^+CD326^+UEA1^+CD205^-$ mTECs isolated from β5t-Cre × loxP-EGFP mice, whereas $EGFP^+CD326^+UEA1^-CD205^+$ cTECs isolated from the same mice concurrently expressed mRNAs specific for EGFP, Cre, and β5t (Fig. 2*E*). Moreover, Cre protein expression was specifically detected in cTECs but not in mTECs (Fig. 2*F*). These results indicate that the majority of mTECs in newborn and adult mice must have previously expressed the β5t gene and that most mTECs must therefore originate from cells that express β5t.

To independently confirm our results, we crossed the β5t-Cre-knock-in mice to a separate reporter mouse strain that carried the CAG-loxP-stop-loxP-Zoanthus green (ZsGreen) gene knocked into the Rosa26 locus (14). To ensure that the Cre-mediated recombination in mTECs was not an artifactual consequence of the engineered β5t locus leaving the neo selection cassette in place, the phosphoglycerate kinase (PGK)-neo sequence was removed by crossing β5t-Cre mice to Flippase (Flp)-deleter animals before breeding to loxP-ZsGreen mice (Fig. S1*A*). On analysis of the resultant β5t-Cre × loxP-ZsGreen mice, we found that ZsGreen was expressed in >99.5% of $CD326^{+}UEA1^{-}CD249^{+}$ cTECs and in >99.5% of $CD326^{+}UEA1^{+}CD249^{-}$ mTECs of the adult thymus (Fig. 3*A*). Moreover, β5t-Cre × loxP-ZsGreen mice displayed normal TEC frequencies and a normal distribution of cTECs and mTECs compared with control loxP-ZsGreen littermates (Fig. 3*A*). Both intrathymic T-cell development and total thymus cellularity were comparable between β5t-Cre × loxP-ZsGreen mice and control loxP-ZsGreen mice (Fig. 3 *B* and *C*). Thus, the expression of either Cre or ZsGreen did not influence TEC viability and function. Immunofluorescence analysis of the thymus tissue sections demonstrated ZsGreen expression that identified most β5t protein–expressing cTECs and K14-expressing mTECs to be positive for ZsGreen (Fig. 3*D*). These results confirm that the β5t-Cre-knock-in locus allows faithful monitoring of present and past β5t expression and that almost all mTECs are derived from cells that previously expressed β5t.

A small subpopulation (~5%) of mTECs did not express β5t-Cre-loxP–mediated EGFP in β5t-Cre × loxP-EGFP mice (Fig. 2 *C* and *D*). However, ZsGreen-negative mTECs were barely detectable (<0.5% of total mTECs) in β5t-Cre × loxP-ZsGreen mice, indicating that the majority (>99.5%) of mTECs are derived from β5t-expressing progenitor cells (Fig. 3*A*). The few EGFP-negative mTECs detected in β5t-Cre × loxP-EGFP mice may reflect a slightly inefficient detection of fluorescence in this particular reporter mouse strain, possibly in part because of the reduced brightness and photo-stability of EGFP compared with ZsGreen (15). Indeed, we detected comparable amount of EGFP mRNA in $EGFP^{-}$ and $EGFP^{+}$ mTECs isolated from β5t-Cre × loxP-EGFP mice. The expression levels of EGFP and ZsGreen are higher in cTECs than in mTECs in both β5t-Cre × loxP-EGFP mice and β5t-Cre ×

loxP-ZsGreen mice (Figs. 2 and 3). This difference in fluorescence may reflect the larger size of cTECs compared with mTECs (16), which in turn accounts for a more abundant accumulation of EGFP protein in cTECs than mTECs.

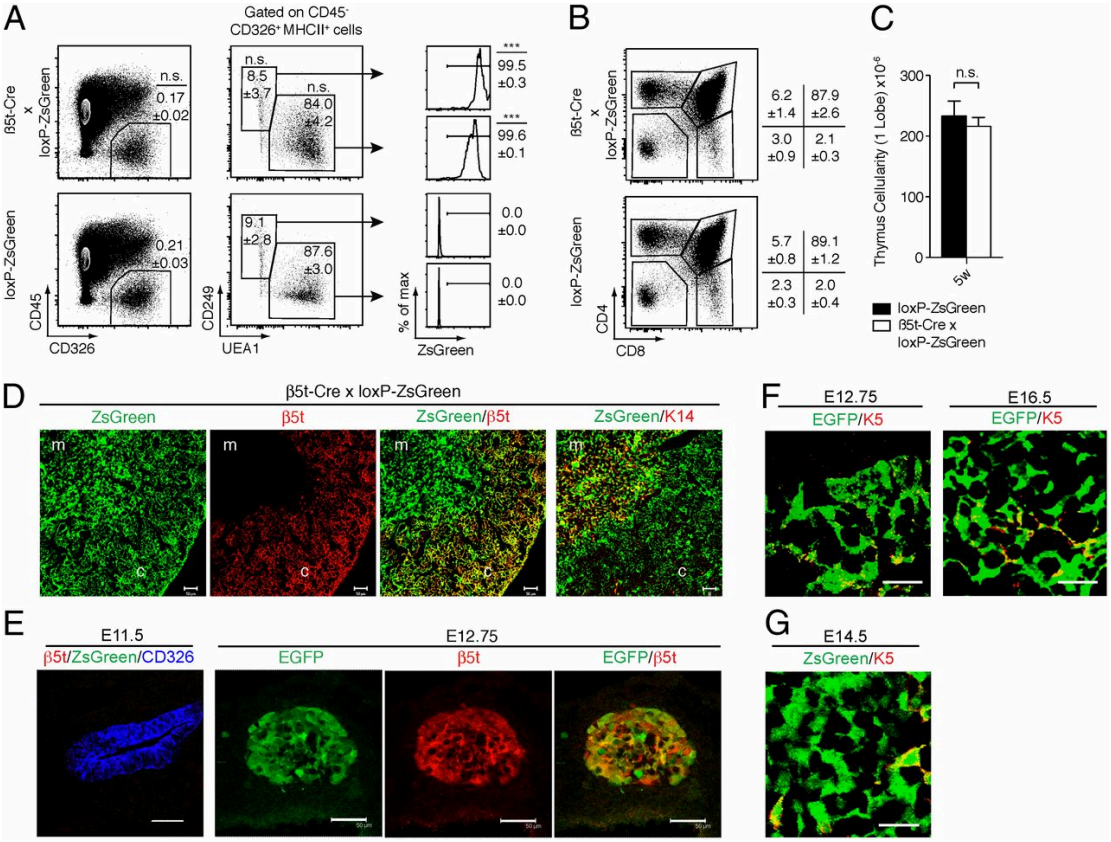

Figure 3.2-3. *β5t-Cre-knock-in locus allows faithful monitoring of present and past β5t expression.* (*A*) Flow cytometric analysis of CD45⁻ CD326⁺ MHC class II⁺ TEC subpopulations from 6-wk-old β5t-Cre × loxP-ZsGreen and loxP-ZsGreen mice. Relative frequencies (means and SEs, $n = 3$) of all TECs, UEA1⁻CD249⁺cTECs, and UEA1⁺CD249⁻ mTECs are indicated in dot plots. Histograms display frequencies (means and SEs, $n = 3$) of ZsGreen-positive cTECs and mTECs. ***$P < 0.001$; n.s., not significant (comparison between β5t-Cre × loxP-ZsGreen and loxP-ZsGreen cells). (*B*) Flow cytometric analysis of thymocytes for the cell surface expression of CD4 and CD8. The cells were isolated from 6-wk-old loxP-ZsGreen and β5t-Cre × loxP-ZsGreen mice. Numbers denote frequency of cells within indicated gates (means and SEs, $n = 3$). (*C*) Total cellularity (means and SEs, $n = 3$) of the thymus in 5-wk-old loxP-ZsGreen (black bar) and β5t-Cre x loxP-ZsGreen (white bar) mice. n.s., not significant. (*D*) Immunofluorescence analysis of thymus tissues from 6-wk-old β5t-Cre x loxP-ZsGreen mice for the expression of ZsGreen (green), β5t (identifying cTEC, red) and K14 (detecting mTECs, red). Data are representative of at least two separate experiments using two mice each. (Scale bar: 50 μm.) c, cortex; m, medulla. (*E*) E11.5 embryos of β5t-Cre × loxP-ZsGreen mice and E12.75 embryos of β5t-Cre × loxP-EGFP mice were stained with anti-β5t antibody. ZsGreen or EGFP fluorescence (green) and anti-β5t immunofluorescence (red) in the pharyngeal region containing the thymic primordium were measured. Where indicated, the sections were additionally stained with anti-CD326 antibody (blue). Shown are representative results of three independent experiments. (Scale bar: 50 μm.) (*F*) E12.75 embryos and E16.5 embryonic thymuses of β5t-Cre × loxP-EGFP mice were stained with anti-K5 antibody. Shown are representative results ($n = 3$) of EGFP fluorescence (green) and anti-K5 immunofluorescence (red) of the thymic primordium (E12.75) and the thymus (E16.5). (Scale bar: 20 μm.) (*G*) E14.5 embryonic thymuses

of β5t-Cre × loxP-ZsGreen mice were stained with anti-K5 antibody. Representative results of ZsGreen fluorescence (green) and anti-K5 immunofluorescence (red) are shown (n = 2). (Scale bar: 20 μm.)

3.2.4.4 β5t-Cre-loxP–Mediated GFP Expression Is Detected in Embryonic mTECs.

EGFP expression in β5t-Cre × loxP-EGFP mice was detectable in TECs as early as embryonic day 12.75 (E12.75) (Fig. 3*E*), approximately half a day after the first detection of β5t protein between E12 and E12.5 (10). Interestingly, β5t protein expression was undetectable in a minor fraction of EGFP$^+$ cells localized in the central region of the E12.75 thymus (Fig. 3*E*), indicating that a minor fraction of TECs localized in the central region of embryonic thymus previously transcribed β5t but have terminated β5t expression before E12.75. Indeed, most TECs in β5t-Cre × loxP-EGFP mice at E12.75 and E16.5 (Fig. 3*F*) and in β5t-Cre × loxP-ZsGreen mice at E14.5 (Fig. 3*G*) that were localized in the central region of fetal thymus and that highly expressed the mTEC-associated marker K5 (17, 18) also expressed EGFP and ZsGreen, respectively. These results suggest that embryonic mTECs, identified by the abundant expression of K5, are derived from β5t-expressing cells.

3.2.4.5 β5t-Cre-loxP–Mediated GFP Expression Is Detected in the Majority of Aire$^+$ mTECs.

Finally, we examined whether Aire-expressing mTECs were derived from β5t-expressing progenitor cells. In the adult thymus of β5t-Cre × loxP-EGFP mice, we found that most Aire$^+$ mTECs were EGFP$^+$ (Fig. 4*A*). Flow cytometric analysis indicated that 97 ± 1% (n = 3) of Aire$^+$UEA1$^+$ mTECs in the adult thymus were EGFP$^+$(Fig. 4*B*). During ontogeny, Aire expression in mTECs was detectable as early as E16 (19, 20). We found that most (99 ± 1% and 93 ± 2%, n = 3) Aire$^+$ mTECs at E16.5 and at postnatal day 1 were EGFP$^+$ (Fig. 4 *C*–*E*). These results indicate that the majority of Aire-expressing mTECs are derived from β5t-expressing progenitor cells throughout ontogeny, including the perinatal period in which Aire expression is important for the establishment of long-lasting self-tolerance in T cells (7). The expression of EGFP is evident in most mTECs, including the majority of Aire-

expressing mTECs, indicating that these cells are derived from progenitor cells that express β5t.

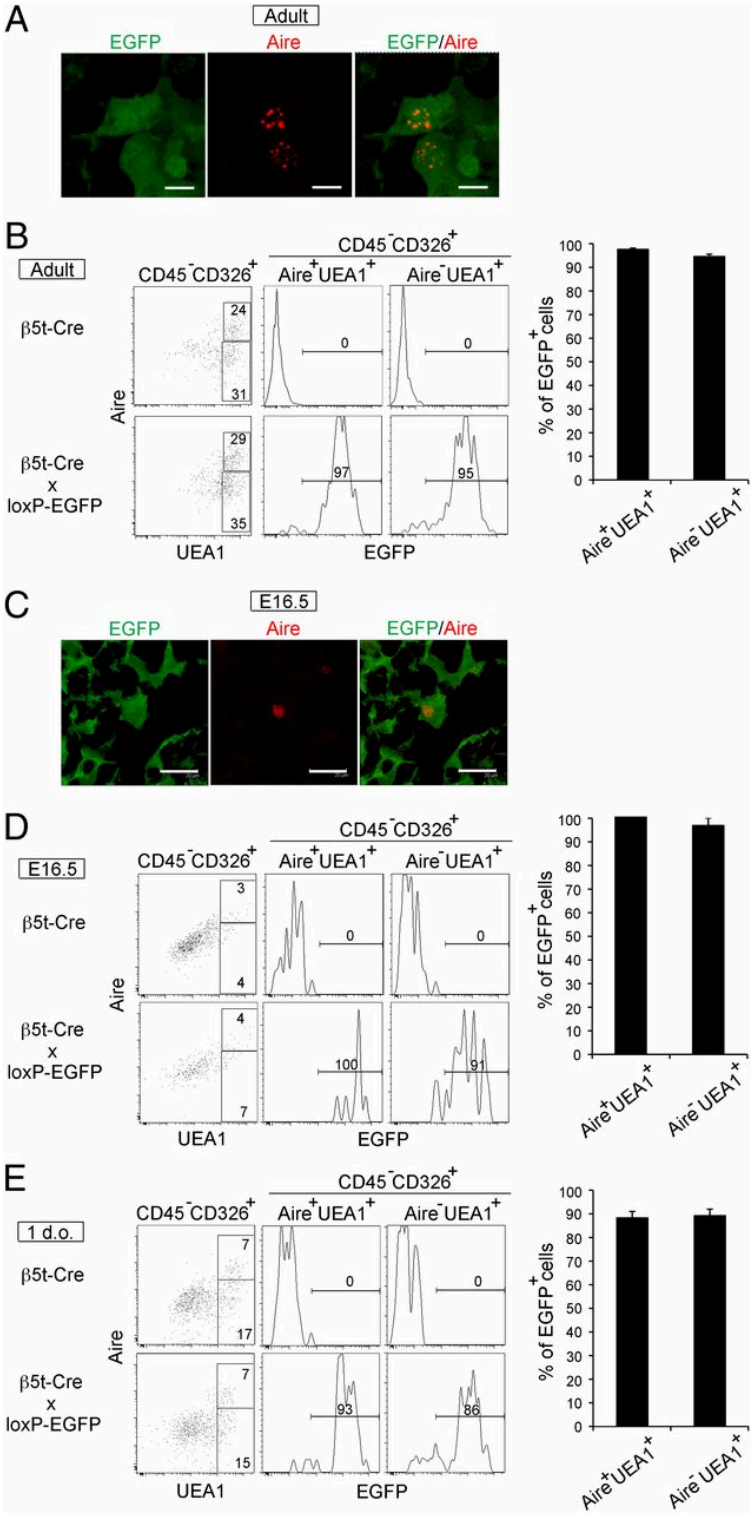

Figure 3.2-4. *β5t-mediated GFP expression is detected in the majority of Aire⁺ mTECs.* Cryosections of the thymus from 6- to 7-wk-old (*A*) and E16.5 (*C*) β5t-Cre × loxP-EGFP mice were analyzed by confocal

microscopy. (Scale bars: *A*, 7 μm; *C*, 20 μm.) Representative images of EGFP (green) and Aire (red) are shown (n = 3). (*B*, *D*, and *E*) Representative flow cytometry profiles of EGFP expression in $CD45^{-}CD326^{+}Aire^{+}UEA1^{+}$ and $CD45^{-}CD326^{+}Aire^{-}UEA1^{+}$ cells from indicated mice at 5–6 wk old (*B*), E16.5 (*D*), and 1 d old (*E*). Numbers in plots indicate frequency within indicated area. Frequencies of $EGFP^{+}$ cells within $CD45^{-}CD326^{+}Aire^{+}UEA1^{+}$ and $CD45^{-}CD326^{+}Aire^{-}UEA1^{+}$ cells are plotted (means and SEs, n = 3).

3.2.5 Discussion

The functional importance of mTECs, particularly Aire-expressing mTECs, in the establishment of self-tolerance in T cells has been well characterized (6, 21). Molecular signals that regulate the development and proliferation of mTECs, such as TNF superfamily receptor signals linked with NF-κB transcription factors, have been described (5, 22). It has further been established that both mTECs and cTECs are derived during embryogenesis from the endodermal epithelium of the third pharyngeal pouch (1). However, developmental pathways from the third pharyngeal pouch epithelial cells to functionally mature TECs remain largely unclear. Progenitor cells capable of giving rise to both cTECs and mTECs are detected in the embryonic thymus (23). These TEC progenitor cells were found to express the transcription factor Foxn1 (8) and the cell-surface molecule placenta expressed transcript 1 (Plet-1) (24). It was also reported that embryonic TECs that highly express Claudins 3 and 4 contained the developmental potential to give rise to mTECs but not cTECs (25). However, TEC progenitor cells that generate the majority of perinatal and postnatal mTECs have not been retrospectively characterized. Our results surprisingly demonstrate that almost all mTECs, including the majority of Aire-expressing mTECs, in embryonic, neonatal, and adult thymus have transiently expressed β5t gene. The expression of β5t-Cre must be transient as Cre and β5t transcripts and proteins cannot be detected in mTECs. Thus, our results reveal that the majority of mTECs originate from progenitor cells that transiently express β5t.

mTECs promiscuously express tissue-restricted self-antigens, which contribute to the establishment of self-tolerance in T cells. Does the β5t-Cre-loxP–mediated EGFP expression in mTECs reflect the promiscuous gene expression in mTECs? Using single-cell analysis of mTECs, promiscuous expression of tissue-restricted self-antigens was measured and found to exhibit expression frequencies between 2% and

15% at mRNAs and between 1% and 3% at proteins (26, 27). On the contrary, our results show that the β5t-Cre-loxP–mediated EGFP expression is detectable in most (>90%) mTECs, including $Aire^{+}$ mTECs and $Aire^{-}$ mTECs (Fig. 4) as well as embryonic mTECs (Fig. 3 *F* and *G*). In addition, neither β5t nor Cre is detected in $EGFP^{+}$mTECs (Fig. 2 *E* and *F*). Thus, it is unlikely that the β5t-Cre-loxP–mediated EGFP expression in mTECs results from the promiscuous expression of β5t, Cre, and/or EGFP. Rather, the detection of EGFP in mTECs of β5t-Cre × loxP-EGFP mice is likely the consequence of β5t expression in precursor cells leading to the development of mTECs.

β5t-Cre-knock-in mice established in this study constitute a potentially useful tool for the study of TEC biology. Foxn1-Cre–expressing mice have been widely used for Cre-loxP–mediated TEC-targeted gain-of-function and loss-of-function studies (28, 29). However, Foxn1 is additionally expressed in the skin epithelium (30, 31). In contrast, our results show that β5t-Cre is specifically expressed in TECs but not in any other cell types or any other tissues, including the skin. Thus, the β5t-Cre-knock-in mice serve as a unique tool for TEC-specific genomic manipulations.

β5t-Cre-loxP–mediated EGFP expression is already detected during thymus organogenesis in early mTECs identified by the expression of K5 (Fig. 3 *F* and *G*). It was reported that $K5^{high}$ mTECs could be detected in the embryonic thymus of Foxn1-deficient mice, suggesting that Foxn1 is not required for the divergence of the mTEC lineage from bipotent cTEC/mTEC progenitors (18). It could therefore be informative to clarify whether progenitor cells that transiently express β5t may also be generated without Foxn1, although the Foxn1 dependence of β5t expression (10) does not readily allow the identification of these cells and their progeny. Nonetheless, because the cellularity and Aire expression of mTECs in β5t-deficient mice are not defective or altered (9, 11), it is conceivable that the transient expression of β5t during early mTEC development is dispensable for the divergence of the mTEC lineage and the consequent development of phenotypically and functionally mature mTECs.

The detection of β5t-Cre-loxP–mediated EGFP expression already in embryonic mTECs points to an early and transient β5t expression during mTEC development. It was previously shown that β5t expression is not detectable in the E11.5 thymus primordium (10), which expresses Foxn1 and presumably contains early TEC progenitor cells. Our results also demonstrate that the β5t-Cre-loxP–mediated reporter expression is not detectable in E11.5 thymus primordia (Fig. 3*E*). These findings suggest that β5t is not expressed in bipotent TEC progenitor cells at E11.5 and that β5t expression is initiated at the stage of TEC differentiation following the initial emergence of common TEC progenitor cells but before the detection of mTEC-restricted progenitor cells. It is possible that bipotent TEC progenitor cells may begin coexpressing a set of cTEC-associated genes, including β5t, and a set of mTEC-associated genes. Once developmental lineage is determined to be either cTECs or mTECs, the expression of lineage-compatible molecules may be secured and the expression of molecules specific for another lineage may be eventually terminated. Alternatively, it is also possible that bipotent TEC progenitor cells may begin expressing a set of cTEC-associated genes, including β5t, rather than a set of mTEC-associated genes. A developmental program driving the cTEC lineage, or the β5t-expressing lineage, may thus represent a default pathway for TEC development, whereas divergence to the mTEC lineage may require additional signals. It is further possible that β5t may be transiently transcribed after commitment to the mTEC lineage and then terminated during the subsequent differentiation into mature mTECs. Nevertheless, our unexpected observation that β5t is transiently expressed during early mTEC development precludes the possibility that mTECs are generated independent of cTEC-associated genetic programs including the expression of β5t, which is essential for cTEC function.

In conclusion, this study demonstrates that most mTECs are derived from β5t-expressing progenitor cells. mTECs play an essential role in the establishment of self-tolerance in T cells that have been newly generated by cTEC-mediated positive selection in the cortex, so that mTECs are important only when cTECs are present and functional. It can be thus speculated that the development of mTECs may be installed as a secondary consequence to the development of cTECs and that the

expression of cTEC-associated β5t during the development of mTECs may reflect the cTEC origin of mTECs. These speculations are supported by the recent observation that Aire-expressing mTECs can be generated upon transplantation of embryonic TECs that express CD205, which is highly expressed by adult cTECs but not mTECs (32). Consequently, it would be interesting to establish whether the mechanisms for the development of mTECs and cTECs are symmetric or asymmetric. Further characterization of TEC progenitors at the clonal level and the molecular mechanisms driving the development of the two distinct TEC lineages will enhance our understanding of how the thymic microenvironment is differentiated into the cortical and medullary compartments and how the separate cortical and medullary regions are maintained.

3.2.6 Materials and Methods

Mice

β5t-Venus knock-in mice (1), CAG-loxP-stop-loxP-EGFPtransgenic mice (2), and Rosa26 knock-in mice that were engineered to contain the CAG-loxP-stop-loxP-ZsGreen sequence (3) were described previously. Flp-deleter (129S4/SvJaeSor-Gt (ROSA)26Sortm1(FLP1)Dym/J) mice were obtained from The Jackson Laboratory. For developmental staging, the day of the vaginal plug was designated as E0.5. Mice were maintained under specific pathogen-free conditions and experiments were carried out under the approval of the Institutional Animal Care and Use Committee of the University of Tokushima and according to Swiss cantonal and federal regulations and permissions.

Generation of β5t-Cre Knock-In Mice

β5t-Cre targeting construct was prepared by subcloning cDNA encoding the codon-improved Cre recombinase (iCre, a gift from Dr. R. Sprengel, Heidelberg, Germany) into the targeting vector with β5t homology arms (1) containing a PGK-neo cassette in a transcriptionally opposite direction that is flanked by flippase recognition target

sites. The linearized vector was electroporated into 129xC57BL/6 ES cells and correctly targeted clones were identified by PCR and verified by Southern blotting. Chimeric mice were generated using standard techniques and further bred to a C57BL/6 background. The genotypes of β5t-Cre mice were determined by PCR analysis of tail DNA using the following three primers: β5t 5′ untranslated region forward primer, 5′-ATCCCTCACCAGCCAATTCCAAAGCC-3′; β5t coding sequence reverse primer, 5′- TGGTGCACAGGAATGACCTTCCGT-3′; and iCre reverse primer, 5′- GAGATGTCCTTCACTCTGATTC-3′. The amplified products were electrophoresed on 1.0% agarose gel and visualized with ethidium bromide.

Immunohistology

Tissues were fixed in 4% (g/vol) paraformaldehyde, embedded in optimum cutting temperature (OCT) compound (Sakura Finetek), and frozen. Thymuses and embryos were sliced into 5-μm-thick and 10-μm-thick sections, respectively. The sections were stained using antibodies specific for GFP (Invitrogen), keratin (K) 5 (Covance), K14 (Covance), CD249 (Ly51, eBioscience), CD326 (EpCAM, BioLegend), β5t (1), and Alexa Fluor 647-conjugated anti-Aire antibody (eBioscience). Alexa-Fluor conjugated anti-IgG antibodies (Invitrogen) were used as secondary reagents. Images were analyzed with a TSC SP2 confocal laser-scanning microscope and Leica Confocal software (version 2.6, Leica).

Cell Preparation

Minced fragments of the thymus and other organs were digested with 0.125% collagenase D (Roche) in the presence of 0.01% DNase I (Roche), as described previously (4). For the analysis and isolation of TECs, CD45+ cells were depleted using magnetic bead–conjugated anti-CD45 antibody (Miltenyi Biotech).

Flow Cytometry

Multicolor flow cytometry and cell sorting were performed with FACSAria II (BD Bioscience). For the analysis of TECs, cells were stained for the expression of CD326 (EpCAM, BioLegend), CD205 (eBioscience), CD249 (Ly51, eBioscience), and CD45 (eBioscience) and for reactivity with UEA1 (Vector Laboratories). For intracellular Aire staining, cells were surfacestained for CD45, CD326, and UEA1 reactivity, fixed in 2% paraformaldehyde, permeabilized with 0.1% saponin, and stained with Alexa Fluor 647-conjugated anti-Aire antibody (eBioscience). For intracellular Cre staining, cells were surface-stained for CD45, CD326, CD80, and CD249, fixed in 2% paraformaldehyde, permeabilized with 0.1% saponin, and stained with biotinylated anti-Cre antibody (Covance) followed by allophycocyanin-conjugated streptavidin. For the analysis of thymocytes, cells were stained with allophycocyanin-conjugated anti-CD4 antibody (BioLegend) and biotinylated anti-CD8 antibody (BioLegend) followed by phycoerythrin-conjugated streptavidin.

Quantitative mRNA Analysis

Total cellular RNA was reverse-transcribed with oligo-dT primer and SuperScript III reverse transcriptase (Invitrogen). Quantitative real-time PCR was performed using SYBR Premix Ex Taq (TaKaRa) and a 7900HT Sequence Detection System (Applied Biosystems). The primers used were as follows: Cre, 5′-GACTACCTCCTGTACCTGCA-3′ and 5′-GAGATGTCCTTCACTCTGATTC-3′; EGFP, 5′-AGCAAGGGCGAGGAGCTGTT-3′ and 5′-GTAGGTCAGGGTGGTCACGA-3′; β5t, 5′-CTCTGTGGCTGGGACCACTC-3′ and 5′-TCCGCTCTCCCGAACGTGG-3′; and GAPDH, 5′-TTGTCAGCAATGCATCCTGCAC-3′ and 5′-GAAGGCCATGCC AGTGAGCTTC-3′. The amplified products were confirmed to be single bands by gel electrophoresis and normalized to the amount of GAPDH amplification products.

3.2.7 References

1. Manley NR, Blackburn CC (2003) A developmental look at thymus organogenesis: Where do the non-hematopoietic cells in the thymus come from? Curr Opin Immunol 15(2):225–232.
2. Boehm T (2008) Thymus development and function. Curr Opin Immunol 20(2): 178–184. 3.
3. Rodewald HR (2008) Thymus organogenesis. Annu Rev Immunol 26:355–388.

4. Klein L, Hinterberger M, Wirnsberger G, Kyewski B (2009) Antigen presentation in the thymus for positive selection and central tolerance induction. Nat Rev Immunol 9(12): 833–844.

5. Anderson G, Takahama Y (2012) Thymic epithelial cells: Working class heroes for T cell development and repertoire selection. Trends Immunol 33(6):256–263.

6. Mathis D, Benoist C (2009) Aire. Annu Rev Immunol 27:287–312.

7. Guerau-de-Arellano M, Martinic M, Benoist C, Mathis D (2009) Neonatal tolerance revisited: A perinatal window for Aire control of autoimmunity. J Exp Med 206(6): 1245–1252.

8. Bleul CC, et al. (2006) Formation of a functional thymus initiated by a postnatal epithelial progenitor cell. Nature 441(7096):992–996.

9. Murata S, et al. (2007) Regulation of CD8+ T cell development by thymus-specific proteasomes. Science 316(5829):1349–1353.

10. Ripen AM, Nitta T, Murata S, Tanaka K, Takahama Y (2011) Ontogeny of thymic cortical epithelial cells expressing the thymoproteasome subunit β5t. Eur J Immunol 41(5):1278–1287.

11. Nitta T, et al. (2010) Thymoproteasome shapes immunocompetent repertoire of CD8+ T cells. Immunity 32(1):29–40.

12. Takahama Y, et al. (2010) Role of thymic cortex-specific self-peptides in positive selection of T cells. Semin Immunol 22(5):287–293.

13. Kawamoto S, et al. (2000) A novel reporter mouse strain that expresses enhanced green fluorescent protein upon Cre-mediated recombination. FEBS Lett 470(3):263–268.

14. Madisen L, et al. (2010) A robust and high-throughput Cre reporting and characterization system for the whole mouse brain. Nat Neurosci 13(1):133–140.

15. Harrell JC, et al. (2006) Estrogen receptor positive breast cancer metastasis: Altered hormonal sensitivity and tumor aggressiveness in lymphatic vessels and lymph nodes. Cancer Res 66(18):9308–9315.

16. Nakagawa Y, et al. (2012) Thymic nurse cells provide microenvironment for secondary T cell receptor α rearrangement in cortical thymocytes. Proc Natl Acad Sci USA 109(50):20572–20577.

17. Klug DB, Carter C, Gimenez-Conti IB, Richie ER (2002) Cutting edge: Thymocyte independent and thymocyte-dependent phases of epithelial patterning in the fetal thymus. J Immunol 169(6):2842–2845.

18. Nowell CS, et al. (2011) Foxn1 regulates lineage progression in cortical and medullary thymic epithelial cells but is dispensable for medullary sublineage divergence. PLoS Genet 7(11):e1002348.

19. Rossi SW, et al. (2007) RANK signals from CD4(+)3(-) inducer cells regulate development of Aire-expressing epithelial cells in the thymic medulla. J Exp Med 204(6): 1267–1272.

20. Gäbler J, Arnold J, Kyewski B (2007) Promiscuous gene expression and the developmental dynamics of medullary thymic epithelial cells. Eur J Immunol 37(12):3363– 3372.

21. Kyewski B, Klein L (2006) A central role for central tolerance. Annu Rev Immunol 24: 571–606.

22. Derbinski J, Kyewski B (2005) Linking signalling pathways, thymic stroma integrity and autoimmunity. Trends Immunol 26(10):503–506.

23. Rossi SW, Jenkinson WE, Anderson G, Jenkinson EJ (2006) Clonal analysis reveals a common progenitor for thymic cortical and medullary epithelium. Nature 441(7096): 988–991.

24. Depreter MG, et al. (2008) Identification of Plet-1 as a specific marker of early thymic epithelial progenitor cells. Proc Natl Acad Sci USA 105(3):961–966.

25. Hamazaki Y, et al. (2007) Medullary thymic epithelial cells expressing Aire represent a unique lineage derived from cells expressing claudin. Nat Immunol 8(3): 304–311.

26. Cloosen S, et al. (2007) Expression of tumor-associated differentiation antigens, MUC1 glycoforms and CEA, in human thymic epithelial cells: Implications for self-tolerance and tumor therapy. Cancer Res 67(8):3919–3926.

27. Derbinski J, Pinto S, Rösch S, Hexel K, Kyewski B (2008) Promiscuous gene expression patterns in single medullary thymic epithelial cells argue for a stochastic mechanism. Proc Natl Acad Sci USA 105(2):657–662.

28. Gordon J, et al. (2007) Specific expression of lacZ and cre recombinase in fetal thymic epithelial cells by multiplex gene targeting at the Foxn1 locus. BMC Dev Biol 7:69.

29. Zuklys S, et al. (2009) Stabilized β-catenin in thymic epithelial cells blocks thymus development and function. J Immunol 182(5):2997–3007.

30. Weiner L, et al. (2007) Dedicated epithelial recipient cells determine pigmentation patterns. Cell 130(5):932–942.

31. Hu B, et al. (2010) Control of hair follicle cell fate by underlying mesenchyme through a CSL-Wnt5a-FoxN1 regulatory axis. Genes Dev 24(14):1519–1532.

32. Baik S, Jenkinson EJ, Lane PJ, Anderson G, Jenkinson WE (2013) Generation of both cortical and Aire(+) medullary thymic epithelial compartments from CD205(+) progenitors. Eur J Immunol 43(3):589–594.

3.2.8 Supplementary Material

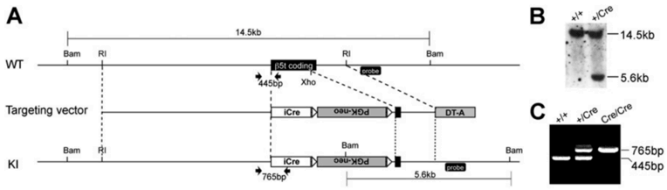

Fig. S1. Generation of β5t-Cre knock-in mice. (*A*) Schematic illustration of β5t genomic locus, targeting vector, and targeted locus. Bam, BamHI; DT-A, diphtheria toxin A; iCre, codon-improved Cre; KI, knock-in; PGK-neo, phosphoglycerate kinase I promoter-driven neomycin resistance gene; RI, EcoRI. Open triangles represent the flippase recognition target (frt) sites. In the KI allele, iCre-encoding cDNA replaces the β5t-encoding sequence. (*B*) Southern blot analysis of BamHI-digested genomic DNA from WT (+/+) and β5t-Cre knock-in heterozygous (+/Cre) mice. The probe is shown in *A*. (*C*) PCR analysis of genomic DNA isolated from WT (+/+), β5t-Cre knock-in heterozygous (+/Cre), and homozygous (Cre/Cre) mice. PCR primers are shown in *A*.

3.3 Embryonic medullary epithelial lineage specification is characterized by an early down-regulation of classical cortical markers

3.3.1 Introductory notes

The work in this chapter is based on the observation that TEC precursors to the cortical and the medullar lineage express the putative cTEC marker β5t very early during thymic organogenesis. Based on this knowledge I am interested to map early TEC differentiation and to characterize more precisely the differentiation of specific subpopulations than what is currently known. In aggregate, this work narrows down the phenotype of progenitor cells at the point of divergence of both individual TEC lineages (i.e. cortical and medullar TEC) early during thymus development.

3.3.2 Introduction

The murine thymus originates from the endodermal lining of the third pharyngeal pouch that develops around embryonic day of development (E) 9.5 (1). This early anlage at the third pharyngeal pouch gives rise to the parathyroid and the thymus, respectively, which are characterized by the expression of Gcm2 from E9.5 onwards and Foxn1 starting on E10.5. While Foxn1 is not required for the generation and maintenance of thymic epithelial cell (TEC) precursors or the initial steps of TEC differentiation, it is required for the proliferation and maturation of those cells by driving the expression of attraction, expansion and maturation molecules that are required to drive T cell development in the developing thymus (2–4). As a consequence of the early expression of Foxn1 during early thymus organogenesis cells of hematopoietic origin migrate to the thymus were they directly engage with TEC. This contact has been shown to play an important role in mTEC differentiation and is in part mediated by signaling through receptors of the tumor necrosis factor receptor superfamily such as Receptor Activator of Nuclear Factor κ B (RANK) (5), Lymphotoxin β receptor (6–9), and CD40 (5). In addition, several components of the canonical and non-canonical NF- κB signaling pathway including relB (10, 11), NF-

κB-inducing kinase (Nik) (12, 13), IkB kinase (IKK) α (14) and TRAF6 (15) have been shown to play essential roles. Furthermore, RANKL and CD40L-mediated signaling initiated by lymphoid tissue-inducer cells (LTi) and invariant Vγ5+ dendritic epidermal T cell (DETC) progenitors promote proliferation and maturation of mTEC progenitor cells (5, 16–18). These two alternative signaling axes are not only important for the initial patterning of the mTEC compartment, but probably remain important later during thymus homeostasis because continuous RANK and CD40 engagement (now mainly provided by post-selection thymocytes) maintain the mature medullary epithelial compartment since deficiencies in these molecules reveal low numbers of the most mature mTEC (18, 19).

The characterization of early TEC differentiation has been challenging due to the lack of appropriate markers. Recently it has been shown that both cortical and medullar TEC emerge from cells that express the classical cTEC markers CD205 and β5t (20, 21). This fits with the previous observations whereby embryonic TEC development, when characterized by flow cytometry through the detection of CD205 (a.k.a. DEC205, Ly75) and CD40, appeared to pass through a stage of CD205-expression (22). The analysis with those markers allowed for the subdivision of developing TEC into very immature TEC (CD40- CD205-), cTEC-like progenitor cells (CD40-/lo CD205+) and mature mTEC (CD40+ CD205-). Nonetheless, early TEC differentiation is still incompletely characterized resulting therefore only in a very coarse "road map" of development. Especially intermediate stages of cells committing to the medullary TEC lineage have so far not properly been captured as only very few markers are currently known to determine individual developmental and maturational mTEC stages. Among the reagents in use for this purpose is the Fucose-binding lectin Ulex europaeus agglutinin 1 (UEA1), which is commonly known as a marker for cells that have fully committed to the medullar epithelial lineage. Expression of the autoimmune regulator (Aire) in the adult mouse is a feature characteristic of very mature mTEC. Curiously, the expressional dynamics of the available mTEC markers are only poorly understood during embryonic mTEC specification.

To contribute to a more detailed description of the individual developmental stages in TEC lineage differentiation, I investigated the dynamics of CD205 and CD40 expression during embryonic mTEC development in combining with various other markers that have so far been mainly used to characterize adult TEC in cortex and medulla. A special focus was given to characterize the progenitor population from which both thymic epithelial lineages emerge.

3.3.3 Results

3.3.3.1 Dynamic phenotypic change of TEC during embryonic mTEC differentiation

I set out to characterize early TEC differentiation through the means of flow cytometry, as this technique offers the advantage to measure the relative expression of several markers on a per-cell basis and in parallel offers the possibility to perform quantitative analyses at the population level. Investigations to analyze TEC phenotypes at time points earlier than E15.5 used C57Bl/6 mice and required owing to the low TEC cellularity the pooling of individual lobes. Mice expressing the green fluorescent protein under the transcriptional control of the Aire promoter (designated Aire-GFP) were time-mated and analyzed at embryonic day (E) 15.5, 16.5 or 17.5.

At E14.5, the thymus contained a high proportion of TEC (~38%) (Figure 1A). This proportion continuously diminished reaching a frequency of 4% in embryos at E17.5 and of ~0.2% in 5 week old mice (Chapter 2, Figure 3A). This decrease in relative TEC cellularity in the course of intrauterine and early postnatal development was paralleled by a massive increase in the absolute (and hence also relative) number of cells of hematopoietic origin (i.e. CD45+) (Figure 1A). To investigate thymic epithelial development during these dynamic changes, we examined TEC for the expression of CD40 and CD205 (Figure 1B, *upper panel*). At E14.5 most TEC revealed a CD40-/lo CD205+ immature phenotype compatible with a presumed cTEC identity and in accordance with previous reports (22). During E15.5-17.5, TEC begun to upregulate CD40 and to downregulate CD205 cell surface expression resulting in a phenotype

commonly associated with mature mTEC in the adult mouse. In parallel with this maturational change, fewer TEC displayed the immature CD40- CD205- and CD40- CD205+ phenotypes. The growth of distinct medullary islets becomes clearly visible between E14.5 and E17.5 when TEC with medullary phenotype can be first detected. To investigate early mTEC differentiation we further analyzed TEC for their reactivity with UEA1, a fucose binding lectin reactive during development and with most adult mTEC, and the expression of CD40. The combined use of these markers allowed to characterize mTEC into several, distinct subpopulations. Importantly, the absolute and relative number of UEA1+ cells expanded during thymus organogenesis parallel with the increase in mTEC cellularity (Figure 1B, *lower panels*).

Differentiation and proliferation of mTEC during embryonic development are known to be dependent on signals originating from the hematopoietic compartment (5, 6, 9); conversely thymocyte differentiation requires signals from TEC. This bi-directional dependence has been termed 'thymic cross-talk' and concerns signals mediated by both cell-surface and soluble molecules (23, 24). It is therefore not surprising that physical TEC::thymocyte-complexes have been identified of the adult thymus that persist after enzymatic digestion (25, 26). Imaging by ImageStreamX (Imaris), a newer technology combining multi-channel flow cytometry and high-resolution microscopy, indeed confirms the existence of these multi-cellular complexes and reveals large, single cTEC (CD45- EpCAM+ MHCII+ UEA1-) that contain more than 10 thymocytes (CD45+ EpCAM- CD4+) (data not shown). These complexes are therefore positive for EpCAM and CD45 expression, two mutually exclusive markers as they stain in the mouse exclusively epithelial and hematopoietic cells, respectively. As specific cell aggregates have not yet been investigated in the embryonic thymus we studied their presence, phenotype and composition throughout foetal life. We found that CD45+ TEC, comparing to the EpCAM+ CD45- population (Figure 1B), expressed higher levels of CD40 and lower levels of CD205, and therefore resembled developing TEC directed towards the mTEC lineage (Figure 1C, *upper panels)*. Moreover the proportion of TEC expressing the mTEC-associated lectin UEA1 was significantly higher in those associated with thymocytes and

increased during development (Figure 1C, *lower panels*). These findings suggest that developing mTEC engage tightly with thymocytes during differentiation.

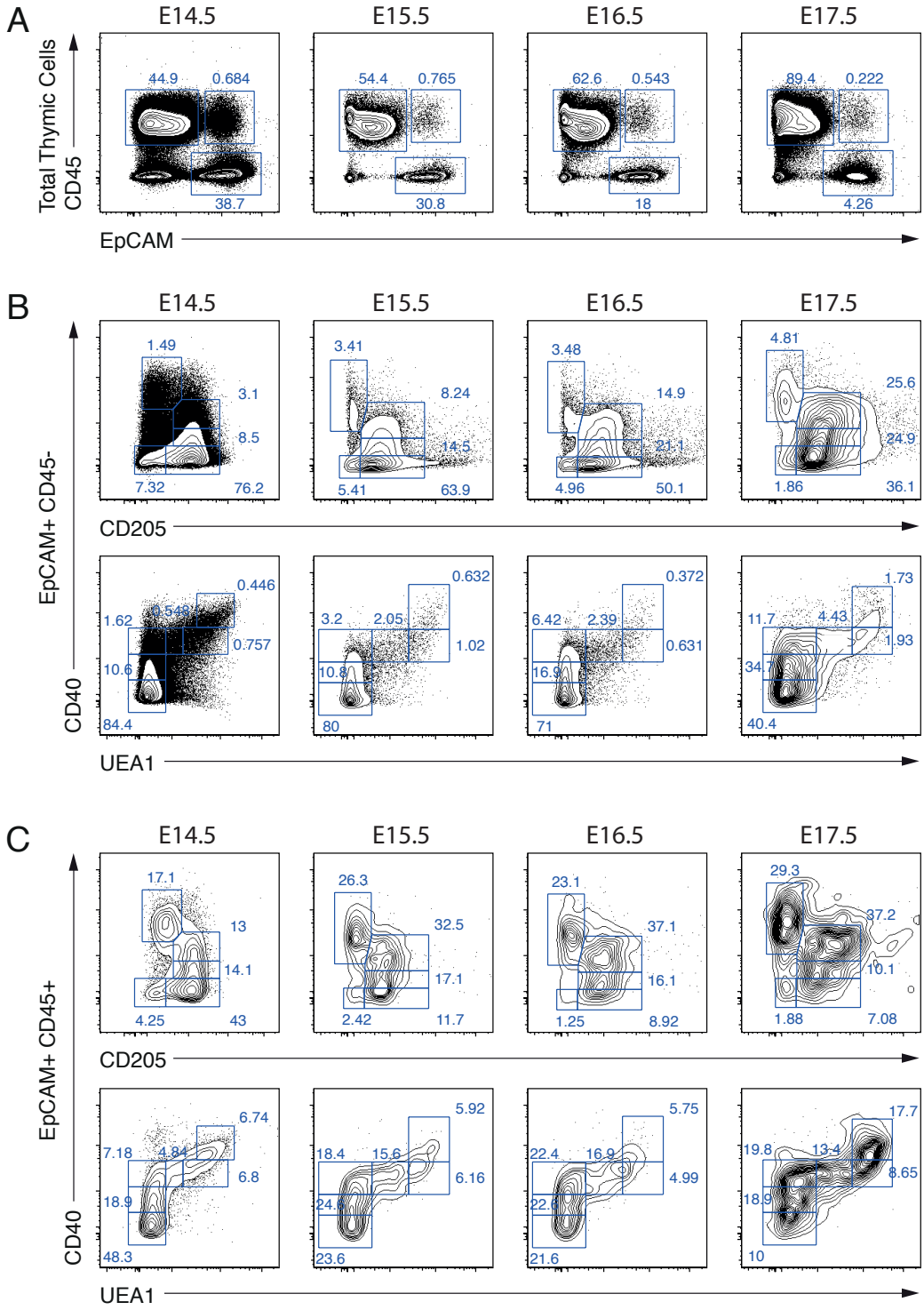

Figure 3.3-1. *Dynamic surface phenotypic changes of thymic epithelial cells during embryonic TEC differentiation.* (A) Flow cytometric analysis of total thymic cell at E14.5 (pooled analysis of approx. 70

C57Bl/6 embryos), and E15.5, E16.5 and E17.5 (representative plots of single Aire-GFP embryos) for the expression of CD45 and EpCAM. (B) Analysis of mice described in (A) for the detection of CD40, CD205 and UEA1 in CD45- EpCAM+ thymic epithelial cells. (C) Comparative analysis to (B) for CD45+ EpCAM+ TEC-thymocyte complexes.

3.3.3.2 Embryonic transcription of the Aire locus is initiated during commitment to mTEC lineage

The expression of the autoimmune regulator (Aire) facilitates the expression of tissue-restricted antigens (TRA) that represent a large portion of the genetic self (27). The precise time point at which point Aire expression is initiated during TEC differentiation in the embryonic thymus has not yet been determined. We used a mouse model (named Aire-GFP) to investigate the emergence of Aire positive mTEC in which the fluorochrome GFP is knocked expressed under the transcriptional control of the *Aire* locus and therefore under the transcriptional control of the native Aire promoter (27). At E15.5 and E17.5, most Aire-GFP expressing TEC belonged to the mTEC with a CD40int/hi CD205lo UEA1+ phenotype but typically could not be detected among CD40-/lo CD205+ UEA1- TEC (Figure 2A). Further, the expression level of Aire-GFP, as measured by geometric mean fluorescence intensity (gMFI), increased in mTEC subpopulations that displayed higher UEA1 reactivity but lost their CD205 expression. These phenotypic changes indicated that the expression of the Aire surrogate GFP correlated with advanced maturation along the mTEC lineage (Figure 2B). Since Aire protein expression is uniquely expressed among TEC in medullary epithelia GFP+ cells had also lost the phenotypic markers characteristic of cTEC. The acquisition of typical mTEC features was also associated with a downregulation or overt lack of other markers typically identifying immature TEC apparent at E14.5 when cells with an intermediate expression of CD40 and UEA1 began to downregulate CD205 and β5t, two typical features of the cTEC lienage. These two markers were found to be mostly absent in the more mature population marked as CD40int and UEA1hi (Figure 3). In aggregate, these results suggest a gradual transcriptional change in cells that enter the mTEC lineage (i.e. CD40int UEA1int).

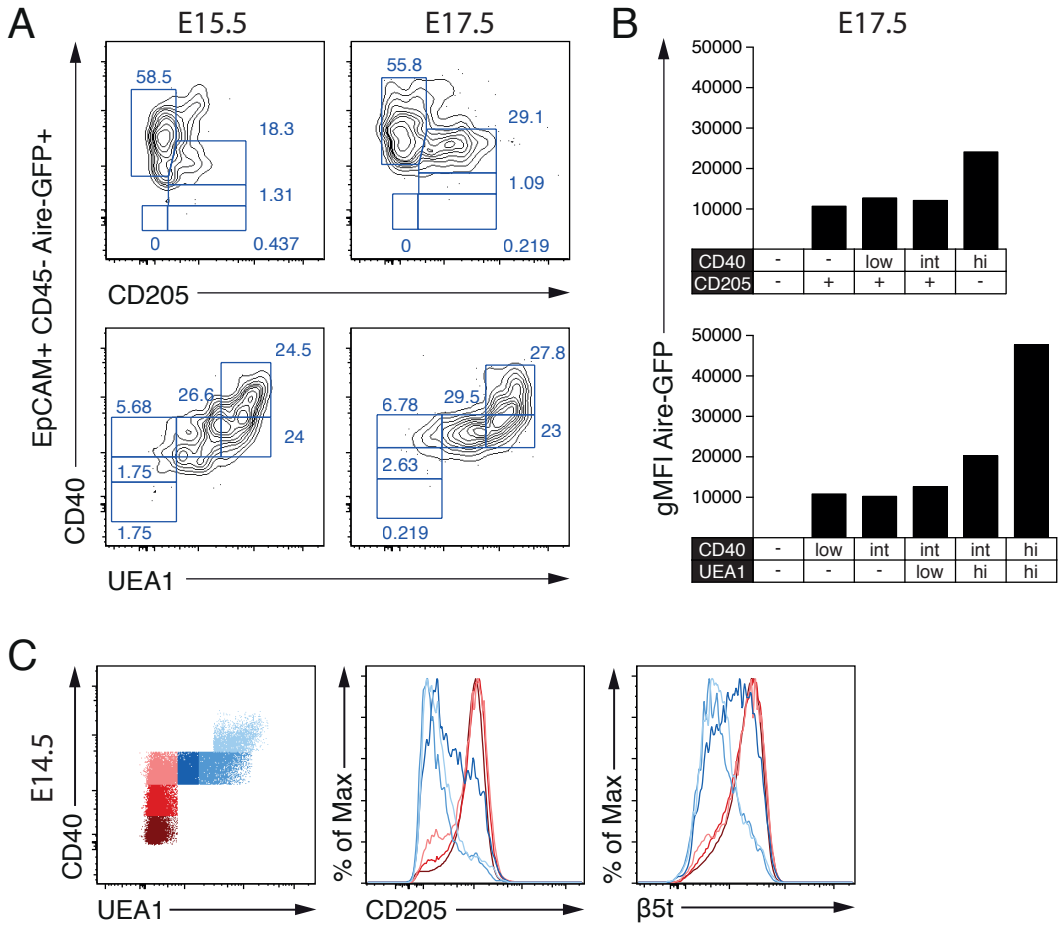

Figure 3.3-2 *Transcription of Aire-GFP is initiated during early embryonic mTEC differentiation.* (A) Aire-GFP mice were time-mated and collected 15 (*left* panels) and 17 days (*right* panels) after detection of vaginal plug that marks E0.5. Flow cytometric analysis was performed for the detection of CD40, CD205 and UEA1 in Aire-GFP+ TEC (CD45- EpCAM+). (B) Analysis of Aire-GFP expression levles detected as the geometric mean fluorescence intensity (gMFI) in the E17.5 embryos described in (A). Columns represent the corresponding gates shown in (A) (*right panels upper and lower plots).* (C) Detection of CD205 and intracellular β5t by flow cytometry in E14.5 C57Bl/6 TEC (CD45- EpCAM+), subdivided into groups determined by the expression of CD40 and UEA1. All plots show the results of single mice representative for that age.

3.3.4 Discussion

The phenotypic dynamics during embryonic TEC development and lineage specification are still only partially characterized. Recent publications have shown that the majority of TEC are derived in the embryo from progenitor cells that express the classical cTEC markers β5t and CD205 (20, 21). The results presented here expand these findings employing now the prototypical mTEC markers UEA1 and Aire, and specify a developmental stage (and hence cellular phenotype) where the cTEC and

mTEC lineage diverge. Stages of embryonic mTEC development have classically been subdivided based on the cell-surface detection of CD40 and CD205 into three consecutive populations, CD40- CD205-, CD40-/lo CD205+, and CD40int/hi CD205-, but failed to identify the point at which the two distinct lineages diverge. Using these two markers together with β5t, UEA1 and Aire we were able to further subdivide embryonic TEC differentiation into 7 stages (Figure 3). Stage I is characterized by the lack of expression of characteristic features of cortical (CD205) and medullary TEC (CD40, UEA1 and Aire). As this stage simultaneously expresses EpCAM and β5t, I conclude that most of these cells are TEC that have committed to a cortical fate. The transition to stage II is defined by the acquisition of CD205 positivity, a feature in keeping with the observation that almost all TEC originate form CD205+ precursors (21). Most, if not all, TEC are derived from cells that have originally adopted a cTEC-like phenotype (as obviated by β5t expression) though some maintain for a time a bi-lineage (20). Whether this population also encompasses cells with a unique cTEC developmental fate will only become established once single cell grafting experiments have been achieved that allow a clonal analysis of these cells. From stage III on all cells display at least low expression levels of CD40, a receptor triggering the canonical NF-κB pathway that is especially required for mTEC maturation. The emerging responsiveness to signals through this pathway renders cells increasingly susceptible to adopt a medullar fate. Additionally, RANK and LTβR could be upregulated together with CD40, as they have also been implicated in mTEC maturation, but this co-expression still needs to be experimentally proven. Intermediate levels of CD40 mark cells at stage IV, which probably represents the last population lacking the mTEC markers UEA1 and Aire. From stages III and IV onwards, TEC are more complexed with CD45+ cells. With the notion that these cells provide the required ligands (i.e. CD40L and RANKL) for mTEC-progenitors to expand and mature, it seems plausible that the close physical contact between developing thymocytes and mTEC identifies the earliest point of mTEC differentiation. However, this relationship has only recently been observed and needs further investigation, including the identification of the CD45+ cells associated with stage IV cells, time point of emergence of this aggregates during embryonic

development, and validation (possibly by imaging flow cytometry) that these are real cell aggregates and not artifacts resulting from the TEC isolation protocol. Indeed, the phenotypic changes observed from stage V on TEC strongly suggests that these cells have irreversibly committed to the medullar lineage. The downregulation of strict cTEC markers CD205 and β5t, and the concomitant upregulation of UEA1 and, in some cells, Aire certainly supports this argument. Lastly, stages VI and VII appear to mark the final differentiation stages in the path leading to a mature mTEC phenotype, as they have been shown to express the mTEC lineage-associated genes Claudin-3, Claudin-4, RANK, Cathepsin-S and Aire (22).

Taken together, the results presented here reveal a complex developmental program of mTEC during thymus organogenesis at mid to late gestation. Further analyses will have to identify the transcriptional identity of each of these subpopulations. With a clear phenotype of the TEC progenitor cells it will be possible to investigate whether corresponding cells can be found in the adult mouse, where it is currently unknown if TEC progenitor cells to both lineages are present at all. Of special interest are the cells at stage IV, which characterize the point of TEC lineage divergence. The CD40lo/int character of these cells could potentially render them susceptible to CD40L, Rank and LTβ signals provided by hematopoietic cells and required to establish a regular thymic medulla. But which TEC subsets exactly participate in this initial engagement and why other cells stay within the cTEC lineage remains unclear. Analyses by imaging flow cytometry using markers identifying LTi and Vγ5 cells will help to identify the precise hematopoietic cell type that is aggregated with developing mTEC. Apart from CD40, alternative receptors of the canonical and non-canonical NF-κB pathway might be important in this process including RANK and LTβR, whose expression levels within each of the seven developmental stages of TEC still have to be assessed. Cells at stage IV are of special interest because they may contain a high number of mTEC progenitors. A close phenotypic characterization of this population could potentially reveal the identity of mTEC progenitor cells that as of now remains elusive. Once this cell type is identified, it will be interesting to investigate adult thymi for their presence, and if present, to test their regenerative potential in the adult mouse. This could potentially lead to treatments where genetic

defects in the tolerance-inducing mTEC compartment can be repaired and autoimmune diseases permanently cured.

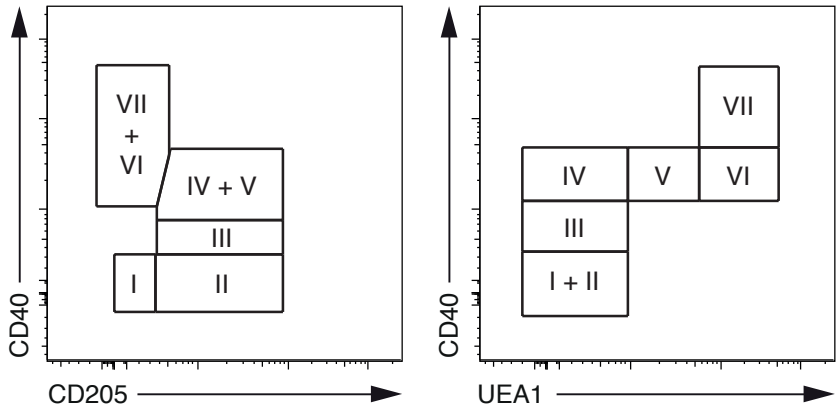

Stage	I	II	III	IV	V	VI	VII
β5t	+	+	+	+	int	-	-
CD205	-	+	+	+	low	-	-
CD40	-	-	low	int	int	int	hi
UEA1	-	-	-	-	low	hi	hi
Aire	-	-	-	- / low	- / int	- / hi	- / hi

Figure 3.3-3 *Overview of TEC markers expressed in the seven stages of embryonic mTEC differentiation.* Description of mTEC differentiation stages contained within individual gates of the flowcytometric plots described in Figures 1 and 2 (*upper panels*). Table showing the expression of 5 markers in each of the seven mTEC differentiation stages.

3.3.5 Materials & Methods

Mice

C57Bl/6 mice were obtained from Janvier Laboratories. Aire GFP-mice have been previously described (27). Developmental staging was determined by the detection of a vaginal plug at 0.5 days post conception (dpc). All mice were kept in specific-pathogen-free conditions and in according to institutional and cantonal guidelines.

Flow Cytometry

Cells were isolated by exposing embryonic thymic lobes to CollagenaseD and DNase I for 30 min and then incubated with antibodies specific for CD45 (30F11; eBioscience), EpCAM (G8.8; DSHB, University of Iowa), CD40 (HM 40-3, BioLegend), CD205 (NLDC-145, BioLegend) and UEA-1 (Reactolab). For intracellular staining, cells were fixed, permeabilized (Cytofix/Cytoperm Kit, BD Biosciences) and labelled for the expression of Psmb11 (MBL). Stained samples were acquired on a FACSAria II flow cytometer and the data was analyzed using the FlowJo (Treestar) software.

3.3.6 References

1. Gordon, J., V. Wilson, N. Blair, J. Sheridan, A. Farley, L. Wilson, N. Manley, and C. Blackburn. 2004. Functional evidence for a single endodermal origin for the thymic epithelium. Nature Immunology.
2. Ucar, A., O. Ucar, P. Klug, S. Matt, F. Brunk, T. G. Hofmann, and B. Kyewski. 2014. Adult thymus contains FoxN1(-) epithelial stem cells that are bipotent for medullary and cortical thymic epithelial lineages. Immunity 41: 257–69.
3. Romano, R., L. Palamaro, A. Fusco, G. Giardino, V. Gallo, L. Del Vecchio, and C. Pignata. 2013. FOXN1: A Master Regulator Gene of Thymic Epithelial Development Program. Frontiers in immunology 4: 187.
4. Nowell, C. S., N. Bredenkamp, S. Tetélin, X. Jin, C. Tischner, H. Vaidya, J. M. Sheridan, F. H. Stenhouse, R. Heussen, A. J. Smith, and C. C. Blackburn. 2011. Foxn1 regulates lineage progression in cortical and medullary thymic epithelial cells but is dispensable for medullary sublineage divergence. PLoS Genet. 7: e1002348.
5. Akiyama, T., Y. Shimo, H. Yanai, J. Qin, D. Ohshima, Y. Maruyama, Y. Asaumi, J. Kitazawa, H. Takayanagi, J. M. Penninger, M. Matsumoto, T. Nitta, Y. Takahama, and J.-I. Inoue. 2008. The tumor necrosis factor family receptors RANK and CD40 cooperatively establish the thymic medullary microenvironment and self-tolerance. Immunity 29: 423–37.
6. Chin, R. K., J. C. Lo, O. Kim, S. E. Blink, P. A. Christiansen, P. Peterson, Y. Wang, C. Ware, and Y.-X. X. Fu. 2003. Lymphotoxin pathway directs thymic Aire expression. Nat. Immunol. 4: 1121–7.
7. Seach, N., T. Ueno, A. L. Fletcher, T. Lowen, M. Mattesich, C. R. Engwerda, H. S. Scott, C. F. Ware, A. P. Chidgey, D. H. Gray, and R. L. Boyd. 2008. The lymphotoxin pathway regulates Aire-independent expression of ectopic genes and chemokines in thymic stromal cells. J. Immunol. 180: 5384–92.
8. White, A. J., K. Nakamura, W. E. Jenkinson, M. Saini, C. Sinclair, B. Seddon, P. Narendran, K. Pfeffer, T. Nitta, Y. Takahama, J. H. Caamano, P. J. Lane, E. J. Jenkinson, and G. Anderson. 2010. Lymphotoxin signals from positively selected thymocytes regulate the terminal differentiation of medullary thymic epithelial cells. J. Immunol. 185: 4769–76.
9. Boehm, T., S. Scheu, K. Pfeffer, and C. C. Bleul. 2003. Thymic medullary epithelial cell differentiation, thymocyte emigration, and the control of autoimmunity require lympho-epithelial cross talk via LTbetaR. J. Exp. Med. 198: 757–69.
10. Weih, F, D Carrasco, SK Durham, DS Barton, and CA Rizzo. 1995. Multiorgan inflammation and hematopoietic abnormalities in mice with a targeted disruption of RelB, a member of the NF-κB/Rel family. Cell .
11. Burkly, L, C Hession, L Ogata, C Reilly, and LA Marconl. 1995. Expression of relB is required for the development of thymic medulla and dendritic cells..
12. Kajiura, F, S Sun, T Nomura, and K Izumi. 2004. NF-κB-inducing kinase establishes self-tolerance in a thymic stroma-dependent manner. The Journal of Immunol.
13. Mouri, Y., H. Nishijima, H. Kawano, F. Hirota, N. Sakaguchi, J. Morimoto, and M. Matsumoto. 2014. NF-κB-inducing kinase in thymic stroma establishes central tolerance by orchestrating cross-talk with not only thymocytes but also dendritic cells. J. Immunol. 193: 4356–67.

14. Kinoshita, D, F Hirota, T Kaisho, and M Kasai. 2006. Essential role of IκB kinase α in thymic organogenesis required for the establishment of self-tolerance. The Journal of Immunol.

15. Inoue, J, J Gohda, and T Akiyama. 2007. Characteristics and biological functions of TRAF6. TNF Receptor Associated Factors (TRAFs) .

16. Rossi, S. W., M.-Y. Y. Kim, A. Leibbrandt, S. M. Parnell, W. E. Jenkinson, S. H. Glanville, F. M. McConnell, H. S. Scott, J. M. Penninger, E. J. Jenkinson, P. J. Lane, and G. Anderson. 2007. RANK signals from CD4(+)3(-) inducer cells regulate development of Aire-expressing epithelial cells in the thymic medulla. J. Exp. Med. 204: 1267–72.

17. Roberts, N. A., A. J. White, W. E. Jenkinson, G. Turchinovich, K. Nakamura, D. R. Withers, F. M. McConnell, G. E. Desanti, C. Benezech, S. M. Parnell, A. F. Cunningham, M. Paolino, J. M. Penninger, A. K. Simon, T. Nitta, I. Ohigashi, Y. Takahama, J. H. Caamano, A. C. Hayday, P. J. Lane, E. J. Jenkinson, and G. Anderson. 2012. Rank signaling links the development of invariant γδ T cell progenitors and Aire(+) medullary epithelium. Immunity 36: 427–37.

18. Desanti, G. E., J. E. Cowan, S. Baik, S. M. Parnell, A. J. White, J. M. Penninger, P. J. Lane, E. J. Jenkinson, W. E. Jenkinson, and G. Anderson. 2012. Developmentally regulated availability of RANKL and CD40 ligand reveals distinct mechanisms of fetal and adult cross-talk in the thymus medulla. J. Immunol. 189: 5519–26.

19. Hikosaka, Y., T. Nitta, I. Ohigashi, K. Yano, N. Ishimaru, Y. Hayashi, M. Matsumoto, K. Matsuo, J. M. Penninger, H. Takayanagi, Y. Yokota, H. Yamada, Y. Yoshikai, J.-I. Inoue, T. Akiyama, and Y. Takahama. 2008. The cytokine RANKL produced by positively selected thymocytes fosters medullary thymic epithelial cells that express autoimmune regulator. Immunity 29: 438–50.

20. Ohigashi, I., S. Zuklys, M. Sakata, C. E. Mayer, S. Zhanybekova, S. Murata, K. Tanaka, G. A. Holländer, and Y. Takahama. 2013. Aire-expressing thymic medullary epithelial cells originate from β5t-expressing progenitor cells. Proc. Natl. Acad. Sci. U.S.A. 110: 9885–90.

21. Baik, S., E. J. Jenkinson, P. J. Lane, G. Anderson, and W. E. Jenkinson. 2013. Generation of both cortical and Aire(+) medullary thymic epithelial compartments from CD205(+) progenitors. Eur. J. Immunol. 43: 589–94.

22. Parnell, SM, EJ Jenkinson, and G Anderson. 2009. Checkpoints in the development of thymic cortical epithelial cells. The Journal of Immunol.

23. Takahama, Y. 2006. Journey through the thymus: stromal guides for T-cell development and selection. Nat. Rev. Immunol. 6: 127–35.

24. Klein, L., B. Kyewski, P. M. Allen, and K. A. Hogquist. 2014. Positive and negative selection of the T cell repertoire: what thymocytes see (and don't see). Nat. Rev. Immunol. 14: 377–91.

25. Nakagawa, Y., I. Ohigashi, T. Nitta, M. Sakata, K. Tanaka, S. Murata, O. Kanagawa, and Y. Takahama. 2013. Thymic nurse cells provide microenvironment for secondary T cell receptor α rearrangement in cortical thymocytes. Proceedings of the National Academy of Sciences of the United States of America 109: 20572–7.

26. Wekerle, H., U. P. Ketelsen, and M. Ernst. 1980. Thymic nurse cells. Lymphoepithelial cell complexes in murine thymuses: morphological and serological characterization. J. Exp. Med. 151: 925–44.

27. Sansom, S. N., N. Shikama-Dorn, S. Zhanybekova, G. Nusspaumer, I. C. Macaulay, M. E. Deadman, A. Heger, C. P. Ponting, and G. A. Holländer. 2014. Population and single-cell genomics reveal the Aire dependency, relief from Polycomb silencing, and distribution of self-antigen expression in thymic epithelia. Genome Res. 24: 1918–31.

3.4 Spatio-temporal contribution of single β5t+ cortical epithelial precursors to the thymus medulla

3.4.1 Introductory notes

3.4.1.1 Summary

Based on the previous results made with the β5t-Cre mouse and the analysis of the phenotypic dynamics during embryonic development we were interested in investigating whether the activity of β5t+ mTEC progenitors is limited during early thymus organogenesis, or alternatively, can also be observed during later stages of development. We therefore created a new experimental mouse model in which the reverse tetracycline transactivator (rtTA) gene was expressed under the transcriptional control of the *Psmb11* locus. These mice were then crossed to animals transgenic for the Cre recombinase (and Luciferase) whose expression is under the control of a Tetracycline Response Element (TRE) (named LC1). Double mutant mice were then bred with ZsGreen reporter mice to gain a tissue (i.e. TEC)-specific, inducible reporter system (designated $3xtg^{\beta5t}$). In a first series of experiments, $3xtg^{\beta5t}$ embryos were exposed to Doxycycline (Dox) from the 7^{th} day post-conception (dpc) to birth exposing the mothers to the drug in the drinking water. 80% of cTEC and mTEC of treated newborn mice were ZsGreen positive indicating that progenitors to both TEC compartments had successfully recombined the stop cassette in front of the ZsGreen reporter allowing the cells to be labeled. Labelled TEC could be detected at high frequency and in absence of Dox for at least 40 days after birth, demonstrating the maintenance of the epithelial stroma over long period of time with cells derived from a β5t-positive precursor. The slightly lower recombination frequency of 80% when compared to 99% of β5t-Cre::ZsGreen mice identified however a limitation in labeling efficiency in utero. Nonetheless, these experiments demonstrated the specificity of labeling because expression of ZsGreen in cells other than TEC coud not be observed in these mice. I next investigated mice in which thymic morphogenesis had changed to a maintenance stage with an established cortico-medullary distinction. For this purpose, 5 week old mice were chosen and treated with Dox for 24 hours. The frequency of ZsGreen+ cTEC was approximately 5%

within 2 days after drug treatment and its frequency increased to 8-10% after one week, a value that remained unchanged for the following 20 weeks. Though lower than expected, the percentage of ZsGreen+ TEC persisted unchanged for at least 20 weeks after drug treatment. The consistent presence of ZsGreen+ cTEC weeks after Dox treatment and the established half-life of cTEC of this age of typically 1-2 weeks, would strongly argue that labeled cells represented a long-lived and stable population. In immunohistochemial analyses of thymic cross-sections, cTEC and mTEC were distributed throughout the entire thymus at all time points investigated. The lack of ZsGreen+ cTEC and mTEC cell clusters even at 20 weeks after induction of recombination suggested that none of these labeled cells participated in maintaining their respective compartment in a large scale. Taken together, these results implied that the genetic labeling of TEC through β5t did not preferentially label TEC progenitors of either compartment. In contrast to the frequency of labeled cTEC, only 1-2% of the mTEC in 5-week-old 3xtg$^{\beta5t}$ mice expressed ZsGreen 2 days after Dox treatment. This low percentage only marginally increased with time to 2-3%, a frequency that persisted at least for 20 weeks following drug treatment. The detection of reporter-positive mTEC shortly after treatment was of surprise because β5t protein detection in adult mice is restricted to the cortex. Since mTEC promiscuously express almost all protein-coding genes for the purpose of efficient thymus negative selection of self-reactive T cells, we tested whether the expression of β5t could be part of the promiscuous gene expression program. Consequently, labeling of mTEC would result from the cells' unique ability to express an almost complete range of tissue-restricted antigens (TRA). Labeled mTEC displayed in comparison to unlabeled mTEC higher levels of MHCII and Aire expression, which identifies them as mature. Transcript analysis in wildtype MHCII^{lo} and MHCII^{hi} mTEC revealed that β5t is expressed in parallel with Aire together with Aire. MHCII^{lo} and Aire-deficient mTEC revealed markedly reduced espression in contrast to MHC^{hi} mTEC. Hence β5t is expressed as part of the Aire-dependent promiscuous TRA expression program. Single cell transcriptomic analyses confirmed these results revealing 4 out of 174 mTEC to contain β5t transcripts and a general transcriptomic landscape that resembled the one of mature mTEC. Taken together, these results

showed that mTEC responded to Dox because they expressed β5t as part of their pGE program.

In adult mice with a fully mature thymic architecture, only low recombination efficiency could beachieved for cTEC and mTEC in mice treated with Dox. This result was unlikely caused by a lack of β5t progeny contributing to more mature epithelia. Rather, changes in pharmacodynamics of Dox distribution could account for this finding. I therefore investigated on e week old mutant mice as the thymic architecture is still being established. For this purpose, mice were treated with a single i.p. injection of Dox and analysed at different time points thereafter. At least half of all cTEC were labeled in these animals 2 days after Dox treatment and this significant frequency persisted for at least 20 weeks. In contrast, only 2% of all mTEC expressed ZsGreen 2 days after Dox treatment, a frequency that was similar to that in 5-week-old mice. However, the frequency of ZsGreen+ cells continuously increased in mutant mice that had been treated at one week of ate reaching a maximum of up to 50% 8 weeks after treatment. This increase paralleled the general growth of the mTEC compartment and suggested that β5t+ cells were contributing to the postnatal expansion of the medulla. BrdU incorporation experiments showed that ZsGreen+ mTEC at 2 days after the initial Dox exposure incorporated lower amounts of BrdU comparing to ZsGreen- cells, possibly due to the fact that those cells were recombined as a result of expressing β5t as part of their Aire-controlled promiscuous gene expression program and which is known to occur in mature and less proliferating cells. Investigating mice at 10 days after Dox treatment I noticed that ZsGreen+ mTEC incorporated significantly more BrdU when compared to ZsGreen- mTEC. This difference likely reflected the cell's active expansion and hence contribution to the medulla. Though, ZsGreen+ mTEC 2 days after Dox treatment were regularly distributed throughout the medulla , labeled cells 2 weeks after drug exposure had formed clusters along the cortical-medullary junction (CMJ). These aggregates were clonal in origin as they expressed only a single fluorochrome when the ZsGreen was replaced by the confetti locus. This construct contains four different fluorescent proteins (CFP, GFP, YFP and RFP) but cells express upon Cre-mediated removal of a stop cassette only a single "color" in their progeny. The results obtained

in 3xtg$^{\beta5t}$ mice treated at one week of age with a single Dox dose demonstrated the contribution of β5t+ progenitor cells to the medulla, which resulted in a progressive increase of their progeny over time. To reveal the developmental potential of cTEC that labeled early after Dox treatment, we isolated ZsGreen+ cTEC and mTEC from 9 day old mice that had been treated with Dox 2 days earlier. Reaggregation of these cells with wild-type C57Bl/6 mouse thymic stroma taken from E14.5 embryos, so called reaggregate thymic organ cultures (RTOC), were cultured for 24 hours in vitro and then transplanted under the kidney capsule of athymic nude mice. Five weeks later, the grafts were analysed. RTOC incorporating ZsGreen+ cTEC contained reporter-positive cell clusters both in the cortex (as expected) and in the medulla, although in the latter compartment at variable frequency. ZsGreen+ mTEC expressed CK14 and Aire and were therefore displayed characteristic features of mature mTEC. In comparison, RTOC formed with ZsGreen+ mTEC had generated only very few ZsGreen+ cells that were located in rare clusters, similarly to the ones observed in RTOC containing ZsGreen+ cTEC.

Taken together, we found that β5t+ TEC progenitor cells actively contribute to the formation of the medulla during embryonic and postnatal thymus development. Moreover, we localize the postnatal medullar growth zones and therefore by proxy the position of the mTEC progenitor to the CMJ. Lastly, we show that the progenitor cell can be transplanted with sorted cTEC, suggesting a progenitor-progeny relationship between a β5t+ precursor and mTEC that are devoid of this characteristic cortical marker. A precise phenotype that unequivocally identifies this cortical progenitor awaits further studies. Moreover, future future analyses will have to show whether these cells are quiescent or even absent in the adult mouse, an aspect that could be of interest in the context of Regenerative Medicine.

3.4.1.2 Contribution

The work described above reflects a body of work to which several have contributed. Together with a colleague I was responsible for the planning of the experiments and the treatment of mice. Moreover, I analyzed TEC in 3xtg$^{\beta5t}$ mice by flow cytometry

(Figures 1B-C, 2A, 3A, 3E, 4A-C, Supplementary Figure 1B-C, 3), sorted TEC subpopulations and tested those cells for the expression of various transcripts (Figure 5A, Supplementary Figure 4A). Further addition I isolated TEC from 3xtg$^{\beta 5t}$ mice and C57Bl/6 embryonic mice, generated the RTOC and assisted in the transplantation of said RTOC under the kidney capsule of nude mice. Finally I conducted the immunohistological and microscopic (Figures 5B-C, Supplementary Figure 1A, 4B) analysis of the ensuing ectopic thymi. These contributions were considered significant so that I was acknowledged as a co-first author of the manuscript that has now been submitted for publication.

3.4.1.3 Authors and affiliations of the publication

Carlos E. Mayer[1#], Saulius Zuklys[1#], Saule Zhanybekova[1], Izumi Ohigashi[2], Hong Ying Teh[1], Stephen N. Sansom[3], Noriko Shikama-Dorn[1], Katrin Hafen[1], Iain C. Macaulay[4], Mary E. Deadman[6], Chris P. Ponting[4,5], Yousuke Takahama[2] and Georg A. Holländer[1,6]

1 Department of Biomedicine, University of Basel, Basel, Switzerland

2 Division of Experimental Immunology, Institute for Genome Research, University of Tokushima, Japan

3 The Kennedy Institute of Rheumatology, University of Oxford, Oxford, United Kingdom

4 Wellcome Trust Sanger Institute-EBI Single Cell Genomics Centre, Wellcome Trust Sanger Institute, Hinxton, Cambridge, United Kingdom

5 MRC Functional Genomics Unit, Department of Physiology, Anatomy and Genetics, University of Oxford, Oxford, United Kingdom

6 Department of Paediatrics and the Weatherall Institute of Molecular Medicine, University of Oxford, Oxford, United Kingdom

[#] These authors contributed equally to this study.

3.4.2 Abstract

Intrathymic T cell development is critically dependent on cortical and medullary thymic epithelial cells (TEC). Both epithelial subsets originate during early thymus organogenesis from progenitor cells that express the thymoproteasome subunit β5t, a typical feature of cortical TEC. Using *in vivo* lineage fate mapping, we demonstrate that β5t$^+$ TEC progenitors give rise to the medullary TEC compartment early in life but significantly limit their contribution once the medulla has completely formed. Lineage- tracing studies at single cell resolution demonstrate for young mice that the post-natal medulla is expanded from individual β5t$^+$ cortical progenitors located at the cortico-medullary junction. These results therefore not only define a developmental window during which the expansion of medulla is efficiently enabled by progenitors resident in the thymic cortex, but also reveal the spatio-temporal dynamics that control the growth of the thymic medulla.

3.4.3 Introduction

The thymus provides the physiological microenvironment for the development of T lymphocytes and is therefore essential for the immune system's ability to distinguish between vital self and injurious non-self. Essential for this competence are thymic epithelial cells (TEC), which classify into separate cortical (c) and medullary (m) lineages with specific molecular, structural and functional characteristics (1). cTEC attract blood-borne precursor cells, commit them to a T cell fate and foster their differentiation to a developmental stage at which individual immature T cells (designated thymocytes) express the T cell antigen receptor (TCR). Because the TCR specificity is generated pseudo-randomly during thymocyte development, its utility for a given individual will need to be assessed. cTEC positively select thymocytes that express a TCR with intermediate affinity for the peptide/MHC complexes on

their surface for survival and further maturation (2). In contrast, mTEC - in collaboration with cTEC, dendritic and other hematopoietic cells situated in the thymic medulla - mediate negative selection through apoptosis, thus removing thymocytes that recognize self-antigens with high affinity (3–5). The selection of thymocytes by both cTEC and mTEC depends on their collective ability to promiscuously express transcripts encoding almost all ubiquitously and tissue-restricted proteins (6) thus enabling these cells to instruct a functional yet self-tolerant T cell repertoire.

Both TEC lineages are derived in the embryo from a common epithelial stem/progenitor population (7–10). Its further differentiation initially leads to a cell stage that simultaneously expresses markers characteristic for either cortical and medullary TEC lineages (11, 12). This finding contests a developmental model in which bi-potent stem/precursor cells lacking cortical or medullary hallmarks segregate synchronously into the two different TEC lineages (13). An overlap in the expression of lineage-specific marks is also observed in transgenic lineage tracing studies (14) where the vast majority of mTEC derive from progenitor cells expressing the cTEC prototypical marker Psmb11, which is encoded by the *β5t* locus. Experimental evidence further suggests that epithelial cells with a bi-potent, self-renewing capacity persist after birth and can give rise to both TEC lineages (15–17). Whether these cells concertedly and unremittingly contribute to both TEC subpopulations, or, alternatively, whether one lineage is maintained after a specific point in time independent of the other owing to lineage-restricted precursors remains unresolved. It is certainly conceivable that TEC stem/precursor cells display a developmental behaviour alike that observed in other epithelial organs where bi-potent cells initially establish a multi-lineage epithelial structure that is later maintained by lineage-specific, uni-potent progenitors (18). Lineage-restricted progenitors within the medullary and cortical compartments have indeed been identified using different experimental approaches including *in vivo* cell lineage studies (15, 19–22) although neither their proportion nor functional importance have so far been defined.

The precise precursor-product relationships between each TEC lineage are still incompletely understood. To resolve this issue, we have developed a novel *in vivo* lineage-tracing model that allows the marking of β5t$^+$ cTEC in an inducible fashion and thus can assess the cells' developmental potential at distinct postnatal stages. Here we report that β5t$^+$ cTEC at the cortico-medullary junction of one-week old mice serve as an efficient progenitor for the mTEC lineage. Contributions from these precursors to the medulla are multi-clonal for individual medullary islands. However, once the medulla has reached its normal cellularity in the postnatal thymus, the differentiation potential of β5t$^+$ precursors to mTEC lineage is markedly restricted.

3.4.4 Results

3.4.4.1 Adult cortical and medullary thymic epithelia are derived from embryonic β5t expressing precursors

Given the unexpected finding that embryonic TEC precursors for both the cortical and medullary lineages express β5t (14), we set out to further identify these cells and their developmental potential throughout the life course of the mouse. For this purpose, we created a new mouse line (designated β5t-rtTA) that expresses the reverse tetracycline transactivator (rtTA) under the transcriptional control of the β5t locus (psmb11; Figure 1A). Correctly targeted mice were crossed to animals transgenic for LC1 and the conditional ZsGreen reporter (23, 24). Treatment of these triple transgenic mice (designated 3xtgβ5t) with doxycyline (dox) produces dox/rtTA complexes that bind to the tetracycline response element (TRE) upstream of the LC1 transcription unit and consequently drive the expression of Cre. As a result, the stop cassette in the reporter construct is removed and the transcription of the fluorescent protein ZsGreen is enabled identifying β5t-expressing TEC and their progeny (Figure 1A, lower panel).

Treating 3xtg^{β5t} mice from embryonic day 7.5 (E7.5) until birth with dox resulted in the expression of ZsGreen in the vast majority of cortical (i.e. EpCAM$^+$ Ly51$^+$ UEA1$^-$

CD45$^-$) and medullary TEC (EpCAM$^+$ Ly51$^-$ UEA1$^+$ CD45$^-$) (Figure 1B and 1C). The frequency of labelled epithelia was comparable for both anatomical compartments and remained largely unchanged during the first 40 days of postnatal life, which includes a phase of significant organ growth. ZsGreen expression was, however, not detected in haematopoietic and non-epithelial stromal cells of treated 3xtg$^{\beta5t}$ mice (Figure 1B) and, likewise, labelling was absent from TEC of untreated triple transgenic mice excluding transgene 'leakiness' as an explanation for these results (Figure S1). In aggregate, these findings suggested the existence of a collective of β5t-positive precursors in fetal mice from which both cTEC and mTEC originate, extending previous results (14).

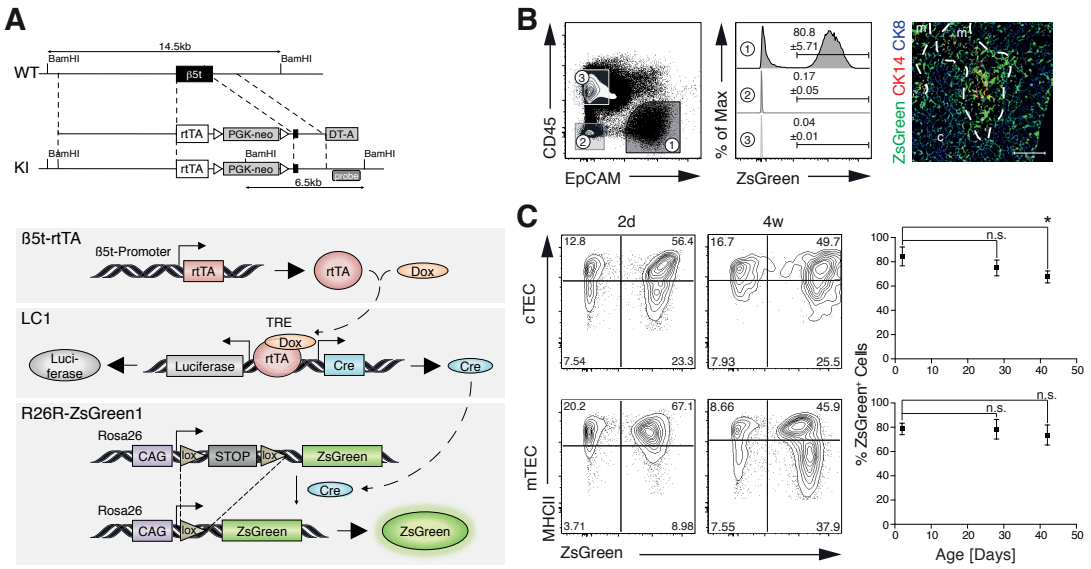

Figure 3.4-1. *Tissue and time controlled expression of the reporter ZsGreen in thymic epithelial cells.* (A) Description of the targeting strategy to achieve rtTA expression under the transcriptional control of the β5t locus and a cartoon depicting the design of β5t promoter driven TEC specific labeling in the triple transgenic mice designated 3xtg$^{\beta5t}$. (B, C) Flow cytometric and immunofluorescent analyses of thymic tissue isolated from mice treated with Dox from embryonic day (E) 7.5 until birth. (B) The left panel depicts the flowcytometric analyses of epithelial (EpCAM$^+$CD45$^-$), haematopoietic (EpCAM$^-$CD45$^+$) and non-epithelial stromal (EpCAM$^-$CD45$^-$) cells 2 days after treatment. The ZsGreen expression is shown in the middle panels for each of the separate cell populations identified in the left panel. The right panel demonstrates immunofluorescence analysis of ZsGreen expression in combination with CK8 (blue) and CK14 (red). The data shown is representative of 2 independent experiments. (C) Flow cytometric analysis of cTEC (EpCAM$^+$Ly51$^+$UEA1$^-$CD45$^-$) and mTEC (EpCAM$^+$Ly51$^-$UEA1$^+$CD45$^-$) for expression of MHCII and ZsGreen 2 days and 4 weeks after treatment (left panels). Frequencies of ZsGreen positive cTEC and mTEC detected at indicated days after Dox treatment are displayed in the right panel. The graph is representative of 2 independent experiments with at least 3 mice per time point. *p<0.05.

3.4.4.2 Time controlled and tissue specific labelling of adult cTEC in triple transgenic mice

We next determined whether a comparable precursor-progeny relationship exists for the postnatal thymus. For this purpose, 5-week old 3xtg$^{\beta5t}$ mice were treated with dox for 24 hours and ZsGreen expression in TEC was subsequently followed for as long as 20 weeks. Under these conditions, fluorescently labelled cTEC could be detected as early as 48 hours after initial drug exposure and were dispersed throughout the cortex (Figure 2A and 2B). Both cTEC with low and high MHCII expression (MHC^{lo} and MHC^{hi}, respectively) remained labelled and were uniformly dispersed throughout the cortex for at least 140 days after completion of dox treatment. We conclude from these lineage-tracing studies that the drug-mediated recombination had likely also occurred in precursors from which mature cTEC derive over time. Alternatively, a relatively small but discernable population of labelled cells (approx. 10%) may either had an extended half life and/or were generated by self-duplication of existing, differentiated ZsGreen+ cTEC dispersed throughout the cortex without any input from stem cells as described for other organ systems (25–27).

The labelling efficiency of adult cTEC was increased with longer exposure to the drug (Figure S1C) but did not reach the high efficiency of dox-induced recombination observed in the thymus of fetal 3xtg$^{\beta5t}$ mice (Figure 1C). This lower recombination efficiency could in part be explained by the decreased promoter activity of the *β5t* locus measured in older animals (accompanying paper by Ohigashi *et al*.). Further, we investigated whether a restricted transcription of the LC1 transgene was responsible for the observed ZsGreen expression and found that mice transgenic for the tetO-Cre transcriptional unit (β5t-rtTA::tetO-Cre1Jaw/J::ZsGreen, designated 3xtg$^{tetO\text{-}Cre}$) in lieu of LC1 transgene demonstrated a higher labelling efficiency (Figures S1A and S1B). Thus, the extent with which triple transgenic cTEC could be labelled was dependent on the length of dox exposure, age of the mouse, and the specific Cre transcriptional unit used. Despite their higher labelling efficiency, 3xtg$^{tetO\text{-}Cre}$ mice were considered unsuitable for our further

studies owing to their high background of spontaneous Cre-mediated recombination (Figure S1A and 1B).

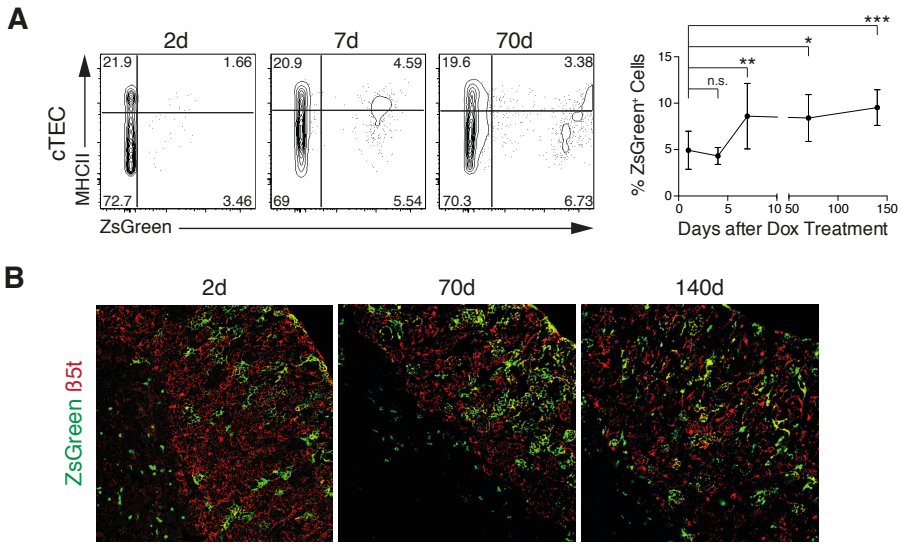

Figure 3.4-2. *Lineage tracing of cortical thymic epithelial cells in adult mice.* (A) Frequency and time course analyses of ZsGreen expression in cTEC of treated 3xtg$^{\beta5t}$ mice. 5-week old 3xtg$^{\beta5t}$ mice were i.p. injected twice within 24hr with Dox (2mg) and given Dox (2mg/ml) supplemented drinking water in that time. The frequency of labeled cTEC was measured at the indicated time points. Left panel: flow cytometric analyses of cTEC (EpCAM^{+}Ly51^{+}UEA1^{-}CD45^{-}) for expression of MHCII and ZsGreen; Right panel: relative frequency of ZsGreen+ cTEC over the course of 140 days. *p<0.05, **p<0.01, ***p<0.001. (B) Immunohistology of the thymic tissue at 2, 70 and 140 days after Dox treatment of 5-week old 3xtg$^{\beta5t}$ mice. Tissue sections were stained with anti-β5t antibodies (red) and analysed for the expression of ZsGreen (green).

3.4.4.3 Aire-controlled promiscuous expression of the β5t locus labels mTEC in triple transgenic mice

Dox-treatement of adult 3xtg$^{\beta5t}$ mice initially resulted in the ZsGreen labelling of mostly MHC^{hi} mTEC at a very low frequency (1-2%; Figure 3A and Figure S2). Over the course of a few days, the rate of labeled MHC^{lo} increased and labeled mTECs with both an MHC^{lo} and MHC^{hi} phenotype persisted for at least 140 days. In comparison to cTEC, the labelling rate was at least 3-7 fold reduced for each of the individual time points tested (Figure 2A and Figure S1B), thus revealing a significant difference in the extent by which mTEC had expressed or continued to transcribe the β5t locus.

At the population level, β5t transcripts were detected in wild type mice by RNA-Seq in all mTEC subpopulations (Figure 3B). At single cell resolution, 4 of 174 wild type MHC^{hi} mTEC transcribed more than one β5t mRNA copy per cell (6.4 on average). Those cells displayed a gene expression profile typical of mature mTEC (Figure 3C) and transcribed Aire-dependent and Aire-independent tissue restricted antigens (TRA) comparable in number to that of other mature mTEC (Figure 3D). Moreover, the relative frequency of ZsGreen+ Aire+ MHC^{hi} mTEC was significantly increased in $3xtg^{\beta5t}$ mice 2 days after dox exposure when compared to ZsGreen- cells with the same phenotype (51.9±4.1 vs 20.7±3.5, Figure 3E). These findings suggested that the early detection of labeled mTEC was primarily the result of promiscuous gene expression.

Given the relatively short half-life of 7-8 days for mTEC of the Aire-expressing lineage (28), ZsGreen+ mTEC labelled as a consequence of Aire expression were progressively replaced in dox-treated adult $3xtg^{\beta5t}$ by cells with an MHC^{low} phenotype (Figure 3A). Their frequency increased by up top 16-fold over the course of the experiment at the expense of labeled MHC^{hi} mTEC (Figure 3A) demonstrating a dynamic change in the contribution of each of these individual mTEC subpopulations to the group of ZsGreen+ mTEC. The relative frequency of labeled mTEC persisted even at later time points (Figure 3A) when MHC^{low} mTEC contributions were more noticeable. These results therefore suggested that TEC other than relatively short lived cells promiscuously expressing β5t were successfully labeled after Dox exposure, persisted and contributed, albeit at a low rate, to both the MHC^{lo} and MHC^{hi} ZsGreen+ mTEC populations.

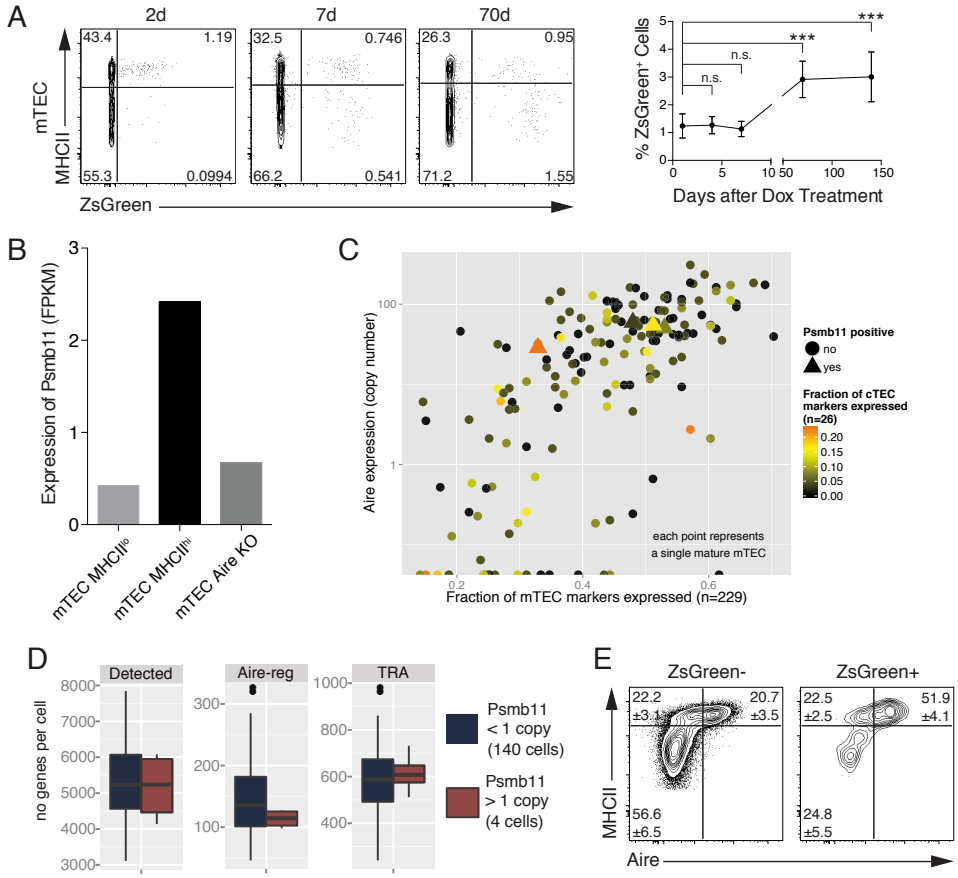

Figure 3.4-3. *Promiscuous gene expression contributes to ZsGreen expression in medullary MHCII^{hi} thymic epithelial cells in adult 3xtg$^{\beta5t}$ mice* (A) Flow cytometric analysis of MHCII and ZsGreen expression (left panel) and relative frequency (right panel) of ZsGreen+ mTEC (EpCAM^{+}Ly51^{-}UEA1^{+}CD45^{-}) of 3xtg$^{\beta5t}$ mice treated at 5 weeks of age with 2 injections of Dox (2mg) within 24hrs and given Dox (2mg/ml) supplemented drinking water during that time. ***p<0.001 (B) Expression of β5t (Psmb11) measured by RNAseq of 4 week old wild-type MHCII^{hi} mTEC, MHCII^{lo} mTEC and MHCII^{hi} Aire-deficient mTEC. (C) Promiscuous expression of Psmb11 in single mature mTEC. Mature mTEC positive for Psmb11 (> 1 copy, triangles) express Aire and show expression of mTEC and cTEC marker genes that is similar to that observed in Psmb11 negative cells (circles). (D) Analysis of gene expression in single Aire-expressing mTEC. No significant difference in the number of Aire-regulated genes or TRA was detected between Psmb11 positive and negative cells (Mann-Whitney U test). (E) Flow cytometric analysis for the expression of MHCII and Aire in ZsGreen- and ZsGreen+ mTEC of 3xtg$^{\beta5t}$ mice 48 hours after Dox treatment.

3.4.4.4 Postnatal β5t^{+} cTEC marked early in Dox-treated 3xtg$^{\beta5t}$ mice contribute to mTEC lineage

To test the precursor potential of postnatal β5t^{+} TEC and probe their competence to give rise to the mTEC lineage, we extended our experiments to the analysis of 1-week old 3xtg$^{\beta5t}$ mice in which the cellularity of the thymic medulla exponentially increases (29). A single dox injection in these young mice resulted in a high and

consistent labeling of cTEC (Figure 4A). Since previous studies had estimated the turn-over of cTEC and mTEC to be 7 to 14 days in young mice (29, 30), the recovery of a significant percentage of ZsGreen+ cTEC as late as 240 days after recombination suggested that precursors must have likely been labeled that gave rise to mature ZsGreen+ cTEC at the end of the experimental observation (Figure 4A, right panel).

In contrast to the cTEC lineage in 1-week old 3xtg$^{\beta5t}$ mice (but similar to mTEC in adult mutant animals), only very few mTEC expressed ZsGreen 2 days after Dox treatment (Figure 4B, left panels). The majority of these mTEC had an MHC^{hi} phenotype and likely expressed the label owing to β5t transcription as part of the cells' promiscuous gene expression program. However, both the frequency of all labeled mTEC as well as that of MHC^{lo} ZsGreen+ mTEC increased progressively over time to reach a plateau at 8 weeks after dox treatment when equal relative numbers of MHC^{lo} ZsGreen+ and MHC^{hi} ZsGreen+ cells were present that jointly constituted one third of the mTEC population (Figure 4B, right panel). The expansion kinetics of labeled cells was therefore significantly different to that of the cTEC lineage and suggested that the higher frequency of ZsGreen+ mTEC observed after the first days following dox exposure must have derived from β5t-expressing cells that served as precursors to the mTEC lineage. These precursors required up to 56 days until their progeny established a constant ratio of MHC^{hi} and MHC^{lo} populations similar to non-labeled mTEC.

We next sought to detail the cell proliferation for stages along the mTEC lineage. For this purpose, we treated 1-week old mice with Dox and analyzed their BrdU incorporation 2 and 10 days later (Figure 4C). At the earlier time point, labeled MHC^{hi} mTEC displayed a lower proliferation rate compared to the population of unlabeled MHC^{hi} mTEC which is consistent with the notion that labeled cells corresponded to epithelia that express β5t as part of their promiscuous gene expression program and Aire^{+} MHC^{hi} mTECs represent mostly postmitotic cells (31). At the later time point, labeled MHC^{hi} mTEC proliferated at an increased rate suggesting that this population now comprised a higher frequency of maturing mTEC.

We next sought to localise these precursor cells and their immediate clonal progeny *in situ* in the thymus of postnatal mice. Tissue sections taken 2 weeks after initiation of Dox treatment demonstrated an accumulation of ZsGreen+ mTEC at the cortico-medullary junction as revealed by noticeable cell clusters whereas the pattern of labelled mTEC in the other parts of the medulla remained unchanged over time (Figure 4D). These tracing results suggested an expansion of precursors but could not inform on the clonality of these clusters. To address this specific aspect of mTEC growth, we generated [β5t-rtTA::LC1::R26R-Confetti] mice (designated 3xtg^{confetti}) which allow the stochastic multicolor labelling of cell clones from an individual β5t^{+} TEC whose progeny is indelibly marked by the same fluorescent protein (32). After a single dose of dox at 1 week of age, thymus tissue was isolated 2 weeks later and sections were screened for fluorochrome-labelled cell clusters. Small aggregates of 5 to 25 monochromatic TEC cells could be detected at the cortical-medullary junction of treated but not untreated 3xtg^{confetti} mice (Figure 4D and data not shown). These data strongly suggested that β5t-expressing precursors localised at the junction between cortex and the medulla had proliferated and contributed to the growth of the epithelial component of the thymic medulla.

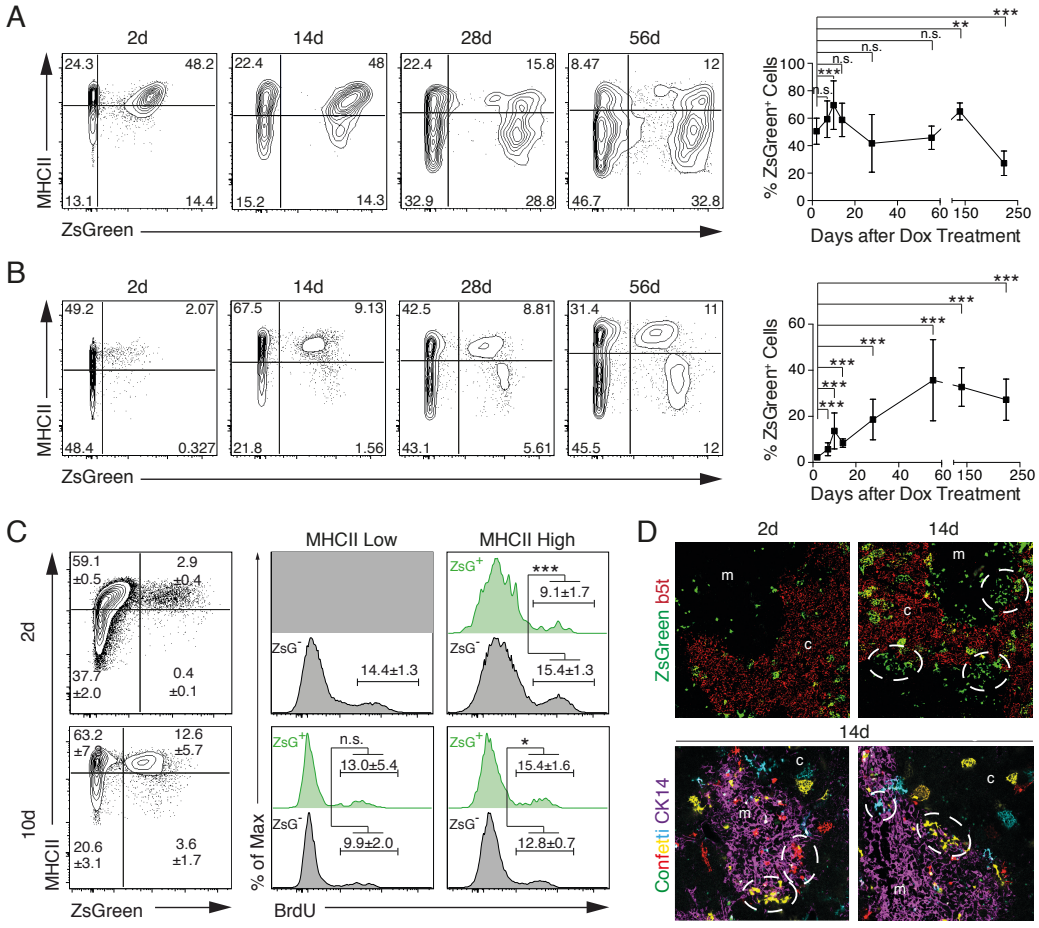

Figure 3.4-4. *Lineage tracing in 1-week old 3xtg$^{\beta5t}$ mice*. (A) Frequency and time course analyses of ZsGreen expression in cTEC. One-week old mice received a single i.p. injection of Dox (1mg) and were subsequently analysed at the indicated times. Flow cytometric analyses of cTEC (EpCAM^{+}LY51^{+}UEA1^{-} CD45^{-}) for the expression of ZsGreen and MHCII (left panel) and relative frequencies of ZsGreen+ cTEC over the course of 250 days after treatment (right panel). (B) Frequency and time course analyses of ZsGreen expression in mTEC from mice described in (A). Flow cytometric analyses of mTEC (EpCAM^{+}LY51^{-}UEA1^{+}CD45^{-}) for the expression of MHCII and ZsGreen (left panel) and relative frequencies of ZsGreen+ mTEC over the course of 250 days after drug treatment (right panel). (C) BrdU incorporation analysis of mTEC (EpCAM^{+}UEA1^{+}CD45^{-}) in 3xtg$^{\beta5t}$ mice treated at 1 week of age and chased for 2 and 10 days respectively. The BrdU incorporation rates are displayed for ZsGreen- and + mTEC subpopulations expressing high or low levels of MHCII. (D) Upper panels show immunohistologal analysis of thymic sections from 3xtg$^{\beta5t}$ mice that had been treated with Dox at 1 week of age and analysed 2 and 14 days after treatment for the expression of β5t (red) and ZsGreen (green) expression. Note the clusters of ZsGreen positive cells positioned at the cortical-medullary junction (dashed circles); lower panel: R26R-confetti mice were crossed with β5t-rtTA and LC1 generating triple transgenic mice, 3xtg^{confetti} [β5t-rtTA::LC1::R26R-confetti]. Triple transgenic mice were treated with a single dose of Dox (1mg) at 1 week of age and analysed 2 weeks later for the expression of the transgenic fluorochromes and cytokeratin 14 (as mTEC marker). Note monochromatic cell clusters exclusively localized to the cortical medullar junction. *p<0.05, **p<0.01, ***p<0.001.

3.4.4.5 Post-natal β5t-positive cTEC serve as precursors for mTEC

Data presented so far suggested that precursors to the mTEC lineage express β5t and are resident at the cortico-medullary junction from where their progeny extends into the medulla early in postnatal life. However, the efficiency with which these precursors seemingly contribute to the mTEC compartment already decreases in the second week of life (Figure S3). To formally test the assertion that β5t+ cTEC indeed serve as precursors for the post-natal mTEC lineage, we isolated ZsGreen+ cTEC two day after Dox treatment of 1-week old 3xtg$^{\beta5t}$ mice, reaggregated 2.5x10^4 of these cells with E14.5 wild type, non-haematopoietic thymic stromal cells (1.5x10^5) and grafted the resultant organoids under the kidney capsule of adult athymic (*nu/nu)* recipients. ZsGreen+ mTEC isolated in parallel served as the corresponding controls. A selection of exemplary cortical and medullary TEC genes, respectively, used to characterize further the grafted cells revealed the expected differences in transcription profiles (Figure 5A). However, the population of ZsGreen+ cTEC used for these grafting studies did not display different transcript levels for markers recently described in endogenous thymic epithelial progenitor cells when compared to unlabeled cTEC (Figure S4 and ref. (16, 17)). This is the likely result of analysing an inhomogeneous population of cTEC at different maturational stages, which includes a low frequency of β5t+ precursors to the mTEC lineage.

The microscopic analysis of reaggregate thymic organ cultures (RTOC) demonstrated the presence of ZsGreen+ TEC in both types of grafts as early as 24 hours after forming the organoids (Figure 5B, upper panels). Five weeks after the placement of grafts under the kidney capsule (Figure S5), the transplanted tissue was further investigated (Figure 5B, lower panels, and Figure 5C). The number of ZsGreen+ TEC in either the cortex or the medulla was limited owing to the ratio of labelled to unlabelled stromal cells used to generate the RTOC and the demonstrated difference in cell proliferation between embryonic and postnatal TEC (30). Tissue sections of grafts in which ZsGreen+ cTEC were admixed with E14.5 wild type stromal cells demonstrated not only the presence of ZsGreen+ TEC in the cortex and medulla but also disclosed mTEC clusters that expressed the typical medullary markers cytokeratin 14 (CK14) and Aire (Figure 5C upper panels). In contrast, tissue

sections from RTOC generated with ZsGreen+ mTEC revealed labelled TEC only in the medulla where the cells displayed an identical phenotype to epithelia derived from ZsGreen+ cTEC (Figure 5C, lower panels). Taken together, these transplantation studies unequivocally demonstrated that within 5 weeks after engraftment ZsGreen+ cTEC gave rise to TEC both in the cortex and the medulla whereas ZsGreen+ mTEC contribute exclusively to the epithelial compartment of the medulla highlighting an essential difference in the developmental potential of these two post-natal cell populations.

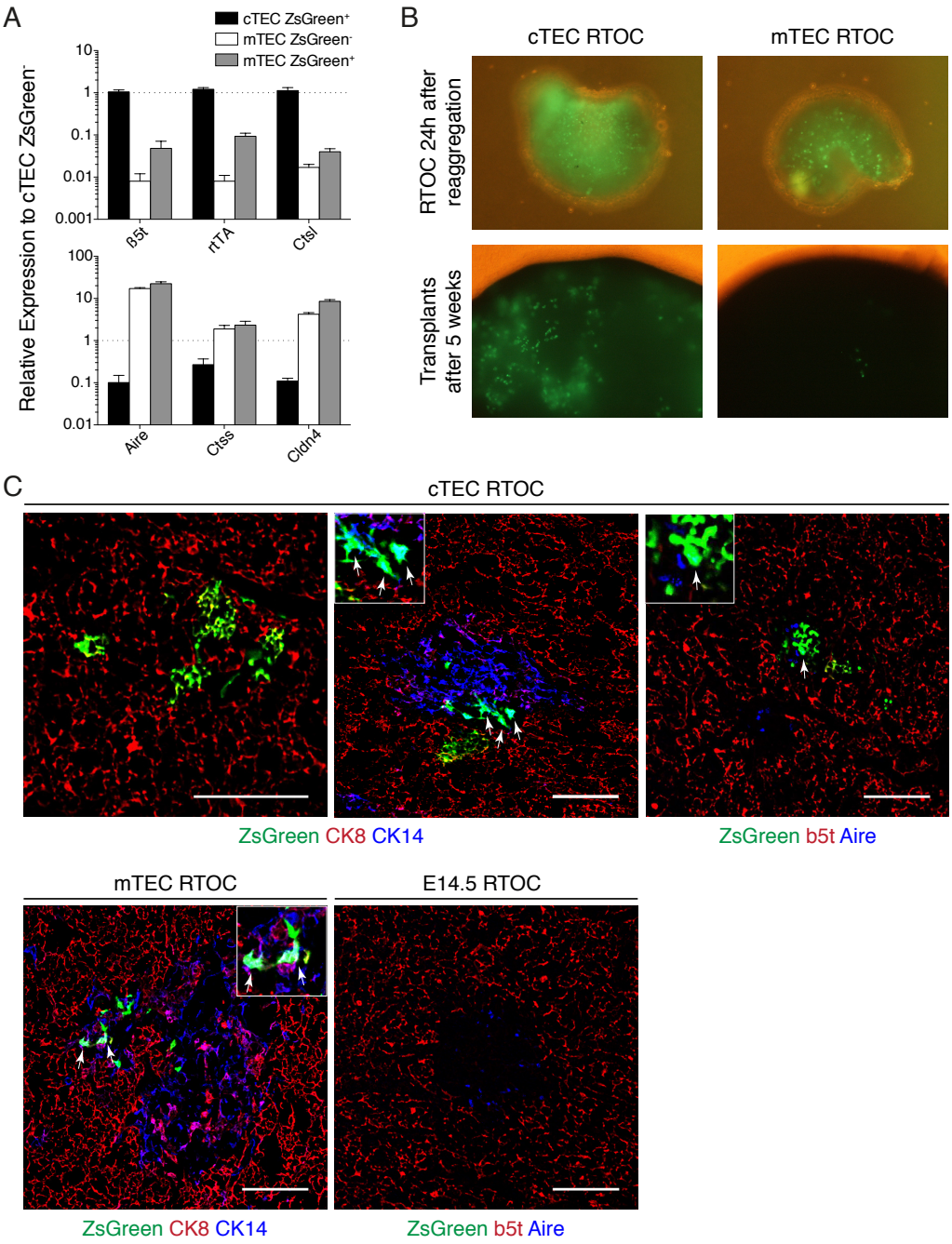

Figure 3.4-5. *Transplantation of ZsGreen+ cTEC from 3xtg^{β5t} mice gives rise to cortical and medullary TEC*. (A) RT-qPCR gene expression analysis of cortical (β5t, rtTA, Ctsl) and medullary (Aire, Ctss, Cldn4) TEC markers in ZsGreen-/+ TEC subpopulations. One-week old mice received a single i.p. injection of Dox (1mg) 48 hours prior to sorting cTEC (EpCAM^{+}LY51^{+}UEA1^{-}CD45^{-}) and mTEC (EpCAM^{+}LY51^{-}UEA1^{+}CD45^{-}), subdivided by the expression of ZsGreen. Gene expression was normalized to EpCAM and is presented as relative expression to cTEC ZsGreen-. (B) Representative macroscopic images of RTOC 24 hours after reaggregation (upper row) and the transplants 5 weeks post transplantation (lower row). (C) Immunofluorescence analysis of thymic sections from transplants made with ZsGreen+ cTEC for the expression of ZsGreen, CK8 and CK14 (upper row, left and middle panel) or ZsGreen, β5t and Aire (upper row, right panel), and the analysis for the expression of ZsGreen, CK8 and CK14 in thymic sections from transplants made with ZsGreen+ mTEC (lower row, left panel) or for ZsGreen, β5t and Aire in transplants originally using embryonic stromal cells alone (lower row, right panel). Arrows indicate cells co-expressing ZsGreen and mTEC marker (CK14 or Aire) in areas that are shown in the close-up. Scale bar = 100μm.

3.4.5 Discussion

TEC patterning is initiated during fetal development and continues throughout postnatal life as reflected by a permanent replacement of TEC in both cortex and medulla (29, 30, 33). The precise developmental point and physical location at which cTECs and mTECs diverge has, however, remained undefined. During embryonic development, the majority of mTECs, including Aire^{+} cells, derive from β5t-expressing progenitors. Using *in vivo* lineage-tracing at population and single cell resolution, we now demonstrate that individual β5t^{+} cortical progenitors located at the cortico-medullary junction contribute to the formation and maintenance of the postnatal medulla. This input parallels the expansion of the thymic medulla and its extent is maximal during the first week of life when compared to later ages. Thus, age determines the degree by which β5t^{+} cortical precursors contribute to the medullary epithelial compartment, revealing a gradual change in the precursor-progeny relationship within the mTEC lineage. These results contribute to an evolving concept that identifies differences between TEC lineage development in the embryo (7–10) and TEC maintenance in the postnatal thymus (15), thus highlighting a unique spatio-temporal contribution of β5t^{+} cortical epithelial precursors to the medullary TEC compartment.

Several developmental models have been suggested to explain the step-wise formation and maintenance of the thymic epithelial scaffold (13). Single epithelial precursors with a developmental potential to contribute to both cortex and medulla can be isolated at E12.5 from the thymus anlage (8, 34). Interestingly, the expression of the epithelial cell-specific transcription factor FoxN1 is not necessary for the formation of the earliest TEC progenitors within the embryo and may only be required to achieve their differentiation into common and eventual lineage-restricted TEC precursors and their progeny (17).

TEC with either cortical (CD205, β5t) or medullary phenotype (MTS10, Claudin3/4) are already detected in embryonic tissue at early stages of development (20, 21, 35, 36). Ontogenic studies in embryos further imply that CD205^{+}CD40^{-} cTEC represent progenitors positioned between the population of bi-potent cTEC/mTEC progenitors

and mature cTEC that require for their continued maturation cell-extrinsic signals provided by early thymocytes (7, 9, 10, 37, 38). The frequency of these cTEC-like progenitors, their precise phenotype and hence the developmental stage at which they reduce or even lose their bi-potency in place of an exclusive contribution to only the cTEC lineage remains yet to be defined. Based on results presented here and published previously (21), it is, however, likely that some or all of these aspects may differ between fetal and postnatal mice.

Distinct maturational stages have also been described for the postnatal mTEC lineage where a single linear differentiation process extends from immature progenitors ($MHCII^{lo}$ $CD80^{lo}$ $Aire^{-}$) to mature epithelia ($MHCII^{hi}$ $CD80^{hi}$ $Aire^{+}$) that may discontinue their Aire expression at a terminal stage (39, 40). Recently $SSEA\text{-}1^{+}$ $Claudin3/4^{+}$ mTEC have been identified that display a remarkable self-renewing capacity and serve as lifelong progenitors for the medullary but not the cortical epithelial compartment (22). Given their specific developmental potential, $SSEA\text{-}1^{+}$ $Claudin3/4^{+}$ mTEC progenitors must be distinct from the cortical $\beta5t^{+}$ precursors described here though they may represent a first unipotent progeny downstream of these cortical $\beta5t^{+}$ precursors. Moreover, our kinetic studies would suggest that cortical $\beta5t^{+}$ precursors represent a rare population because following dox treatment of 1-week old $3xtg^{\beta5t}$ mice up to 56 days are required to achieve maximum labeling of the mTEC compartment. Assuming that mature mTEC are still largely derived from $\beta5t^{+}$ precursors under these conditions (comparable to the fetal labeling experiments), we reason that their frequency must be low as a significant expansion is needed to label eventually as many as one third of all mTEC after a single dox dose. This interpretation is in keeping with our finding that only few clonal TEC clusters are detected at the cortico-medullary junction of individual medullary islets within 2 weeks following dox treatment. Moreover, the relatively low frequency of cortical $\beta5t^{+}$ precursors among early labelled cTEC precluded efforts to identify at the population level a particular gene expression signature of these cells. The reconstitution efficiency of early-labeled $\beta5t^{+}$ cTEC was however low, which is likely owing to the relatively low number used for reaggregates and the competitive advantage of fetal over adult TEC. The frequency of mTEC that express the label as a

result of promiscuous gene expression is very low, not least owing to the cells' relatively short half-life in young mice (average 0.9 weeks; ref. (29)).

In view of the labeling kinetics observed, it is likely that in young mice cortical β5t$^+$ precursors with a developmental potential for the mTEC lineage give first rise to a larger number of epithelia that lack β5t expression but have a self-renewing capacity and can replenish mTEC at all ages to suit the homeostatic needs of the medulla. This population of epithelia may represent the earliest post β5t-stage in the mTEC lineage and could function comparable to transit-amplifying cells (TAC) that balance precursor usage with tissue generation (41). Whether these cells are indeed the aforementioned SSEA-1$^+$ Claudin3/4$^+$ TEC progenitors remains, however, to be determined. Should this be the case, then experimental evidence suggests that these uni-potent precursors are already being generated at E14.5 (22). Once the exponential growth of the medulla has seized, mTEC development may largely be drawn from the TAC-like population with cortical β5t$^+$ precursors contributing now only to a limited extent to the maintenance of the medulla. Mutually not exclusive, the detection of labelled cells as late as 240 days after Dox treatment may, in part, also be the result of mTEC with an extended half-life (on average 10.9 weeks in older mice) (29).

MHC-mismatched ES ± blastocyst chimaeras and fetal thymus reaggregate grafts have suggested that individual progenitor cells generate, at least during fetal thymus development, individual medullary islet (19). In the young mouse most of these are not connected to each other or to a major medullary compartment (19, 42), thus creating a 3-dimensional branched medulla with an extended cortico-medullary junction. The resultant fractal geometry of the medulla therefore optimizes the recruitment of early stage mTEC precursors differentiating from β5t$^+$ precursors positioned in the cortex. Considering the increasing size of individual medullary islets in young mice, our results and previously published results (19) are compatible in demonstrating that individual islets are generated during fetal organogenesis from a single precursor but are later in life derived from an oligoclonal origin. While it had so far remained untested whether these epithelial progenitors are only able to

establish the correct medullary architecture during ontogeny, lineage tracing and competitive grafting experiments presented here now demonstrate that this capacity of β5t$^+$ cortical epithelial precursors is maintained into postnatal life. However, contributions from these precursors are significantly diminished in older mice and are not reactivated following thymic injury in adult mice (data not) thus inferring a regenerative process that is compartment-intrinsic.

The persistence of ZsGreen$^+$ TEC in both cortex and medulla over an extended period following short time labelling is remarkable and can best be explained by a pool of long-lived precursors in which recombination had successfully occurred and from which mature TEC are eventually generated. Alternative mechanisms may exist but have to date not yet been established for TEC. For example, a fraction of differentiated ZsGreen+ TEC could be generated *in situ* via a process of self-duplication in the absence of any contribution from progeny of labeled precursor cells, a phenomenon reported for other epithelial cell lineages (25–27). However, this mechanism would need to be stochastic and independent of specific developmental niches, as individual clusters of ZsGreen$^+$ TEC cannot be discerned in the cortex or the medulla of older mice that had been treated with Dox at one or five weeks of age.

In summary, we demonstrate to our knowledge for the first time that a population of β5t$^+$ cortical progenitors positioned adjacent to the medulla gives rise to mTEC. The extent of this contribution changes considerably during the first postnatal weeks when number and proportion of mTEC dramatically increase due to extensive proliferation. The precise signals and their down-stream molecular events responsible for this change remain presently undefined. However, insight into this process and the isolation and manipulation of β5t$^+$ cortical epithelial precursors constitute a novel rationale for therapeutic strategies to restore immune function.

3.4.6 Experimental procedures

Mice

C57BL/6 mice were obtained from Janvier (France). LC1-Cre transgenic, CAG-loxP-STOP-loxP-ZsGreen, CAG-loxP-stop-loxP-EGFP, R26R-Confetti, β5t-Cre and tetO-Cre1Jaw/J mice were described previously (14, 23, 24, 32, 43, 44). Mice were crossed to obtain double or triple heterozygous mutant animals as indicated in the text. For developmental staging, the day of a visible vaginal plug was designated in timed pregnancies as embryonic day 0.5 (E0.5). Mice were kept under specific pathogen-free conditions and all experiments were in accordance with local and national regulations and permissions.

Generation of β5t-rtTA mice

β5t-rtTA mice were generated analogous to the β5t-Cre animals previously reported (14).

Doxycycline Treatment

Fetal [β5t-rtTA::LC1-Cre::CAG-loxP-STOP-loxP-ZsGreen] mice (designated triple transgenic, 3xtg^{β5t}) were exposed to Doxycycline (Dox) via the mother's drinking water which was supplemented with the drug (2mg/ml) and sucrose (5% w/v) from E7.5 until birth. One-week-old 3xtg^{β5t} mice were treated with a single intraperitoneal (i.p.) injection of Dox (0.3mg) whereas older mice received two i.p. injections of Dox (2mg, each) in the course of 24 hours during which they were in addition exposed to drinking water supplemented with the drug.

BrdU Labelling

Mice were injected i.p. with 1mg BrdU (BrdU Kit, BD Pharmingen) and kept for 16 hours prior to analysis.

Cell Preparation

Thymic lobes were cut up into fragments, incubated in PBS containing 0.2mg/ml Liberase TM (Roche Diagnostics) and 30μg/ml DNaseI (Roche Diagnostics) at 37˚C for 60 min with occasional pipetting to facilitate digestion. Embryonic thymic tissue was incubated in PBS with 2% FCS (Perbio), 1mg/ml Collagenase D (Roche Diagnostics) and 30μg/ml DNaseI at 37˚C for 30 min. For the specific analyses of TEC, cells were enriched using magnetic beads (autoMACS Pro Separator, Miltenyi Biotech) and sorted using a FACSAria II (BD Bioscience).

Flow Cytometry

Cells were incubated with antibodies specific for CD45 (30F11; eBioscience), EpCAM (G8.8; DSHB, University of Iowa), MHCII (M5/114.15.2; BioLegend), Ly51 (6C3; BioLegend), UEA-1 (Reactolab), Aire (5H12; eBioscience) and BrdU. For intracellular staining, cells were fixed, permeabilized (Cytofix/Cytoperm Kit, BD Biosciences) and labelled for the expression of Aire or the incorporation of BrdU. Stained samples were acquired on a FACSAria II flow cytometer and the data was analyzed using the FlowJo (Treestar) software.

Quantitative PCR analysis

Total RNA was isolated from sorted cells with the RNeasy Micro Kit (Qiagen), validated using a NanoDrop 2000 (Thermo Scientific). cDNA was synthesized using SuperScriptIII (Live Technologies) and assessed by quantitative real-time PCR with SYBR Green (SensiMix; Bioline). Primer sequences are available upon request. *Epcam* specific transcripts were used as an internal control and PCR data was analysed using the LinRegPCR software (45).

Transcriptomic analyses

The transcriptomes of 174 single mature mTEC expressing more than 3000 genes (copy numbers from ref. (6), GEO accession GSE60297) were examined for Psmb11 expression. 26 cTEC and 229 mTEC marker genes (Fig 3C) were identified from cTEC and Aire-KO mTEC population RNA-seq data (GEO accession GSE53110 (6)). Here the mature Aire-KO mTEC population was used to avoid confounding Aire-induced promiscuous gene expression. Marker genes were required to be expressed at > 20 FPKM in the population of interest and < 1 FPKM in the other. Aire-regulated genes and TRA definitions are taken from (6).

Histological analyses

Prior to freezing, thymic lobes were fixed in 3.7% Formalin (Sigma) for 2-4 hours and dehydrated over night in a 20% w/v Sucrose solution. Thymic sections (8μm) were stained using Abs specific for Psmb11 (MBL), CK8 (Progen), CK14 (Covance) and Aire (eBioscience). Alexa Fluor-conjugated anti-IgG Abs (Invitrogen) were used as secondary reagents. Images were acquired using a Zeiss LSM510 (Carl Zeiss).

RTOC transplants

25'000 sorted transgenic TEC were mixed with 150'000 wild type embryonic (E14.5) cells depleted of $CD45^+$ and $Ter119^+$ subpopulations (autoMACS Pro Separator, Miltenyi Biotech), spun down and incubated at 37°C over night. Reaggregates were placed under the kidney capsule of the recipient *nu*/*nu* mice and analysed 5 weeks later.

Statistical analyses

Statistical analyses were performed using Students *t* test (unpaired, two-tailed). Probability values were classified into four categories: P>0.05 (n.s.), 0.05≥P>0.01 (*), 0.01≥P>0.001 (**) and P≤0.001 (***).

3.4.7 References

1. Anderson, G., and Y. Takahama. 2012. Thymic epithelial cells: working class heroes for T cell development and repertoire selection. *Trends Immunol.* 33: 256–63.

2. Klein, L., B. Kyewski, P. M. Allen, and K. A. Hogquist. 2014. Positive and negative selection of the T cell repertoire: what thymocytes see (and don't see). *Nat. Rev. Immunol.* 14: 377–91.

3. Metzger, T. C., and M. S. Anderson. 2011. Control of central and peripheral tolerance by Aire. *Immunol. Rev.* 241: 89–103.

4. Daley, S. R., D. Y. Hu, and C. C. Goodnow. 2013. Helios marks strongly autoreactive CD4+ T cells in two major waves of thymic deletion distinguished by induction of PD-1 or NF-κB. *J. Exp. Med.* 210: 269–85.

5. Stritesky, G. L., Y. Xing, J. R. Erickson, L. A. Kalekar, X. Wang, D. L. Mueller, S. C. Jameson, and K. A. Hogquist. 2013. Murine thymic selection quantified using a unique method to capture deleted T cells. *Proc. Natl. Acad. Sci. U.S.A.* 110: 4679–84.

6. Sansom, S. N., N. Shikama-Dorn, S. Zhanybekova, G. Nusspaumer, I. C. Macaulay, M. E. Deadman, A. Heger, C. P. Ponting, and G. A. Holländer. 2014. Population and single-cell genomics reveal the Aire dependency, relief from Polycomb silencing, and distribution of self-antigen expression in thymic epithelia. *Genome Res.* 24: 1918–31.

7. Gill, J., M. Malin, G. A. Holländer, and R. Boyd. 2002. Generation of a complete thymic microenvironment by MTS24(+) thymic epithelial cells. *Nat. Immunol.* 3: 635–42.

8. Rossi, S. W., W. E. Jenkinson, G. Anderson, and E. J. Jenkinson. 2006. Clonal analysis reveals a common progenitor for thymic cortical and medullary epithelium. *Nature* 441: 988–91.

9. Rossi, S. W., A. P. Chidgey, S. M. Parnell, W. E. Jenkinson, H. S. Scott, R. L. Boyd, E. J. Jenkinson, and G. Anderson. 2007. Redefining epithelial progenitor potential in the developing thymus. *European journal of immunology* 37: 2411–2418.

10. Bennett, A. R., A. Farley, N. F. Blair, J. Gordon, L. Sharp, and C. C. Blackburn. 2002. Identification and characterization of thymic epithelial progenitor cells. *Immunity* 16: 803–14.

11. Baik, S., E. J. Jenkinson, P. J. Lane, G. Anderson, and W. E. Jenkinson. 2013. Generation of both cortical and Aire(+) medullary thymic epithelial compartments from CD205(+) progenitors. *Eur. J. Immunol.* 43: 589–94.

12. Ribeiro, A. R., P. M. Rodrigues, C. Meireles, J. P. Di Santo, and N. L. Alves. 2013. Thymocyte selection regulates the homeostasis of IL-7-expressing thymic cortical epithelial cells in vivo. *J. Immunol.* 191: 1200–9.

13. Alves, N. L., Y. Takahama, I. Ohigashi, A. R. Ribeiro, S. Baik, G. Anderson, and W. E. Jenkinson. 2014. Serial progression of cortical and medullary thymic epithelial microenvironments. *Eur. J. Immunol.* 44: 16–22.

14. Ohigashi, I., S. Zuklys, M. Sakata, C. E. Mayer, S. Zhanybekova, S. Murata, K. Tanaka, G. A. Holländer, and Y. Takahama. 2013. Aire-expressing thymic medullary epithelial cells originate from β5t-expressing progenitor cells. *Proc. Natl. Acad. Sci. U.S.A.* 110: 9885–90.

15. Bleul, C. C., T. Corbeaux, A. Reuter, P. Fisch, J. S. Mönting, and T. Boehm. 2006. Formation of a functional thymus initiated by a postnatal epithelial progenitor cell. *Nature* 441: 992–6.

16. Wong, K., N. L. Lister, M. Barsanti, J. M. Lim, M. V. Hammett, D. M. Khong, C. Siatskas, D. H. Gray, R. L. Boyd, and A. P. Chidgey. 2014. Multilineage potential and self-renewal define an epithelial progenitor cell population in the adult thymus. *Cell Rep* 8: 1198–209.

17. Ucar, A., O. Ucar, P. Klug, S. Matt, F. Brunk, T. G. Hofmann, and B. Kyewski. 2014. Adult thymus contains FoxN1(-) epithelial stem cells that are bipotent for medullary and cortical thymic epithelial lineages. *Immunity* 41: 257–69.

18. Van Keymeulen, A., A. S. Rocha, M. Ousset, B. Beck, G. Bouvencourt, J. Rock, N. Sharma, S. Dekoninck,

and C. Blanpain. 2011. Distinct stem cells contribute to mammary gland development and maintenance. *Nature* 479: 189–93.

19. Rodewald, HR, S Paul, C Haller, H Bluethmann, and C Blum. 2001. Thymus medulla consisting of epithelial islets each derived from a single progenitor. *Nature* .

20. Hamazaki, Y., H. Fujita, T. Kobayashi, Y. Choi, H. S. Scott, M. Matsumoto, and N. Minato. 2007. Medullary thymic epithelial cells expressing Aire represent a unique lineage derived from cells expressing claudin. *Nat. Immunol.* 8: 304–11.

21. Parnell, SM, EJ Jenkinson, and G Anderson. 2009. Checkpoints in the development of thymic cortical epithelial cells. *The Journal of … .*

22. Sekai, M., Y. Hamazaki, and N. Minato. 2014. Medullary thymic epithelial stem cells maintain a functional thymus to ensure lifelong central T cell tolerance. *Immunity* 41: 753–61.

23. Schönig, K., F. Schwenk, K. Rajewsky, and H. Bujard. 2002. Stringent doxycycline dependent control of CRE recombinase in vivo. *Nucleic Acids Res.* 30: e134.

24. Madisen, L., T. A. Zwingman, S. M. Sunkin, S. W. Oh, H. A. Zariwala, H. Gu, L. L. Ng, R. D. Palmiter, M. J. Hawrylycz, A. R. Jones, E. S. Lein, and H. Zeng. 2010. A robust and high-throughput Cre reporting and characterization system for the whole mouse brain. *Nat. Neurosci.* 13: 133–40.

25. Schaub, J. R., Y. Malato, C. Gormond, and H. Willenbring. 2014. Evidence against a stem cell origin of new hepatocytes in a common mouse model of chronic liver injury. *Cell Rep* 8: 933–9.

26. Yanger, K., D. Knigin, Y. Zong, L. Maggs, G. Gu, H. Akiyama, E. Pikarsky, and B. Z. Stanger. 2014. Adult hepatocytes are generated by self-duplication rather than stem cell differentiation. *Cell Stem Cell* 15: 340–9.

27. Dor, Y., J. Brown, O. I. Martinez, and D. A. Melton. 2004. Adult pancreatic beta-cells are formed by self-duplication rather than stem-cell differentiation. *Nature* 429: 41–6.

28. Nishikawa, Y., H. Nishijima, M. Matsumoto, J. Morimoto, F. Hirota, S. Takahashi, H. Luche, H. J. Fehling, Y. Mouri, and M. Matsumoto. 2014. Temporal lineage tracing of Aire-expressing cells reveals a requirement for Aire in their maturation program. *J. Immunol.* 192: 2585–92.

29. Dumont-Lagacé, M., S. Brochu, C. St-Pierre, and C. Perreault. 2014. Adult thymic epithelium contains nonsenescent label-retaining cells. *J. Immunol.* 192: 2219–26.

30. Gray, D. H., N. Seach, T. Ueno, M. K. Milton, A. Liston, A. M. Lew, C. C. Goodnow, and R. L. Boyd. 2006. Developmental kinetics, turnover, and stimulatory capacity of thymic epithelial cells. *Blood* 108: 3777–85.

31. Gray, D., J. Abramson, C. Benoist, and D. Mathis. 2007. Proliferative arrest and rapid turnover of thymic epithelial cells expressing Aire. *J. Exp. Med.* 204: 2521–8.

32. Snippert, H. J., L. G. van der Flier, T. Sato, J. H. van Es, M. van den Born, C. Kroon-Veenboer, N. Barker, A. M. Klein, J. van Rheenen, B. D. Simons, and H. Clevers. 2010. Intestinal crypt homeostasis results from neutral competition between symmetrically dividing Lgr5 stem cells. *Cell* 143: 134–44.

33. Rodewald, H.-R. R. 2008. Thymus organogenesis. *Annu. Rev. Immunol.* 26: 355–88.

34. Depreter, M. G., N. F. Blair, T. L. Gaskell, C. S. Nowell, K. Davern, A. Pagliocca, F. H. Stenhouse, A. M. Farley, A. Fraser, J. Vrana, K. Robertson, G. Morahan, S. R. Tomlinson, and C. C. Blackburn. 2008. Identification of Plet-1 as a specific marker of early thymic epithelial progenitor cells. *Proc. Natl. Acad. Sci. U.S.A.* 105: 961–6.

35. Ripen, A. M., T. Nitta, S. Murata, K. Tanaka, and Y. Takahama. 2011. Ontogeny of thymic cortical epithelial cells expressing the thymoproteasome subunit β5t. *Eur. J. Immunol.* 41: 1278–87.

36. Muñoz, J. J., T. Cejalvo, E. Tobajas, L. Fanlo, A. Cortés, and A. G. Zapata. 2014. 3D Immunofluorescence analysis of early thymic morphogenesis and medulla development. *Histol. Histopathol.* .

37. Van Ewijk, W., G. Holländer, C. Terhorst, and B. Wang. 2000. Stepwise development of thymic microenvironments in vivo is regulated by thymocyte subsets. *Development* 127: 1583–91.

38. Holländer, G. A., B. Wang, A. Nichogiannopoulou, P. P. Platenburg, W. van Ewijk, S. J. Burakoff, J. C. Gutierrez-Ramos, and C. Terhorst. 1995. Developmental control point in induction of thymic cortex regulated by a subpopulation of prothymocytes. *Nature* 373: 350–3.

39. Rossi, S. W., M.-Y. Y. Kim, A. Leibbrandt, S. M. Parnell, W. E. Jenkinson, S. H. Glanville, F. M. McConnell, H. S. Scott, J. M. Penninger, E. J. Jenkinson, P. J. Lane, and G. Anderson. 2007. RANK signals from CD4(+)3(-) inducer cells regulate development of Aire-expressing epithelial cells in the thymic medulla. *J. Exp. Med.* 204: 1267–72.

40. Nishikawa, Y., F. Hirota, M. Yano, H. Kitajima, J. Miyazaki, H. Kawamoto, Y. Mouri, and M. Matsumoto. 2010. Biphasic Aire expression in early embryos and in medullary thymic epithelial cells

before end-stage terminal differentiation. *J. Exp. Med.* 207: 963–71.

41. Hsu, Y.-C. C., L. Li, and E. Fuchs. 2014. Transit-amplifying cells orchestrate stem cell activity and tissue regeneration. *Cell* 157: 935–49.

42. Irla, M., J. Guenot, G. Sealy, W. Reith, B. A. Imhof, and A. Sergé. 2013. Three-dimensional visualization of the mouse thymus organization in health and immunodeficiency. *J. Immunol.* 190: 586–96.

43. Kawamoto, S., H. Niwa, F. Tashiro, S. Sano, G. Kondoh, J. Takeda, K. Tabayashi, and J. Miyazaki. 2000. A novel reporter mouse strain that expresses enhanced green fluorescent protein upon Cre-mediated recombination. *FEBS Lett.* 470: 263–8.

44. Perl, A.-K. T. K., S. E. Wert, A. Nagy, C. G. Lobe, and J. A. Whitsett. 2002. Early restriction of peripheral and proximal cell lineages during formation of the lung. *Proc. Natl. Acad. Sci. U.S.A.* 99: 10482–7.

45. Ramakers, C., J. M. Ruijter, R. H. Deprez, and A. F. Moorman. 2003. Assumption-free analysis of quantitative real-time polymerase chain reaction (PCR) data. *Neurosci. Lett.* 339: 62–6.

3.4.8 Supplementary Material

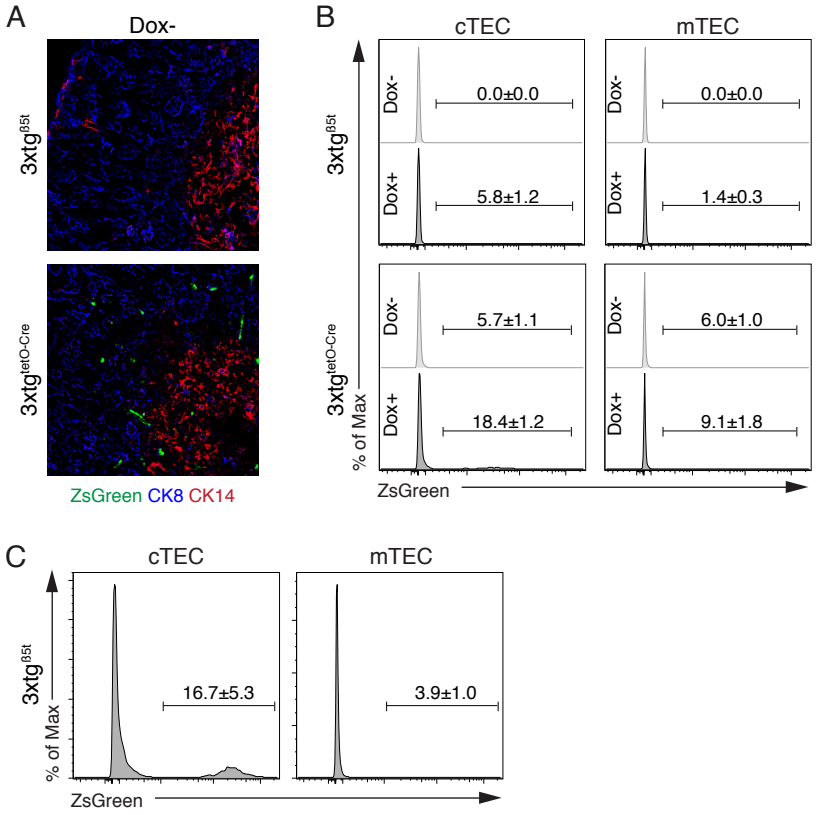

Figure S1. *Comparative analysis of triple-transgenic mice in which Cre expression is driven by different transgenes.* (A) Thymic cross-sections of untreated 5-week old 3xtg$^{\beta 5t}$ and 3xtg$^{tetO\text{-}Cre}$ mice were analysed by immunofluorescence for the expression of ZsGreen, CK8 and CK14. (B) Flow cytometric analysis of cTEC (EpCAM^{+}LY51^{+}UEA1^{-}CD45^{-}) and mTEC (EpCAM^{+}LY51^{-}UEA1^{+}CD45^{-}) for the expression of ZsGreen in 5-week old 3xtg$^{\beta 5t}$ (*upper* panel) and 3xtg$^{tetO\text{-}Cre}$ (*lower* panel) mice that were i.p. injected twice within 24hr with Dox (2mg) and given Dox (2mg/ml) supplemented drinking water in that time. (C) Flow cytometric analysis of cTEC and mTEC for the expression of ZsGreen in 6-week old 3xtg$^{\beta 5t}$ mice i.p. injected with Dox (2mg) at 5 weeks of age and then given Dox (2mg/ml) supplemented drinking water for the following week.

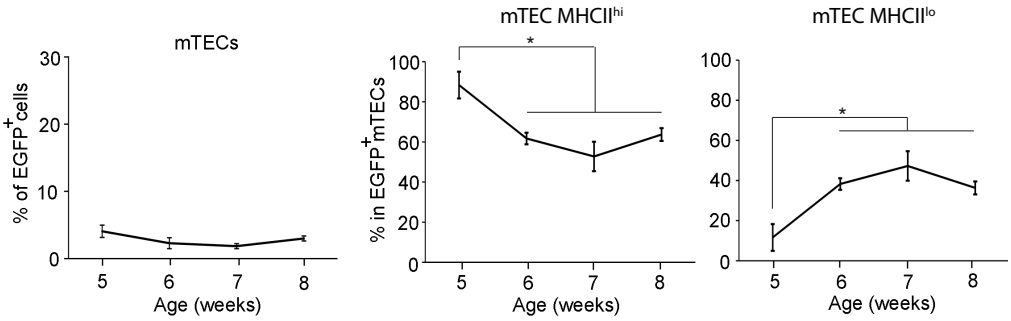

Figure S2. *Kinetic changes of MHCII expression in EGFP+ mTEC.* Flow cytometric analysis of MHCII^{hi} and MHCII^{lo} mTEC (EpCAM^{+}Ly51^{-}UEA1^{+}CD45^{-}) in β5t-rtTA::LC1::CAG-EGFP mice treated at 4 weeks of age for one week with Dox (2mg/ml) supplemented drinking water. Percentage of EGFP+ cells for each of the indicated TEC subpopulations is plotted against the age of the mice. *P<0.05.

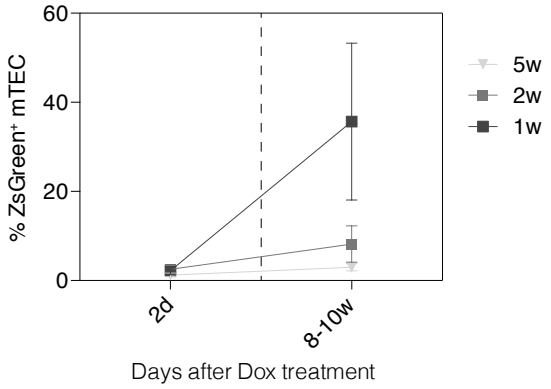

Figure S3. *Contribution of β5t+ progenitor cells to the postnatal medulla growth is reduced with age.* 3xtg^{β5t} mice were treated with Dox at either 1 week, 2 weeks or 5 weeks of age and chased for 2 days or 8 to 10 weeks. Percentage of ZsGreen+ mTEC (EpCAM^{+}Ly51^{-}UEA1^{+}CD45^{-}) was determined at each time point by flow cytometry. Values represent mean ± SD of at least three independent experiments with at least three mice per time point each.

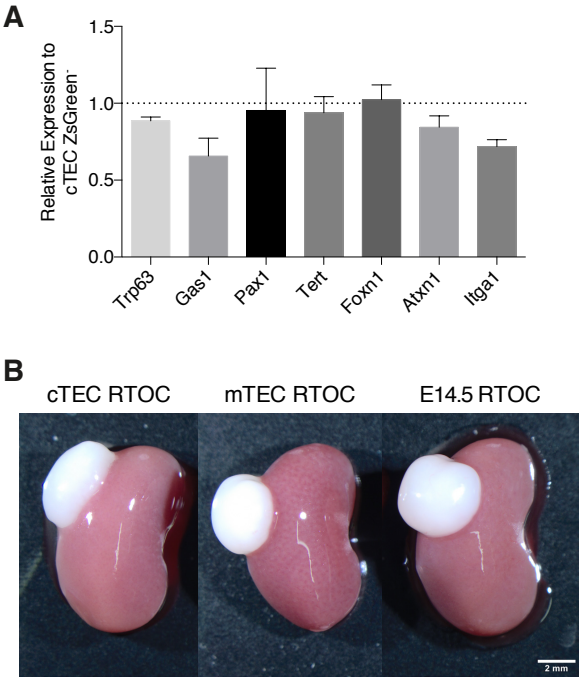

Figure S4. *ZsGreen+ cTEC used for RTOC contribute to the formation of the thymus when transplanted into recipient mouse.* (A) ZsGreen-/+ cTEC were sorted from 3xtg$^{\beta 5t}$ mice treated with a single injection of Dox (1mg) at one week of age and kept for two days. RT-qPCR analysis of selected genes in ZsGreen+ cTEC shown relative to ZsGreen- cTEC. Values represent the mean ± SD. (B) Macroscopic image showing kidneys of *nu/nu* mice 5 weeks after transplanting RTOC containing either ZsGreen+ cTEC or mTEC mixed with embryonic cells, or embryonic cells alone. Scale bar = 2mm.

4 Discussion

The thymic epithelial cells (TEC) are required for thymopoiesis and play an important role in the establishment of central tolerance. TEC in the cortex (designated cTEC) guide the first steps of T cell development by expressing factors that attract, commit and select T cell progenitor cells (1–4). The subsequent steps in T cell development are controlled by medullary TEC (mTEC), which are specialized in the ectopic expression and presentation of tissue-restricted antigens (TRA) (5, 6). These are required for the correct negative selection of potentially auto-reactive T cells (2). Due to their importance in the establishment of T cell tolerance, the study of mTEC development and function has been a strong focus of thymic research. In spite of the difficulty to investigate TEC precursors due to the lack of appropriate markers that define this rare cell population, several important findings were made in recent years. Two groups have reported the existence of bi-potent TEC progenitor cells during embryogenesis and in postnatal mice, defining a shared developmental origin of cTEC and mTEC (7, 8). Recent publications extended this relationship reporting that progenitor cells to the mTEC lineage express β5t and CD205, molecules characteristic for adult cTEC, during embryonic development (9, 10). Similar observations were made in adult mice, in which label-retaining cells were characterized and tested for their progenitor capacity (11, 12). These experiments identified a subpopulation of cTEC that gave rise to mTEC in reaggregation and transplantation experiments. In addition, adult cTEC revealed a significant regenerative capacity upon drug-induced injury of the thymic cortex, implying the presence of TEC progenitor cells in within the cTEC compartment (13). In parallel to the accumulating cTEC-centric evidence, mTEC lineage-restricted progenitor cells were identified in the medullar compartment during embryogenesis and in adult mice (14–16). Moreover, TEC with progenitor capacities were reported in EpCAM-Foxn1- TEC, and in animals in which Foxn1, a transcription factor that is required for the expansion and final maturation of TEC, was induced in adulthood (17–19). In aggregate, these publications show that progenitor cells to the mTEC lineage are present during thymic organogenesis and in the adult mouse, and that cTEC-like cells as well as mTEC lineage-restricted progenitors in the medulla contribute to the development of the medullary compartment.

The study presented in chapter 3.1 describes the involvement of Dicer and miRNA in TEC development, differentiation and function. This investigation concluded that Dicer is largely dispensable during embryonic TEC development because no changes were observed in architecture or function of thymi in which Dicer was selectively deleted in TEC at embryonic day of development (E) 12.5. Therefore the initial wave of T cell development was undisturbed. However, the lack of Dicer disturbed the postnatal formation of the medulla because mTEC failed to expand in numbers in mice of one week of age and older. In keeping with this conclusion, the thymic epithelial identity and function were lost, as observed in 2-week-old mice when the overall thymic micro-architecture displayed aberrant expression of markers characteristic for cTEC and mTEC and defects in thymic T cell positive selection emerged. In light of the data presented in chapter 3.4, I now interpret the observed changes that occurred after the loss of Dicer expression in TEC, as follows: The postnatal development of the thymus is marked by a significant growth of the medulla and hence an increase in mTEC numbers. Mice, in which Dicer was specifically deleted in TEC, revealed normal number of mTEC until 1 week of age. However, in 2-week-old mice we detected that the number of cTEC was slightly increased, while mTEC cellularity was markedly diminished. A deficiency in Dicer, and consequently most miRNA, could thus have impaired the postnatal cTEC-like progenitor cell and, as a consequence, affected the formation of the medulla. Unfortunately, the precise phenotypic identity of that cell remains unknown, which limits the ability to verify this hypothesis. However, the work presented here significantly advanced our understanding of embryonic and postnatal mTEC development in as much as it identified β5t as a marker in cells that serve as mTEC progenitors. In addition, I characterized the branching point of cortical and medullar lineage divergence during embryonic development, giving insights into the phenotypic dynamics during lineage commitment. Because we have shown that β5t+ mTEC progenitor cells continue to contribute to the growth of the medulla during the first weeks of live, the phenotypic identification of mTEC at distinct steps during differentiation could potentially help understanding the mechanisms that drive the development of this compartment in the postnatal mouse. Unfortunately, β5t is not a

specific to mTEC progenitor cells but a protein expressed in almost all cTEC. This broad expression pattern limits the isolation of only progenitor cells based on β5t-expression for the analysis of their gene expression profile and progenitor capacity. To overcome this issue I propose three strategies that focus on the investigation of 3xtg$^{\beta5t}$ mice treated with Dox at 1 week of age. ZsGreen+ cTEC detected at 2 days after treatment could be subdivided based on their expression of different cell surface markers that have been proposed for adult TEC progenitor cells (e.g. Ly51^{low}, MHCII^{low}, Atxn1^{+}, Itga1^{+}) and tested for their progenitor capacities in reaggregation and transplantation experiments, such as the ones described in chapter 3.4.5 (12, 17). This approach would specify the phenotype of a cTEC subpopulation that is enriched in mTEC progenitor cells. Unfortunately, this strategy is unlikely to lead to the clean isolation of progenitor cells, because, due to the scarcity of candidate progenitor markers, the isolated subpopulations would likely contain mature, non-progenitor cTEC. Although many mature cTEC could be excluded following this procedure, an analysis of such a mixture of cells would unlikely provide the clear phenotypic identity of the unknown progenitor cell.

In chapter 3.4 I found that β5t was expressed as part of the promiscuous gene expression program in mature mTEC, which lead to the expression of ZsGreen in approximately 2% of mTEC at 2 days after Dox treatment. Because the relative and absolute number of ZsGreen+ mTEC increased during the following 8 weeks after treatment of 1-week-old mice, I concluded that β5t+ progenitor cell-derived, newly generated mTEC contributed to the growth of the medulla during the postnatal development of the thymus. I propose that the ZsGreen+ fraction of cells within the medulla at 2 days after the Dox treatment of 1-week-old mice is composed of two very different cell populations: mature mTEC that expressed β5t as part of their promiscuous gene expression (pGE) program, and newly generated epithelia that are committed to the mTEC-lineage. It is likely that these two populations can be differentiated owing to their transcription of cell markers associated with mature mTEC (e.g. UEA1^{high}, CD80^{high}, CD86^{high}, Aire^{+}, Involucrin^{+}, CK10^{+}), or expression of molecules characteristic for cTEC (e.g. β5t, CD205, Ly51). This expected phenotype would therefore be the cumulative result of a progression from a cTEC-like

progenitor cell to an epithelium with an mTEC fate. The availability of a set of specific cell surface markers would allow to purify mTEC progenitor cells in unmanipulated thymi and to map their differentiation pathway. An analysis of the transcriptional landscape of these β5t+ progenitor cell-derived, differentiating mTEC could therefore provide an approximate phenotype of the enigmatic cTEC-like progenitor. The progenitor cells themselves are, however, unlikely to be identified using this approach.

Should the distinction between β5t+ progenitor-derived cells and those expressing β5t as part of their pGE prove to be difficult, alternative approaches will have to be considered. For example, individual ZsGreen+ mTEC, isolated at 2 days after the treatment of 1-week-old mice, could be analyzed for their transcriptional landscapes on a per-cell basis. Using computer-assisted cluster matching profiling a precise developmental pathway could be suggested that can subsequently be tested. In spite of holding some challenges, including a lower sensitivity in detecting lowly abundant transcripts, this last approach is the most likely in succeeding to identify the phenotype of the β5t+ mTEC progenitor cell.

Once the cTEC-like progenitor cell is phenotypically identified it will be interesting to test the progenitor capacity of that cell. Specifically it would be informative to elucidate whether these precursors are restricted to the mTEC lineage in neonatal mice and if so, when during thymic organogenesis they establish this capacity. Indeed, single cell evidence has yet to be produced as to the existence of a truly bi-potent TEC progenitor in the adult thymus, comparable to Plet1+ (a.k.a. MTS20 and MTS24) cells described in the early bot not late embryo (8). Data presented in chapter 3.4 demonstrates that mTEC progenitor cells are located in the neonatal thymus at the cortico-medullary junction, a structure that has long been hypothesized as the site where bi-potent precursor cells should be placed (20, 21). Traditionally, extrapolation from results obtained studying thymus organogenesis has linked bi-potency to a TEC phenotype that is Plet1+, CK5+ and CK8+ (22). And in fact CK5+CK8+ cells can be detected in the adult thymus located near the cortico-medullary junction, which has made this population very attractive as a potential

postnatal bi-potent progenitor population. Experiments showed that in thymi of human CD3ε transgenic mice, in which T cell development is blocked at a very early CD44+CD25- DN stage, CK5+CK8+ TEC were most abundant (20). These cells gave rise to CK5-CK8+ cTEC when transplanted into Rag1-/- mice, enforcing this phenotype to be typical for TEC progenitor cells. In contrast I do not know whether the β5t+ progenitor cells to the mTEC lineage express indeed CK5 or CK8 and whether they contribute to the formation of the cortex. Because the percentage of ZsGreen+ cTEC remained stable for at least 20 weeks in $3xtg^{\beta5t}$ mice that were treated at one week of age, I hypothesize that β5t is does not preferentially label cTEC progenitor cells at that age. To investigate whether β5t+ progenitor cells contribute to the formation of the cortical compartment I propose to pulse-treat $3xtg^{confetti}$ mice with Dox during embryogenesis and follow the quantity and localization of reporter-positive cells after short periods of chase. The detection of reporter-positive clusters would provide more insights into cTEC development during thymic organogenesis. An alternative explanation to the stable percentage of ZsGreen+ cTEC would be that β5t is not preferentially expressed (or not-expressed) in postnatal cTEC progenitors, which would lead to a continuous contribution of ZsGreen+ and ZsGreen- progenitor cells to the cortical epithelial compartment in which the overall percentage of reporter positive cells does not change over time. However, this alternative explanation is less likely to be correct because ZsGreen+ cTEC progenitors would still participate to the cortex (even though equally to ZsGreen- ones), which would lead to regional clusters of reporter positive cells in the vicinity of precursors. Yet we did not observe any cluster formation during short or long chases after Dox treatment when investigating thymic cross-sections, nor did we detect a biased distribution of same-colored cells in the cortex of $3xtg^{confetti}$ mice. In addition we did not find cluster formation in thymic injury models, i.e. mice that received sub-lethal total body irradiation (data not shown). I therefore conclude that the contribution of β5t+ progenitor cells to the cortex after one week of life is very limited.

In light of the results presented in chapter 3.4, I would like to propose a model of postnatal TEC development (Figure 1) in which β5t+ progenitor cells sitting at the cortico-medullary junction actively contribute to the growth of the medulla during

the first weeks of life, as observed in the in vivo tracing studies of 3xtg$^{\beta5t}$ mice treated at one week of age and the transplantation experiments of RTOC generated with sorted ZsGreen+ cTEC. The immediate progeny of those progenitors would give rise to a transiently amplifying immature, mTEC-lineage restricted population (based on the BrdU incorporation data and the examination of transplants originating from RTOC generated with ZsGreen+ mTEC). Ultimately, after the amplification phase, the mTEC lineage-committed progenitor would develop into the various mature mTEC lineages.

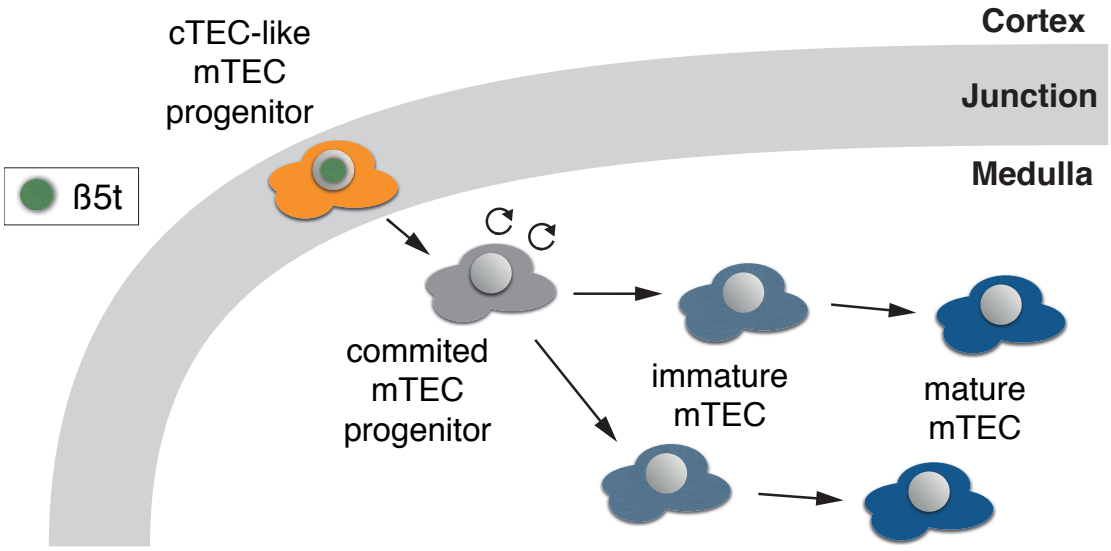

Figure 3.4-1. *Model for postnatal mTEC development.* During the postnatal expansion of the medulla β5t+ progenitor situated at the cortico-medullary junction give rise to a transiently amplifying population of mTEC lineage-restricted cells, which, upon several round of proliferation, develop into the mature mTEC lineages observed in the adult thymus.

In summary, the results presented in this thesis provide an insight into the complex spatio-temporal dynamics of thymic epithelial cell development. cTEC-like (i.e. β5t+ and CD205+) cells appear very early during thymic organogenesis and are required for the production of signals that attract and commit immigrating hematopoietic progenitor cells. Later in development, cTEC are involved in the processes of positive selection, a critical step during T cell development, and even negative selection, as adult cTEC have been shown to express TRA (5). Thus mTEC provide

addition to a function already largely provided by cTEC and hence not critically needed for the generation of T cells. However, mTEC clearly refine the overall competence of the thymus. The delayed developmental appearance of mTEC and the possible continuous contribution of cTEC-like cells to the growing medulla could therefore drive an evolutionary evolved fine-tuning of the thymic function that allows the creation of a secondary specialized compartment able to secure the correct selection of the T cell antigen receptor repertoire.

References

1. Rothenberg, EV, JE Moore, and MA Yui. 2008. Launching the T-cell-lineage developmental programme. Nature Reviews Immunology .
2. Klein, L., B. Kyewski, P. M. Allen, and K. A. Hogquist. 2014. Positive and negative selection of the T cell repertoire: what thymocytes see (and don't see). Nat. Rev. Immunol. 14: 377–91.
3. Klein, L., M. Hinterberger, G. Wirnsberger, and B. Kyewski. 2010. Antigen presentation in the thymus for positive selection and central tolerance induction. Nature reviews. Immunology 9: 833–44.
4. Takahama, Y. 2006. Journey through the thymus: stromal guides for T-cell development and selection. Nat. Rev. Immunol. 6: 127–35.
5. Sansom, S. N., N. Shikama-Dorn, S. Zhanybekova, G. Nusspaumer, I. C. Macaulay, M. E. Deadman, A. Heger, C. P. Ponting, and G. A. Holländer. 2014. Population and single-cell genomics reveal the Aire dependency, relief from Polycomb silencing, and distribution of self-antigen expression in thymic epithelia. Genome Res. 24: 1918–31.
6. Kyewski, B., and L. Klein. 2006. A central role for central tolerance. Annual review of immunology 24: 571–606.
7. Bleul, C. C., T. Corbeaux, A. Reuter, P. Fisch, J. S. Mönting, and T. Boehm. 2006. Formation of a functional thymus initiated by a postnatal epithelial progenitor cell. Nature 441: 992–6.
8. Rossi, S. W., W. E. Jenkinson, G. Anderson, and E. J. Jenkinson. 2006. Clonal analysis reveals a common progenitor for thymic cortical and medullary epithelium. Nature 441: 988–91.
9. Ohigashi, I., S. Zuklys, M. Sakata, C. E. Mayer, S. Zhanybekova, S. Murata, K. Tanaka, G. A. Holländer, and Y. Takahama. 2013. Aire-expressing thymic medullary epithelial cells originate from β5t-expressing progenitor cells. Proc. Natl. Acad. Sci. U.S.A. 110: 9885–90.
10. Baik, S., E. J. Jenkinson, P. J. Lane, G. Anderson, and W. E. Jenkinson. 2013. Generation of both cortical and Aire(+) medullary thymic epithelial compartments from CD205(+) progenitors. Eur. J. Immunol. 43: 589–94.
11. Dumont-Lagacé, M., S. Brochu, C. St-Pierre, and C. Perreault. 2014. Adult thymic epithelium contains nonsenescent label-retaining cells. J. Immunol. 192: 2219–26.
12. Wong, K., N. L. Lister, M. Barsanti, J. M. Lim, M. V. Hammett, D. M. Khong, C. Siatskas, D. H. Gray, R. L. Boyd, and A. P. Chidgey. 2014. Multilineage potential and self-renewal define an epithelial progenitor cell population in the adult thymus. Cell Rep 8: 1198–209.
13. Rode, I., and T. Boehm. 2012. Regenerative capacity of adult cortical thymic epithelial cells. Proc. Natl. Acad. Sci. U.S.A. 109: 3463–8.
14. Onder, L., V. Nindl, E. Scandella, Q. Chai, H. Cheng, S. Firner, M. Novkovic, D. Bomze, R. Maier, and F. Mair. 2015. Alternative NF B signaling regulates mTEC differentiation from podoplanin expressing presursors in the cortico medullary junction. European journal of immunology .
15. Hamazaki, Y., H. Fujita, T. Kobayashi, Y. Choi, H. S. Scott, M. Matsumoto, and N. Minato. 2007. Medullary thymic epithelial cells expressing Aire represent a unique lineage derived from cells expressing claudin. Nat. Immunol. 8: 304–11.
16. Sekai, M., Y. Hamazaki, and N. Minato. 2014. Medullary thymic epithelial stem cells maintain a functional thymus to ensure lifelong central T cell tolerance. Immunity 41: 753–61.
17. Ucar, A., O. Ucar, P. Klug, S. Matt, F. Brunk, T. G. Hofmann, and B. Kyewski. 2014. Adult thymus contains FoxN1(-) epithelial stem cells that are bipotent for medullary and cortical thymic epithelial lineages. Immunity 41: 257–69.

18. Jin, X., C. S. Nowell, S. Ulyanchenko, F. H. Stenhouse, and C. C. Blackburn. 2014. Long-term persistence of functional thymic epithelial progenitor cells in vivo under conditions of low FOXN1 expression. PLoS ONE 9: e114842.

19. Bredenkamp, N., C. S. Nowell, and C. C. Blackburn. 2014. Regeneration of the aged thymus by a single transcription factor. Development 141: 1627–37.

20. Klug, D., C. Carter, E. Crouch, D. Roop, C. Conti, E. Richie, and C. Conti. 1997. Interdependence of cortical thymic epithelial cell differentiation and T-lineage commitment. Proceedings of the National Academy of Sciences of the United States of America .

21. Park, C.-S., Lee, Yang, Ahn, Kim, Shin, and Kim. 2013. Differential lineage specification of thymic epithelial cells from bipotent precursors revealed by TSCOT promoter activities. Genes Immun .

22. Bennett, A. R., A. Farley, N. F. Blair, J. Gordon, L. Sharp, and C. C. Blackburn. 2002. Identification and characterization of thymic epithelial progenitor cells. Immunity 16: 803–14.

5 Appendix